ADVANCED LECTURES ON DYNAMICAL METEOROLOGY

Roger K. Smith

Fassung: WS 02/03

Contents

PREFACE

These notes are an outgrowth of various advanced courses on dynamical meteorology given over a period of years at Monash University in Australia and the University of Munich. They are an extension of my earlier set 'Lectures on Dynamical Meteorology', to which frequent reference is made. The notes include in places material adapted from course notes kindly given to me by Dr. John Green, formerly of Imperial College, London and Dr. Michael McIntyre from the University of Cambridge. I gratefully acknowledge these two colleagues for providing me with their unpublished lecture material.

I would like to thank Anna-Riitta Järvinen for her care and patience in preparing the typescript and to the many people who have pointed out errors in previous versions.

Roger Smith, Munich, August 2002.

Chapter 1

INTRODUCTION

Dynamical meteorology concerns itself with the theoretical study of *atmospheric motion*. It aims to provide an understanding of such motion as well as a rational basis for the prediction of atmospheric events, including short and medium weather prediction and the forecasting of climate.

The atmosphere is an extremely complex system involving motions on a very wide range of space and time scales. As a result, the dynamic and thermodynamic equations which describe the motions are too general to be solved easily. Thus, invariably, they have solutions representing phenomena that may not be of interest in the study of a particular problem: for example, we do not believe that acoustic (sound) waves are important in cyclogenesis, but such motions are described by the general equations of motion.

As in earlier courses (Smith, 1992; Lectures on Modern Synoptic Meteorology, henceforth referred to as SM; Smith, 2000; Lectures on Dynamical Meteorology, henceforth referred to as DM) we attempt to reduce the complexity of the equations by scaling whilst aiming to retain a reasonably accurate description of motion within certain limits of temporal and spatial scales. In doing this we need first to ascertain the essential physical aspects of the motion we hope to study. Then we seek ways of making approximations that are consistent in all equations by using quantitative estimates based on our physical perception of the problem. Finally, we need to determine for what scales the estimates accurately reflect physical reality.

It is necessary to be aware of the various types of waves motion which can occur in the atmosphere. Certain wave types play an important role in atmospheric dynamics and they may propagate significant amounts of energy from one place to another in a manner analogous to the propagation of energy by electromagnetic waves. Moreover, because waves are solutions of the equations, they will appear when the equations are integrated numerically. Some of these wave types cause difficulties in attempts to make numerical

weather predictions and we shall seek ways to modify the equations in order to *filter* them out; an example is a modification that makes the equations 'sound-proof' discussed in Chapter 2. Under some circumstances, waves may grow rapidly in amplitude, often as a result of *instability*. For example, Kelvin-Helmholtz instability may arise when a strong vertical shear occurs in the neighbourhood of large stable density gradient such as an inversion layer; this is one mechanism thought to be responsible for clear air turbulence (CAT). Another example is baroclinic instability, a process responsible for extra-tropical cyclogenesis; this instability has consequences for the *predictability* of the atmosphere. Examples of waves we shall study are listed in Table 1.

Table 1.1: General wave types in the atmosphere.

Wave type	**Speed controlled by:**
acoustic waves	temperature
gravity waves	static stability
inertial waves	Coriolis forces
Rossby waves	latitudinal variation of the Coriolis parameter

1.1 Some revision

1.1.1 The momentum equation in height coordinates

The momentum equation for a rotating stratified fluid may be written as

$$\frac{D\mathbf{u}}{Dt} + f\mathbf{k} \wedge \mathbf{u} = -\frac{1}{\rho}\nabla p + \sigma\mathbf{k} - \mathbf{D}, \tag{1.1}$$

where

$f = 2\Omega sin\phi$	is the Coriolis parameter,
ϕ	is the latitude,
$p = p_T - p_0(z)$	is the perturbation pressure,
p_T	is the total pressure,
$\rho_0(z)$	is the reference pressure; this satisfies the hydrostatic equation: $dp_0/dz = -g\rho_0(z)$,
$\sigma = g(\rho_0 - \rho)/\rho$	is the buoyancy force per unit mass, and
$\mathbf{D}$	is the frictional force per unit mass.

A further discussion of Eq. (1.1) is given in DM Chapter 3. Recall that p and σ are NOT uniquely defined, being dependent on the arbitrarily chosen definition of the reference density and pressure.

1.2 The Boussinesq approximation

This is an approximation which enables considerable simplification to the equations for a stably stratified fluid when density variations are not too large. In it, density variations are considered only in as much as they give rise to buoyancy forces in 1.1). In particular, $1/\rho$ in (1.1) is set equal to $1/\overline{\rho}$, a constant $\overline{\rho}$, $\overline{\rho}$ being, for example, the average density over the whole flow domain. Also $\sigma \approx g(\rho_0(z) - \rho)/\overline{\rho}, \rho_0(z)$ being the horizontal average of r at height z, or the ambient density, for example. Density variations are neglected also in the continuity equation which takes the approximate form $\nabla \cdot \mathbf{u} = 0$.

1.3 The anelastic approximation

In meteorology, the Boussinesq approximation is sometimes too restrictive. For example, in motions which occupy the entire depth of the troposphere, density variations in the vertical are considerable. The density near the tropopause is only about one quarter to one fifth of that at the surface. In such circumstances the anelastic approximation is more accurate. In this, the effect of the decrease in density with height on the fluid inertia is taken into account by setting $\rho^{-1} \approx \rho_0(z)^{-1}$, and the approximate forms of the buoyancy and of the continuity equation are

$$\sigma = g(\rho_0(z) - \rho)/\rho_0(z), \tag{1.2}$$

and

$$\nabla \cdot (\rho_0(z)\mathbf{u}) = 0. \tag{1.3}$$

The anelastic approximation is best handled by a change of pressure variable to $\pi = (p/p^\star)^\kappa$, the so-called *Exner function*, where $p^\star = 1000$ mb. This is especially the case for an atmosphere which is close to adiabatic. For further information see: Ogura and Phillips (1962), Dutton and Fichtl (1969), Lipps and Helmer (1982, 1985), Durran (1989, 1990), Fiedler (1990), Lipps (1990), Nance and Durran (1994), and Bannon (1995).

1.4 Pressure coordinates

For *hydrostatic* motions, such as large-scale atmospheric motions, the use of pressure or some function of pressure as vertical coordinate instead of height simplifies the equations. More details of the transformations involved are given in Chapter 10. In particular, in pressure coordinates the continuity equation takes a simpler form than (1.3) and density does not appear explicitly. The full set of equations is listed below:

$$\frac{D_p}{Dt}\mathbf{u}_h + \omega\frac{\partial \mathbf{u}_h}{\partial p} + f\mathbf{k}\wedge\mathbf{u}_h = -\nabla_p\phi, \tag{1.4}$$

$$\frac{\partial \phi}{\partial p} = -\frac{RT}{p}, \tag{1.5}$$

$$\nabla_p\cdot\mathbf{u}_h + \frac{\partial \omega}{\partial p} = 0, \tag{1.6}$$

$$\frac{D_p}{Dt}\ln\,\theta + \omega\frac{\partial}{\partial p}\ln\theta = \frac{1}{c_pT}\frac{DQ}{Dt}, \tag{1.7}$$

$$\theta = T\left(\frac{p_*}{p}\right)^{\kappa}, \tag{1.8}$$

and

$$\omega = \frac{Dp}{Dt}. \tag{1.9}$$

Here, $D_p/Dt \equiv \partial/\partial t + \mathbf{u}_h\cdot\nabla_p$ is the derivative in an isobaric surface ($p =$ constant, where here, p is the total pressure) and

$$\nabla_p \equiv \left(\frac{\partial}{\partial x},\ \frac{\partial}{\partial y},\ 0\right)_p.$$

Note that an isobaric surface is almost horizontal in large-scale motion. The quantity ϕ, essentially equal to gz, is the *geopotential height* of an isobaric surface. The relationship between height coordinates and pressure coordinates is summarized in Fig. 1.1. In pressure coordinates the quantity w plays the role of vertical velocity w, but note that since pressure decreases with height, ascent ($w > 0$) corresponds with $\omega < 0$, and subsidence ($w < 0$) with $\omega > 0$. The quantity DQ/Dt denotes the diabatic heating rate per unit mass.

1.5 Other pressure coordinate systems

Sometimes a function of p is used as the vertical coordinate rather than p. Two commonly used choices are: $Z(p) = -H_s ln(p/p\star)$, introduced by Eliassen (1949), and $\chi(p) = [1 - (p/p*)^\kappa]\ H/\kappa$, introduced by Hoskins and Bretherton (1972). Here, $H_s = RT_0/g$ is a constant scale height, T_0 is a constant temperature, and $H = p_0/(\rho g)$, is also a constant, where p_0 and ρ_0 are the pressure and density at some level. Convenient attributes of these functions are that $Z(p)$ equals the exact height above the 1000 mb level in an *isothermal* atmosphere, and $\chi(p)$ is the exact height in an *adiabatic* atmosphere. The (x, y, χ) coordinate system is used in Chapter 7 to study the dynamics of fronts. In both cases, the equations of motion are structurally similar to those with pressure as vertical coordinate, although the continuity equation is less simple in form.

1.6 Isentropic coordinates

In a stably-stratified atmosphere, the potential temperature, θ, is an increasing function of height z. In this case there is a one-to-one correspondence between θ and z and we can use θ as a vertical coordinate instead of z. Then, $D/Dt = \partial/\partial t + u(\partial/\partial x) + v(\partial/\partial y) + \dot{\theta}(\partial/\partial\theta)$, where $\dot{\theta} = D\theta/Dt$. Thus in isentropic coordinates (x, y, θ), $\dot{\theta}$ plays the role that w plays in height coordinates. One advantage of this formulation is that for adiabatic motion, $\dot{\theta} = 0$, the effects of vertical advection do not appear explicitly in the equations. See Chapter 10, for further details.

1.7 Sigma coordinates

A major disadvantage of formulations with pressure or a function of pressure as the vertical coordinate is the uncertainty involved in prescribing the surface boundary condition on velocity. For example, in contrast to the condition $w = 0$ at $z = 0$, appropriate for motion over level ground, we need to impose a condition on ω at some pressure level $p = p_1$, say. From (1.9) and the hydrostatic equation $(dp/dz = -\rho g)$, $\omega = (\partial p/\partial t + \mathbf{u}_h \cdot \nabla p) - \rho g w$. Thus, $w = 0$ at $z = 0$ corresponds with $\omega = \partial p/\partial t + \mathbf{u}_h \cdot \nabla p$ at $z = 0$, but the location of "the ground" in pressure coordinates cannot be determined. One way out of this difficulty is to use 'sigma' coordinates, (x, y, σ), where $\sigma = p(x, y, z)/p_s(x, y)$, p_s being the surface pressure. Then the surface is always at the level $\sigma = 1$ and the 'top' of the atmosphere is at $\sigma = 0$. However, the dynamical equations are then more complicated and interpolation procedures

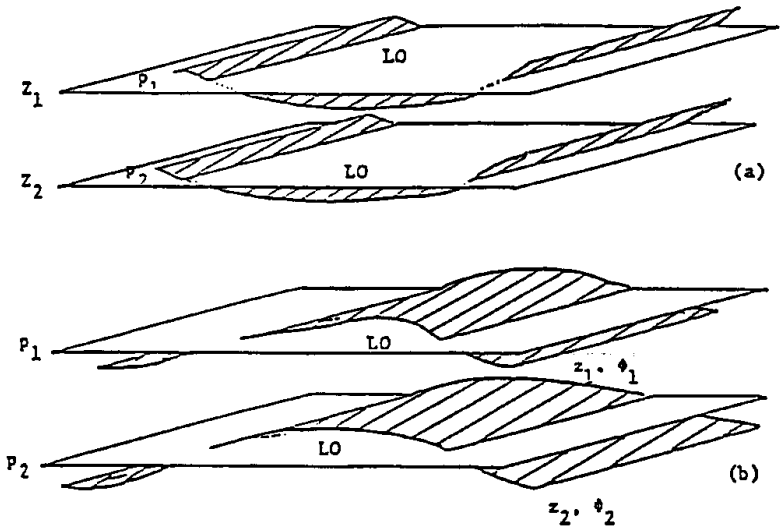

Figure 1.1: (a) Two isobaric surfaces in a low pressure trough as they might appear in (x, y, z) coordinates and (b) as the corresponding geopotential surfaces might appear in (x, y, p) coordinates. In the figure, $z_1 > z_2$, $\phi_1 > \phi_2$ and $p_2 > p_1$. Note that, since pressure decreases with height, the areas of low pressure on z_1 and z_2 in (a) correspond with the region of low geopotential on p_1 and p_2, respectively, in (b).

are necessary for converting between σ and p or z. Sigma coordinates are used widely for operational numerical weather prediction (NWP) models, but rather less for research or illustrative purposes.

Chapter 2

SMALL-AMPLITUDE WAVES IN A STABLY-STRATIFIED ROTATING ATMOSPHERE

In[1] a stably-stratified atmosphere at rest, the pressure $p_o(z)$ and density $\rho_o(z)$ are in hydrostatic equilibrium and related by the formula

$$\frac{dp_o}{dz} = -g\rho_o. \tag{2.1}$$

We consider small-amplitude perturbations to such an atmosphere. The most general equations for inviscid, isentropic motion are

$$\frac{D\mathbf{u}}{Dt} + f\mathbf{k} \wedge \mathbf{u} = -\frac{1}{\rho}\nabla p_T - g\mathbf{k}, \tag{2.2}$$

$$\frac{1}{\rho}\frac{D\rho}{Dt} + \nabla \cdot \mathbf{u} = 0, \tag{2.3}$$

$$\frac{Ds}{Dt} = 0, \tag{2.4}$$

and

$$p = \rho RT, \tag{2.5}$$

in standard notation (see DM). The specific entropy s is related to the potential temperature θ through the formula

$$s = c_p \; ln \; \theta + \text{constant} = \phi + \text{constant}, \tag{2.6}$$

[1]Based on lectures by J. S. A. Green, formerly of Imperial College, London.

where

$$\phi = ln\ \theta. \tag{2.7}$$

Various parameters characterizing the basic state of the atmospheric are the *Brunt-Väisälä frequency*, or *buoyancy frequency, N*; the *sound speed* c_o; and the *density scale height*, H_s. These quantities are defined by the formulae:

$$N^2 = g\frac{d\phi_o}{dz} = \frac{g}{\theta_o}\frac{d\theta_o}{dz}, \tag{2.8}$$

$$c_o^2 = \gamma R T_o = \gamma\frac{p_o}{\rho_o} \tag{2.9}$$

and

$$\frac{1}{H_s} = -\frac{1}{\rho_o}\frac{d\rho_o}{dz} = \frac{g}{RT_o} + \frac{1}{T_o}\frac{dT_o}{dz}. \tag{2.10}$$

Here is γ the rate of specific heats c_p/c_v.

For algebraic simplicity we assume two-dimensional perturbations ($\partial/\partial y \equiv 0$) to the basic state of rest, characterized by a subscript $'o'$. The small-amplitude assumption implies that $\mathbf{u}\cdot\nabla << \partial/\partial t$ in D/Dt, except when acting on a basic state quantity. Denoting $p = p_0 + p'$ etc., and *omitting primes*, we obtain from (2.1) - (2.7) the following equations for perturbed quantities:

$$u_t - fv + [p/\rho(z)]_x = 0, \tag{2.11}$$

$$v_t + fu = 0, \tag{2.12}$$

$$n_4 w_t + p_z/\rho_o + g\rho/\rho_o = 0, \tag{2.13}$$

$$u_x + w_z + n_1\frac{1}{\rho_o}\frac{d\rho_o}{dz}w + n_2\frac{\rho_t}{\rho_o} = 0, \tag{2.14}$$

$$\phi_t + w\phi_{oz} = 0, \tag{2.15}$$

$$\phi = \frac{p}{\gamma p_o} - \frac{\rho}{\rho_o} = \frac{p}{\rho_o c_o^2} - \frac{\rho}{\rho_o}. \tag{2.16}$$

The n_i are tracer quantities, allowing us to follow the terms they multiply through the subsequent analysis; at a later stage these tracers will be set

equal to either unity or zero. Eliminating ρ from (2.13) using (2.16) and (2.10) gives

$$n_4\omega_t + \left(\frac{p}{\rho_o}\right)_z \underbrace{-\frac{p}{\rho_o}\frac{1}{H_s} + g\left(\frac{p}{\rho_o c_o^2} - \phi\right)} = 0. \tag{2.17}$$

The terms grouped with braces may be combined using (2.10) to give, with tracer n_3:

$$-(N^2/g)(p/\rho_o)n_3$$

Eliminating ρ from (2.14) using (2.16) and (2.10) gives

$$u_x + w_z - n_1\frac{w}{H_s} + \frac{n_2}{c_o^2}\left[\frac{p}{\rho_o}\right]_t - n_2\phi_t = 0. \tag{2.18}$$

Writing[2] $\sigma = g\phi$ $(= g\theta'/\theta_o)$ and $P = p/\rho_o$, Eqs. (2.11 - 2.18) become

$$u_t - fv + P_x = 0, \tag{2.19}$$

$$v_t + fu = 0, \tag{2.20}$$

$$n_4 w_t + P_z - n_3\frac{N^2}{g}P - \sigma = 0, \tag{2.21}$$

$$u_x + w_z - n_1\frac{w}{H_s} + \frac{n_2}{c_o^2}P_t - \frac{n_2}{g}\sigma_t = 0, \tag{2.22}$$

$$\sigma_t + N^2 w = 0. \tag{2.23}$$

We investigate travelling-wave solutions of the form

$$(u, v, w, \sigma, P) = (\hat{u}(z), \ldots)e^{i(kx-\omega t)}, \tag{2.24}$$

to Eqs. (2.19-2.23)[3]. Substitution leads to a set of ordinary differential equations for the vertical structure of the waves, characterized by the functions $\hat{u}(z)$ etc.. Thus

$$-i\omega\hat{u} - f\hat{v} + ik\hat{P} = 0, \tag{2.25}$$

[2]Note σ is not equal to buoyancy force; see Ex. (1.1).

[3]Solutions of this form are anticipated because the equations have coefficients which don't depend on x and t.

$$-i\omega\hat{v} + f\hat{u} = 0, \tag{2.26}$$

$$-i\omega n_4\hat{w} + \hat{P}_z - (N^2/g)n_3\hat{P} - \hat{\sigma} = 0, \tag{2.27}$$

$$ik\hat{u} + \hat{w}_z - n_1\frac{\hat{w}}{H_s} - i\omega n_2\left(\frac{\hat{P}}{c_o^2} - \frac{\hat{\sigma}}{g}\right) = 0, \tag{2.28}$$

$$-i\omega\hat{\sigma} + N^2\hat{w} = 0. \tag{2.29}$$

Equations (2.25, 2.26 and 2.29) give

$$\hat{u} = \frac{k\omega}{\omega^2 - f^2}\hat{P}\,, \quad \hat{v} = -\frac{ikf}{\omega^2 - f^2}\hat{P}, \quad \text{and} \quad \hat{\sigma} = \frac{N^2}{i\omega}\hat{w}, \tag{2.30}$$

and using these equations, (2.27) and (2.28) give

$$\frac{d\hat{w}}{dz} + \left(\frac{N^2}{g}n_2 - \frac{1}{H_s}\right)\hat{w} + i\omega\left(\frac{k^2}{\omega^2 - f^2} - \frac{n_2}{c_o^2}\right)\hat{P} = 0, \tag{2.31}$$

$$\left(\frac{d}{dz} - \frac{N^2}{g}n_3\right)\hat{P} - i\omega\left(n_4 - \frac{N^2}{\omega^2}\right)\hat{w} = 0. \tag{2.32}$$

Finally, eliminating[4] $\hat{P}$ we obtain the single equation for $\hat{w}(z)$,

$$\left(\frac{d}{dz} - \frac{N^2}{g}n_3\right)\left[\left(\frac{k^2}{\omega^2 - f^2} - \frac{n_2}{c_0^2}\right)^{-1}\left(\frac{d}{dz} + \frac{N^2}{g}n_2 - \frac{n_1}{H_s}\right)\right]\hat{w} \quad - \\ (\omega^2 n_4 - N^2)\hat{w} = 0. \tag{2.33}$$

This is a homogeneous, second-order, ordinary differential equation for $\hat{w}(z)$. When solved, $\hat{P}(z)$ can be determined from (2.31) and the other quantities can be obtained from (2.30).

If the boundary conditions on $\hat{w}(z)$ are homogeneous, for example $\hat{w}(0) = 0$, then (2.33) must be solved as an eigenvalue problem. It is usual to regard k as given, in which case the eigenvalue problem is to find values of $\omega(k)$ for which nontrivial solutions to (2.33) exist, and to determine the corresponding eigenfunctions, $\hat{w}(z; k, \omega(k))$.

In general, the quantities N^2, c_o^2 and H_s all vary with z and in this case the eigenvalue problem is difficult to solve, at least analytically. However, for

[4]These equations can be written in the operator form $L_1 + A(z)\hat{P} = 0$, $B(z)\hat{w} + L_2\hat{P} = 0$ whereupon elimination of $\hat{P}$ leads to $\left[L_2(A^{-1}L_1) - B(z)\right]\hat{w} = 0$.

an isothermal atmosphere, these quantities are all constants (Ex. 2.1) and sinusoidal or exponential solutions of (2.33) are then possible. Henceforth in this course we assume an *isothermal* atmosphere, except where otherwise stated.

First we consider waves in an unbounded region of fluid assuming that all terms are important, i.e., $n_i \equiv 1$. Note that solutions of (2.33) exist in the form

$$\hat{w}(z) \exp\left(imz + \frac{z}{2H_s}\right), \tag{2.34}$$

provided that

$$\frac{\omega^4}{c_0^2} - \omega^2\left(k^2 + m^2 + \frac{1}{4H_s^2} + \frac{f^2}{c_0^2}\right) + N^2k^2 + f^2\left(m^2 + \frac{1}{4H_s^2}\right) = 0, \tag{2.35}$$

obtained by substituting (2.34) into (2.33) and using (2.35). Equation (2.35) is the *dispersion relation* for small amplitude waves. Referring to (2.24) and (2.34) we see that each of the perturbation quantities u, v, w, σ, P, varies in proportion to $\hat{w}(z) \propto exp\left[i(kx + mz - \omega t) + z/2H_s\right]$, or

$$\exp\left[i(\mathbf{k}\cdot\mathbf{x} - \omega t\right] \exp\left[z/2H_s\right], \tag{2.36}$$

where $\mathbf{k} = (k, m)$ [*here, it is not the unit vector in the vertical!*]. Thus the planes $\mathbf{k}\cdot\mathbf{x} =$ constant are surfaces of constant phase; in particular the wave 'crests' and 'troughs' are planes oriented normal to the vector $\mathbf{k}$ as shown in Fig. 2.1. The wavelength is the distance in the direction of $\mathbf{k}$ over which $\mathbf{k}\cdot\mathbf{x}$ increases (or decreases) by 2π; i.e., $\lambda = 2\pi/\left|\mathbf{k}\right|$.

Note that the wave amplitude is appreciably uniform over height ranges small compared with H_s, but increases exponentially as $z \to \infty$; this is related to the exponential decrease of the density with height.

Using the result (2.35), the dispersion relation can be displayed graphically as shown in Fig. 2.2. For waves propagating in the x-direction, k is real and therefore k^2 must be positive and only the upper right quadrant of the diagram is relevant. We consider now the various possible wave modes.

Geostrophic motion, $\omega = 0$.

Equations (2.11-2.18) have a steady solution with $\partial/\partial t \equiv 0$ (equivalent to $\omega = 0$). In this solution, Eqs. (2.11-2.18) give

$$-fv = -p_x/\rho_o, \; u = 0, \text{ and } p_z/\rho_o = \sigma.$$

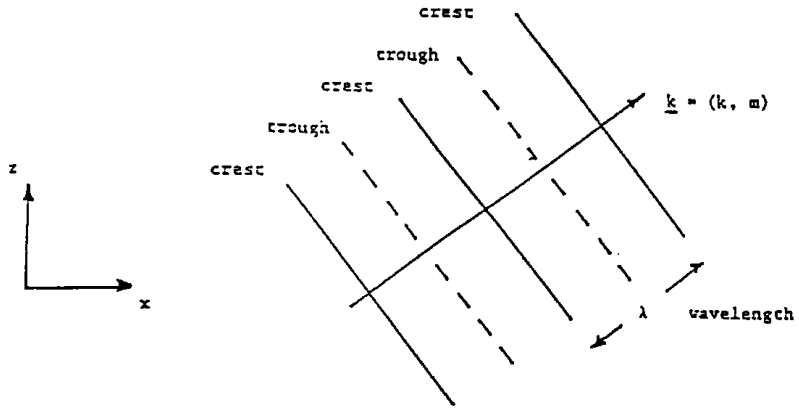

Figure 2.1: Wave crests and troughs of an unbounded plane wave proportional to (2.36).

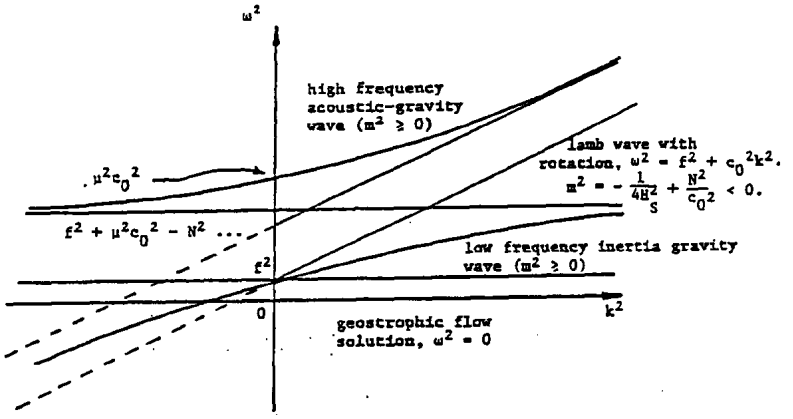

Figure 2.2: Dispersion relation in (k^2, ω^2) space.

Thus air parcels are displaced in the y-direction ($v \neq 0$) and the solution, which holds whether or not N^2, c_o^2 and H_s are constant, corresponds with a thermal wind in this direction.

Inertia-gravity waves: $\omega << (k^2 + m^2)c_o^2$

In this situation, (2.35) gives

$$\omega^2 \approx \frac{N^2k^2 + f^2(m^2 + 1/4H_s^2)}{k^2 + m^2 + 1/4H_s^2 + f^2/c_o^2}. \tag{2.37}$$

Note that in the atmosphere, at middle latitudes, $f \sim 10^{-4}$ s^{-1}, $N \sim 10^{-2}$ s^{-1}, $H_s \sim 10^4$ m and $c_0 \sim 10^3/3$ ms^{-1}, in which case $\varepsilon^2 = f^2/N^2 = 10^{-4} << 1$. Also, $1/4H_s^2 + f^2/c_0^2 = (1 + 4H_s^2 f^2/c_0^2)/4H_s^2$ and the last term in parentheses is $\sim 4 \times 10^{-5}$ and can be neglected.

Equation (2.37) indicates that stratification and rotation are equally important when

$$N^2k^2 \sim f^2(m^2 + 1/4H_s^2).$$

Assuming that $m^2 \leq 1/4H_s^2$, the criterion is $k^2 \sim f^2/4N^2H_s^2$, i.e., $\lambda \sim \ \lambda_o = 4\pi N H_s/f \approx 12{,}000$ km in the atmosphere. Thus for $\lambda << \lambda_o$, rotation effects are negligible unless $|m|$ is sufficiently large, implying a vertical wavelength that is much less than H_s.

With the assumption that $k >> (m^2 + 1/4H_s^2)^{1/2}$, then (2.37) implies that $|m| \leq N$ and Eqs. (2.30) show that

$$\hat{v} \sim \varepsilon\hat{u}, \ \hat{P} \sim (\omega/k)\hat{u} \ \text{ and } \ \hat{\sigma} \sim (N^2/\omega)\hat{w}. \tag{2.38}$$

With the variation (2.36), (2.32) gives

$$i\omega(1 - N^2/\omega^2) = (1/2H_s + im - N^2/g)\hat{P} = \mu\hat{P}, \text{ say,}$$

and since

$$2N^2H_s/g \sim 1.6 \times 10^{-1}, \ |u| \sim (m^2 + 1/4H_s^2)^{1/2},$$

then

$$(m^2 + 1/4H_s^2)^{1/2}\hat{w} \sim (k^2/\omega)\hat{P}. \tag{2.39}$$

It follows that

$$\hat{\sigma} \sim \frac{N^2}{\omega^2}k^2(m^2 + 1/4H_s^2)^{-1/2}\hat{P},$$

and finally

$$\frac{\hat{w}}{\hat{u}} \sim \frac{k}{(m^2 + 1/4H_s^2)^{1/2}} >> 1 \tag{2.40}$$

Thus, in this limit, the wavenumber vector is nearly horizontal ($|k| >> |m|$) and the motion is essentially an oscillation in the vertical plane ($w >> u, \ w >> v$) as indicated in Fig. (2.3); i.e., the waves are *transverse*.

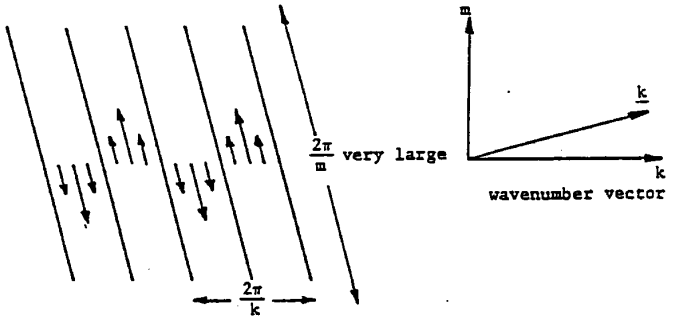

Figure 2.3: Particle motions in an inertial gravity wave with $k^2 >> m^2 + 1/4H_s^2$.

In this limit also, the vertical acceleration due to the buoyancy term is much greater than that due to the pressure gradient, i.e., from (2.27) and (2.29),

$$\frac{\hat{P}_z - (N^2/g)\hat{P}}{\hat{\sigma}} = 1 - \frac{\omega^2}{N^2} = \frac{(m^2 + 1/4\mathrm{H_s^2})(1 - f^2/N^2)}{\mathrm{k^2{+}m^2{+}1/4H_s^2}} << 1,$$

whereas

$$\frac{\hat{w}_t}{\hat{\sigma}} \sim \left| \frac{i\omega(k^2/\omega)\,(m^2 + 1/4\mathrm{H_s^2})^{-1/2}}{\mathrm{k^2(m^2{+}1/4H_s^2)^{-1/2}}} \right| \sim 1.$$

Thus the vertical acceleration of a displaced air parcel is due to its buoyancy and the motion is essentially a gravity wave in which the displacement of isopycnal (constant-density) surfaces supplies the restoring force.

Ultra-long waves, $k \to 0$.

In this limit, $\omega \to f$. Then only Coriolis forces are important and the motion is purely horizontal. Neither buoyancy nor pressure forces are significant. Such waves are called *inertial* waves. Pure inertial waves are regarded often as a meteorological curiosity (Holton, 1992, pp64-65, §3.2.3), although they may be important in atmospheric tidal motions. They are certainly observed in the oceans. In addition, since their phase speed $c_p = \omega/k = f/k$ is large, they may be a computational nuisance. Nevertheless, *inertial effects* are observed in the atmosphere (see DM, Chapter 11). When both rotation and stratification are important, though not necessarily comparable in

magnitude, the waves are called inertial-gravity waves. In the atmosphere, gravity waves usually have horizontal wavelengths 10 km and may be excited, for example, by airflow over orography, by convection penetrating a stably stratified air layer, or by shearing instability.

Acoustic waves, $\omega^2 >> N^2, f^2$.

In this case, (2.35) gives

$$\omega^2 \approx (k^2 + m^2 + 1/4H_s^2)c_0^2.$$

Let us consider the special case where $mH_s >> 1$. Then $(\hat{u}, \hat{w}) \approx \omega^{-1}(k, m)\hat{P}$; i.e., the particle motions are in the direction of the wave $\mathbf{k}$, and are associated with negligible entropy change, $\hat{\phi} \approx 0$. These are well known properties of acoustic waves; the waves are longitudinal and the phase speed $c_p = \omega/|\mathbf{k}| \approx c_0$ is large. Mechanisms of excitation include lightening discharges and aeroplane noise (a rumble when clouds are around).

Lamb waves, $\mathbf{w = 0}$.

Equation (2.33) has the trivial solution $\hat{w} = 0$. However, this does not lead to a trivial solution of the complete system of equations (2.25-2.29). Indeed, it is easily verified that $\hat{w}(z) = 0$ is a solution of (2.31), provided that $\omega^2 = f^2 + k^2c_o^2$, and of (2.32) provided that $\hat{P}(z) = \hat{P}(0)\exp(N^2z/g)$. Furthermore, using (2.30), these solutions correspond to $\hat{u} \approx (k/\omega)\hat{P}$, $\hat{v} \approx 0$ and $\hat{\sigma} \equiv 0$. This solution is a so-called *Lamb wave*, modified slightly by rotation. Its existence requires the ground ($z = 0$) to be flat, so that $\hat{w}(0) = 0$. The pressure perturbation in the Lamb wave is essentially supported by the ground. See Ex. (2.6).

2.1 Boundary waves

The upper and lower limits of the atmosphere, or a layer of it, are defined by boundary conditions in mathematical formulations. These conditions give additional constraints on the possible wave types and their scales. An example is the free-surface boundary condition. The stable boundary separating the troposphere and stratosphere, *the tropopause*, is sometimes modelled as a rigid lid on which $w = 0$. Alternatively it may be modelled as a free surface on which the total pressure is a constant. Suppose the total pressure

along some layer of particles is unaffected by the motion, even though the individual particles may move. An example is a water surface. If the surface is at $h + \zeta(x,t)$, where h is a constant, the condition is expressed by

$$\frac{Dp_{_T}}{Dt} = 0 \text{ at } z = h + \zeta.$$

The linearized version of this condition is

$$\frac{\partial p}{\partial t} + w\frac{dp_o}{dz} = \frac{\partial p}{\partial t} - \rho_o w g = 0 \text{ at } z = h.$$

For waves proportional to (2.36) this condition gives $\hat{P} = -(g/i\omega)\hat{w}$, and using (2.31), we obtain

$$\frac{d\hat{w}}{dz} + \left[\left(\frac{N^2}{g} + \frac{g}{c_o^2}\right) n_2 - \frac{n_1}{H_s} - \frac{gk^2}{\omega^2 - f^2}\right] \hat{w} = 0 \text{ at } z = h. \tag{2.41}$$

The solution of (2.33) subject to (2.41) is straightforward, but no essential features are omitted if we:

(a) neglect the stratification; i.e., set $N^2 = 0$ and omit the σ equation (Eq. 2.29, and

(b) assume the motion to be hydrostatic, $w_t << g$; i.e., set $n_4 = 0$ (this assumption is valid provided that the waves are long enough), and

(c) assume there is no coupling between pressure and density in the continuity equation[5]; i.e., set $n_2 = 0$.

Then Eqs. (2.25-2.28) become

$$\begin{aligned} -i\omega\hat{u} - f\hat{v} + ik\hat{P} &= 0, \\ -i\omega\hat{v} + f\hat{u} &= 0, \\ \hat{P}_z &= 0, \\ ik\hat{u} + \hat{w}_z - \hat{w}/H_s &= 0 \end{aligned}$$

and (2.33) becomes

$$\frac{d}{dz}\left[\frac{d}{dz} - \frac{1}{H_s}\right] \hat{w} = 0 \tag{2.42}$$

[5]This suppresses acoustic waves; see later.

The solution of (2.42) for motion over level ground (i.e., with $\hat{w}(0) = 0$) is

$$\hat{w}(z) = W\left[\exp\left(z/H_s\right) - 1\right], \tag{2.43}$$

where W is a constant. Note that $\hat{u}$, $\hat{v}$ and $\hat{P}$ are related to W and, as $\hat{P}_z = 0$, $\hat{P}$ is a constant. If this solution satisfies (2.41) also, it is easy to verify that

$$\omega^2 = f^2 + gH_sk^2\left[\exp(h/H_s) - 1\right]. \tag{2.44}$$

The solution corresponding with (2.43) and (2.44) includes the case of surface waves in a liquid, for which h/H_s is small[6], and gives also a definite 'surface wave' solution for a deep gas, where h/H_s is large and the mass of air above h is very small. Thus, in a deep atmosphere, the 'free-surface wave' travels with the approximate phase speed $\omega/k \approx \sqrt{(gH_s)}$, unless the wavelength is extremely large, in which case Coriolis effects are important and $\omega/k \approx f/k$. Coriolis effects are comparable with gravitational effects if $k \sim f/\sqrt{(gH_s)}$, i.e. $\lambda \sim 2\pi\sqrt{(gH_s)}/f$. At latitude 45°, $f \sim 10^{-4}$ s^{-1} and when $T = 275$ K, $\sqrt{(gH_s)} \sim 281$ m s^{-1} giving $\lambda \sim 1.8 \times 10^4$ km, which is more than one half of the distance around the latitude circle at 45°, i.e., $2\pi \times 6370 \times \sin 45 = 2.8 \times 10^4$ km. Thus the gravitational term is always important.

Although not an acoustic wave, the free surface wave has a phase speed comparable with the speed of sound c_o, and may be a computational nuisance.

2.2 The effects of shear

At a later stage we shall consider the effects of shear in detail. For the present we note that if shear is included, the foregoing solutions are significantly modified. Briefly,

- **acoustic waves** are refracted by superimposed shear; enhanced downwind audibility results from the convergent refraction of sound waves, usually due to wind shear, but, occasionally, temperature variations may play a role also.

- **gravity waves** may be severely modified by shear. The refraction effect is considerable and leads to the total reflection of some (shorter) components, which may be trapped in channels as well marked trains of lee waves downstream of mountains (see Chapter 3). In certain situations waves may be absorbed also.

[6]Note that for $h/H_s << 1$, (2.44) reduces to $\omega^2 = f^2 + ghk^2$, which is the dispersion relation for inertia-gravity waves on a shallow water layer (see DM, Chapter 11).

- where vorticity gradients are large, gravity waves may grow spontaneously by Kelvin- Helmholtz instability, giving rise to *billows or clear air turbulence* (CAT); see Chapter 5.

2.3 The energy equation

The kinetic energy equation in any dynamical problem is normally[7] derived by taking the scalar product of the velocity with the momentum equation. Thus, in the context of small-amplitude waves studied above, it is obtained by multiplying (2.11), (2.12) and (2.17) by u, v, and w, respectively, and adding, i.e.,

$$\frac{1}{2}(u^2+v^2+n_4w^2)_t + u\left(\frac{p}{\rho_o}\right)_x + w\left(\frac{p}{\rho_o}\right)_z - n_3\frac{pw}{\rho_o}\frac{N^2}{g} - gw\phi = 0. \quad (2.45)$$

Other components of the total energy are obtained by multiplying (2.18) by p/ρ_o, i.e.,

$$\frac{p}{\rho_o}(u_x+w_z) - \frac{n_1}{H_s}\frac{pw}{\rho_o} + n_2\frac{p}{\rho_o}\left(\frac{p_t}{\rho_o c_o^2} - \phi_t\right) = 0. \quad (2.46)$$

Adding (2.45) and (2.46), and using (2.15) and the fact that $\phi_{oz} = N^2/g$, we obtain the *total energy equation*,

$$\frac{\partial}{\partial t}\frac{1}{2}\left[(\mathrm{u}^2+\mathrm{v}^2+\mathrm{n}_4\mathrm{w}^2) + \mathrm{n}_2\frac{p^2}{\rho_o^2 c_o^2} + \frac{g^2\phi^2}{N^2}\right] +$$
$$\left(\frac{up}{\rho_o}\right)_x + \left(\frac{wp}{\rho_o}\right)_z - \frac{n_1}{H_s}\frac{pw}{\rho_o} + \frac{pw}{\rho_o}\frac{N^2}{g}(n_2-n_3) = 0\ . \quad (2.47)$$

This may be written more concisely as

$$\rho_o\frac{\partial E}{\partial t} = -\nabla\cdot F + (n_1-1)\frac{pw}{H_s} + pw\frac{N^2}{g}(n_3-n_2)\,, \quad (2.48)$$

where

$$E = \frac{1}{2}\left[(\mathrm{u}^2+\mathrm{v}^2+\mathrm{n}_4\mathrm{w}^2) + \mathrm{n}_2\frac{p^2}{\rho_o^2 c_o^2} + \frac{g^2\phi^2}{N^2}\right], \quad (2.49)$$

[7] An exception is the derivation for quasi-geostrophic motion which starts from the potential vorticity equation (see Chapter 6).

is the *total wave energy* per unit mass, and $\mathbf{F} = (pu, 0, pw)$ can be interpreted as the flux of wave energy per unit mass. Note that the energy equation does not include f and recall that Coriolis forces do no work (see DM, p.21). Note also that when $n_1 = n_2 = n_3 = 1$, the second and third terms on the right of (2.48) are zero and the equation then shows that *the local rate of change of total wave energy equals the convergence of wave energy flux.*

In any particular type of wave motion, the energy will fluctuate between kinetic energy and some other energy form. Pure wave types are:

(a) *gravity waves*, in which the energy is stored in *potential energy* form $\frac{1}{2}\sigma^2/N^2$, when not in kinetic energy form, and

(b) *compressible*, or acoustic waves, in which the energy is stored as *internal energy* $\frac{1}{2}p^2/\rho_o^2\, c_o^2$, when not in kinetic energy form.

Inertia-gravity waves undergo energy conversions similar to pure gravity waves. In general, waves of the *mixed gravity-acoustic* type are such that kinetic energy is converted partly into potential energy and partly into internal energy. However, in this case, the interpretations of $\frac{1}{2}\sigma^2/N^2$ as potential energy and $\frac{1}{2}p^2/\rho_o^2\, c_o^2$ as internal energy are not strictly correct.

2.4 Simplified solutions and filtered equations

If the tracers n_i are retained and the expression $\hat{w}(z) \propto exp\,[(im + n_1/2H_s)\, z]$, is substituted into (2.33) instead of (2.34), we obtain, after using (2.54) and a little algebra, the dispersion relation

$$m^2 + \frac{n_1^2}{4H_s^2} + \frac{N^2}{g}\left[im(n_3 - n_2) + n_2(n_3 - 1)\frac{N^2}{g} + \frac{1}{H_s}\left\{n_2 - \tfrac{1}{2}n_1(n_2 + n_3)\right\}\right] + (n_4\omega^2 - N^2)\frac{k^2}{\omega^2 - f^2} - n_2 n_4 \frac{\omega^2}{c_o^2} = 0. \tag{2.50}$$

The consequences of omitting certain terms in the equations of motion (2.11, 2.12, 2.15, 2.17 and 2.18) may now be investigated. It is desirable that any approximation yields a consistent energy equation.

2.5 'Sound-proofing' the equations

Examination of (2.47) suggests that setting $n_2 = 0$ in (2.18) will remove the acoustic mode from the equations. Equation (2.50) then gives

$$\omega^2 = \frac{N^2k^2 + f^2\left(m^2 + \frac{n_1^2}{4H_s^2} + n_3\frac{N^2}{g}\left(im - \frac{n_1}{2H_s}\right)\right)}{n_4k^2 + m^2 + \frac{n_1^2}{4H_s^2} + n_3\frac{N^2}{g}\left(im - \frac{n_1}{2H_s}\right)}, \tag{2.51}$$

which, when $n_1 = n_4 = 1$, differs from the dispersion relation for inertia-gravity waves (2.37), only in respect of the terms involving n_3. But (2.51) shows that ω^2 is complex, implying that ω is complex, and hence there exist exponentially growing solutions (c/f (2.36) with ω complex)! Such solutions must have an energy source, although none is available in the unapproximated system. Equation (2.48) shows that with $n_2 = 0$, there is, indeed, an energy source represented by the last term, unless $n_3 = 0$ also. Hence, to filter sound waves from the system of equations (2.11-2.18), we must take both n_2 and n_3 to be zero to preserve energetic consistency.

Note that sound waves are filtered out also by letting $c_o^2 \to \infty$. However this device is clumsy and inaccurate, particularly when applied to (2.54); recall from Ex. (2.2) that

$$(-g/c_o^2)/(1/H_s) = gH_s/c_o^2 = O(1)!$$

Setting $n_2 = n_3 = 0$ in (2.50) instead of $n_2 = n_3 = 1$ results only in the term ω^2/c_o^2 being omitted. The condition for this term to be negligible is complicated; the worst situation is clearly for high frequency waves when ω^2 is large, in which case the term is negligible provided that $\omega^2 c_o^2 << k^2 + m^2 + (4H_s^2)^{-1}$, equivalent to $c_p << c_o$; see Eq. (2.35). The frequency of the inertia-gravity wave is given then by

$$\omega^2 = f^2 + \frac{(N^2 - f^2)k^2}{k^2 + m^2 + 1/4H_s^2}, \tag{2.52}$$

which agrees closely with accurate solutions of (2.35) under typical conditions.

When $n_2 = 0$, the Lamb wave no longer exists when $\hat{w} = 0$, since (2.31) then gives $\hat{P} = 0$. This is a computational advantage, but the free surface wave still exists if the surface condition (2.41) is used. Putting $n_2 = n_3 = 0$ in the full nonlinear equations gives the anelastic system of equations (see Chapter 1). Sound waves are absent and the whole flow is instantly aware of any adjustment to the pressure field. This approximation may be used for practically all meteorological problems, including phenomena in which the pressure is nonhydrostatic, e.g., cumulonimbus convection. If the vertical scale of the motion is much less than the density scale height, i.e., $mH_s >> 1$, then (2.52) becomes

$$\omega^2 = f^2 + \frac{(N^2 - f^2)k^2}{k^2 + m^2}, \tag{2.53}$$

which is identical with the dispersion relation for waves in a Boussinesq liquid (see Ex. 2.10).

2.6 The hydrostatic approximation

In many atmospheric situations, the pressure is very close to its hydrostatic value. In the foregoing analysis, pressure is hydrostatic if $n_4 = 0$ (this eliminates Dw/Dt, or in linearized form $\partial w/\partial t$, from the vertical momentum equation). Now, with $n_1 = n_2 = n_3 = 1$, the dispersion relation (2.50) gives

$$-n_4\frac{\omega^4}{c_o^2} + \omega^2\left(m^2 + \frac{1}{4H_s^2} + n_4\frac{f^2}{c_o^2} + n_4k^2\right) - N^2k^2 - f^2\left(m^2 + \frac{1}{4H_s^2}\right) = 0.$$

Clearly, the terms involving n_4 are negligible if

(i) $\omega^2/c_o^2 << m^2 + 1/4H_s^2$, and

(ii) $\omega^2 << N^2$.

The first of these conditions is typically well satisfied for inertia-gravity waves; however the second is more discriminating. If a layer is close to adiabatic, then $N_2 \approx 0$, and the dispersion relation becomes $\omega^2(m^2 + n_4k^2 + 1/4H_s^2) = f^2(m^2 + 1/4H_s^2)$, requiring that $k^2 << m^2$. But, since for finite N^2,

$$\omega^2 = (N^2k^2 + f^2(m^2 + 1/4H_s^2))/(n_4k^2 + m^2 + 1/4H_s^2),$$

the condition $k^2 << m^2$ implies that $\omega^2 << N^2$ and hence the hydrostatic approximation may be considered appropriate whenever it is satisfied. In other words, the hydrostatic approximation is valid for waves whose horizontal wavelength is much larger than the vertical wavelength. It is important to note that the magnitude of $g^{-1}Dw/Dt$ is irrelevant to the usefulness of the hydrostatic approximation for finding the acceleration. Even if this quantity is small, the dynamics will be incorrectly modelled by its neglect if the motion is in tall narrow columns ($k^2 >> m^2$).

The condition $k^2 << m^2$ is usually well satisfied for large scale atmospheric motions and the hydrostatic approximation is used exclusively in 'primitive equation' (PE) numerical weather prediction (NWP) models.

2.7 Sound-proofed hydrostatic approximation

If we formally set $n_1 = 1$ and $n_2 = n_3 = n_4 = 0$, valid under the same conditions (i) and (ii) for the hydrostatic approximation alone, the dispersion relation gives

$$\omega^2 = f^2 + N^2k^2/(m^2 + 1/4H_s^2).$$

The Lamb wave now disappears (c/f Ex. 2.9) as it does when the other acoustic waves are eliminated. However, the free surface wave still exists and leads to a spurious fast moving wave. It is filtered out by using a rigid-lid condition. A primitive equation, numerical weather prediction model can be devised for the set of equations with $n_1 = 1$ and $n_2 = n_3 = n_4 = 0$ together with a rigid upper boundary condition.

2.8 Variation of mean density with height; the equivalent incompressible atmosphere

The upward decrease of mean density that distinguishes between continuity of volume and mass is represented by the term in n_1 and appears in the multiplier $\exp(z/2H_s) \propto \rho_o^{-1/2}$ in $\hat{w}$ etc.. Over tropospheric depths this factor is significant, but elsewhere n_1 appears only in the combination $m^2 + n_1/4H_s^2$ and then it is often negligible. For example, if $m = \pi/H_s$, $(4H_s^2)^{-1} = \frac{1}{4}(m/\pi)^2 \approx m^2/40$. Thus in many applications, particularly where the vertical length scale of the motion is not large, the density variation can be neglected by setting $n_1 = 0$ as long as the $\rho_0^{1/2}$ factor is included implicitly. A prediction of u, for example, obtained from the incompressible (Boussinesq) model should then be compared with $(\rho_o/\rho_s)^{1/2}u$ observed in the (compressible) atmosphere, where $\rho_s = \rho_o(0)$.

2.9 Geostrophic motion

The solution of (2.35) corresponding with $\omega = 0$ is independent of the values of $n_1 \to n_4$, but the more general "quasi-geostrophic" solutions are not. If we are interested only in the slowly-moving, nearly geostrophic waves, we can omit sound waves and suppose that the pressure is hydrostatic, i.e., put $n_2 = n_3 = n_4 = 0$.

Exercises

(1.1) Neglecting friction effects, the momentum equation may be written as

$$\frac{D\mathbf{u}}{Dt} + f\mathbf{k} \wedge \mathbf{u} = -\frac{1}{\rho}\nabla p\prime + \ g\left(\frac{\rho_0 - \rho}{\rho}\right)\mathbf{k}.$$

Show that

$$-\frac{1}{\rho}\frac{\partial p\prime}{\partial z} = -\,c_p\theta\frac{\partial}{\partial z}(\pi - \pi_0) - W$$

and

$$g\left(\frac{\rho_0 - \rho}{\rho}\right) = g\left(\frac{\theta - \theta_0}{\theta_0}\right) + W,$$

where θ is the potential temperature, π is the Exner function and a subscript 'o' denotes a horizontal average or reference state value. Note that although

$$W = g\frac{\theta}{\theta_0}\left[\left(\frac{\pi}{\pi_0}\right)^{1-1/\kappa} - 1\right],$$

the terms on the RHS can be interpreted as the 'perturbation pressure gradient' and 'buoyancy force' respectively, *only if* the horizontal pressure deviation is small enough for W to be negligible. This is not valid, for example, in a tornado (Leslie and Smith, 1978).

(1.2) The equation of motion for rotating stratified flow of an inviscid fluid is

$$\frac{D\mathbf{u}}{Dt} + f\mathbf{k} \wedge \mathbf{u} = -\frac{1}{\rho_*}\nabla p\prime + \sigma\mathbf{k},$$

where the Boussinesq assumption has been made. Obtain the vorticity equation and identify that part of it which corresponds with the thermal wind equation,

$$f\frac{\partial \mathbf{u}_h}{\partial z} = \mathbf{k} \wedge \nabla_h\sigma.$$

[Hint: it may help to write the total vorticity $\boldsymbol{\omega} = \boldsymbol{\omega}_h + \zeta\mathbf{k}$, where $\boldsymbol{\omega}_h$ is the horizontal component and ζ is the vertical component. The following formulae may to be useful also:

$$\left[\mathbf{u} \wedge \boldsymbol{\omega} = \tfrac{1}{2}\nabla(\mathbf{u}^2) - \mathbf{u}\cdot\nabla\mathbf{u}, \nabla \wedge (\boldsymbol{\omega} \wedge \mathbf{u}) = \mathbf{u}\cdot\nabla\boldsymbol{\omega} - \boldsymbol{\omega}\cdot\nabla\mathbf{u} + \boldsymbol{\omega}(\nabla\cdot\mathbf{u}).\right]$$

(1.3) Show that

$$Z(p) = -\frac{RT_o}{g} \ln (p/p*)$$

measures actual height above the pressure level $p\star$ (= 1000 mb) in an isothermal atmosphere with temperature T_o.

(1.4) Show that $\chi(p) = [1 - (p/p*)^{\kappa}]\, \mathrm{H_s}/\kappa$ measures actual height above the $p\star$ level in an adiabatic atmosphere. Determine the characteristic height scale $z = H_s/k$ appropriate to the atmosphere.

(2.1) Show that for an isothermal atmosphere, N, c_0 and H_s are constants. Show that for $T_0 = 275$ K, $c_0 = 332\ ms^{-1}$, $H_s = 8054$ m and the Brunt-Väisälä period, $2\pi/N$, equals 5.6 minutes.

(2.2) Show that

$$\frac{N^2}{g} = -\frac{g}{c_o^2} + \frac{1}{H_s}. \tag{2.54}$$

Deduce that for an isothermal atmosphere, the ratio $2N^2H_s/g$ is of order unity (use $\gamma = 1.4$).

(2.3) Show that $\phi = \gamma^{-1}\ ln\ p - ln\ \rho +$ constant.

(2.4) Show that the phase speed of the plane wave represented by (2.36) is $\omega/\left|\mathbf{k}\right|$. Show that the phase speed is *not* a vector; i.e., the components of the vector $\omega/\left|\mathbf{k}^2\right|$ are in general not equal to the components of the phase speed in the x and z directions.

(2.5) Show that with the substitutions $\omega^2 = Y + b$, $\mathbf{k}^2 = X + d$ and $\mu^2 = m^2 + 1/4H_s^2$ in (2.35) and with appropriate choices for b and d, the equation represents a hyperbola in the X, Y plane with equation

$$\frac{Y^2}{c_o^2} - XY = (N^2 - f^2)\left(\mu^2 - \frac{N^2}{c_o^2}\right). \tag{2.55}$$

(2.6) Verify that $\omega^2 = f^2 + k^2c_0^2$ is a solution of (2.35) provided that $m^2 = -(1 - 4H_s^2\ N^2/c_0^2)\,/4H_s^2$, and show that for $T_o = 275$ K, $m^2 < 0$.

(2.7) Verify that in the limit as $k \to 0$, the pressure perturbation drops out of the momentum equation and that $\hat{\sigma}$, and $\hat{P} \to 0$.

(2.8) Deduce the following properties of acoustic waves:

$$\hat{u} \sim \frac{k}{\omega}\hat{P}\ , \quad \hat{w} \sim \frac{(im/\omega)(m^2\mathrm{H_s^2}+\frac{1}{4})\hat{P}}{im^2\mathrm{H_s^2}+(\frac{1}{2}-\mathrm{gH_s}/c_o^2)mH_s} \quad , \quad \hat{v} \sim 0,\ \hat{\phi} \sim 0.$$

(2.9) Show that the assumption $n_4 = 0$ does not filter out the Lamb wave from (2.19, 2.20, 2.21, 2.22 and 2.23), even though it removes all other acoustic wave modes. Show also that when $n_4 = 0$ and the condition (2.41) is used, the free surface wave exists even when N^2 is not negligible.

(2.10) The Boussinesq equations for a non-rotating stratified liquid are

$$\frac{D\mathbf{u}}{Dt} = -\frac{1}{\rho_*}\nabla p + \sigma k, \quad \nabla \cdot \mathbf{u} = 0, \quad \text{and} \quad \frac{D\rho}{Dt} = 0$$

where ρ_* is a constant. Show that the dispersion relation for small-amplitude waves in the $x - z$ plane is

$$\omega^2 = \frac{N^2k^2}{k^2 + m^2}.$$

(2.11) Show that in the absence of a basic mean flow, the energy equation for small amplitude waves in a nonrotating Boussinesq liquid is

$$\frac{\partial \tilde{E}}{\partial t} = -\nabla \cdot \tilde{\mathbf{F}}$$

where $\tilde{\mathbf{E}} = \frac{1}{2}\rho_*(u^2 + w^2 + \sigma^2/N^2)$ is the energy density, and $\tilde{F} = (pu, 0, pw)$ is the energy flux. Deduce that

$$\frac{\partial E}{\partial t} = -\frac{\partial F}{\partial z},$$

where E is the *mean energy density* and F is the *mean vertical energy* flux averaged over a horizontal wavelength of a wave. Calculate E and F for a plane wave, for which

$$(u, w, \sigma, P) = \mathrm{Re}\ \left[\left(-\frac{m}{k},\ 1\ ,\ \frac{iN^2}{\omega}, -\frac{\omega m}{k^2}\right)\hat{w}\, e^{i(kx+mz-\omega t)}\right],$$

and show that $F = Ew_g$, where w_g is the *vertical component* of the *group velocity vector*, $\partial\omega/\partial m$.

(2.12) Find the solution of (2.33), with $n_2 = n_3 = 0$, $n_1 = n_4 = 1$, (the sound-proof system) which satisfies $\hat{w}(0) = 0$ and the free surface condition

$$\hat{w}_z - \left(\frac{1}{H_s} + \frac{gk^2}{\omega^2 - f^2} \right) \hat{w} = 0 \ \ at \ \ z = h.$$

Show that, in addition to the dispersion relation for inertia-gravity waves, ω satisfies also the equation

$$\omega^2 = f^2 + \frac{gH_s k^2}{mH_s \ \text{cot mh} \ - \frac{1}{2}}.$$

For $k = 1/(2H_s)$, corresponding with a horizontal wavelength of about 100 km, compare the phase speed of the fastest moving wave in this case with the phase speed obtained from the formula (2.44), assuming that $T_o = 275$ K and $f = 0$.

Chapter 3

WAVES ON MOVING STRATIFIED FLOWS

In Chapter 2 we studied small-amplitude waves in a compressible, stably-stratified, rotating gas when there is no basic flow. We turn now to consider the propagation of small-amplitude internal gravity waves in a stratified shear flow $\mathbf{U} = (U(z), 0, 0)$, including the special case of uniform flow $U(z) =$ constant. The linearized form of the anelastic equations is

$$u_t + Uu_x + wU_z = -P_x, \tag{3.1}$$

$$w_t + Uw_x = -P_z + \sigma, \tag{3.2}$$

$$\sigma_t + U\sigma_x + N^2 w = 0, \tag{3.3}$$

$$u_x + w_z - w/H_s = 0. \tag{3.4}$$

Proceeding as before, we seek travelling-wave solutions of the form (2.24) to obtain

$$-i(\omega - Uk)\hat{u} + \hat{w}U_z = -ik\hat{P}, \tag{3.5}$$

$$-i(\omega - Uk)\hat{w} = -\hat{P}_z + \hat{\sigma}, \tag{3.6}$$

$$-(\omega - Uk)\hat{\sigma} + N^2\hat{w} = 0, \tag{3.7}$$

$$ik\hat{u} + \hat{w}_z - \hat{w}/H_s = 0. \tag{3.8}$$

Equations (3.8), (3.5) and (3.7) lead respectively to expressions relating $\hat{u}$, $\hat{P}$ and $\hat{\sigma}$ to $\hat{w}$:

$$(\hat{u}, \hat{P}, \hat{\sigma}) = \left[\frac{i}{k} \left(\hat{w}_z - \frac{\hat{w}}{H_s} \right), \ \frac{i}{k^2} \left\{ \omega^* \hat{w}_z + \left(kU_z - \frac{\omega^*}{H_s} \right) \hat{w} \right\}, \ \frac{N^2 \hat{w}}{i\omega^*} \right], \quad (3.9)$$

where

$$\omega^* = \omega - Uk, \quad (3.10)$$

is the *intrinsic frequency*[1] of the wave; the frequency measured by an observer moving with the local flow speed $U(z)$. Then (3.6) together with (3.9) gives a second order ordinary differential equation for $\hat{w}$, i.e.

$$\hat{w}_{zz} - \frac{1}{H_s} \hat{w}_z + \left[\frac{k}{\omega^*} U_{zz} + \frac{k}{\omega^*} \frac{U_z}{H_s} - \left(\frac{1}{H_s} \right)_z + \left(\frac{N^2}{\omega^{*2}} - 1 \right) k^2 \right] \hat{w} = 0. \quad (3.11)$$

This equation may be further simplified by taking

$$\tilde{w}(z) = \exp(z/2H_s) \tilde{w}(z), \quad (3.12)$$

as suggested by the analysis in Chapter 2. We set $c = \omega/k$ so that $\omega^* = k(c - U)$. Then, assuming that H_s is a constant, $\tilde{w}(z)$ satisfies the equation

$$\tilde{w}_{zz} + (l^2(z) - k^2) \tilde{w} = 0, \quad (3.13)$$

where

$$l^2(z) = \frac{N^2}{(U - c)^2} - \frac{U_{zz} + U_z/H_s}{U - c} - \frac{1}{4H_s^2}. \quad (3.14)$$

There are two types of problem; one concerned with free waves, the other with forced waves.

3.1 Free waves

When w, and hence $\hat{w}(z)$, satisfies homogeneous boundary conditions at two particular levels, we have an eigenvalue problem. For a given horizontal wavenumber k, free waves are possible only for certain phase speeds c. Alternatively, when c is fixed, there is a constraint on the possible wavenumbers.

[1] It is sometimes referred to alternatively as *Doppler-shifted frequency.*

The possible values of $c(k)$, or given c, the possible values of k, and the corresponding vertical wave structure $\hat{w}(z, k, c(k))$ are obtained as solutions of the eigenvalue problem. Unfortunately, except for one or two simple expressions for $U(z)$, the eigenvalue problem is analytically intractable and, in general, one must resort to numerical methods.

Two examples of free wave problems are shown schematically in Figs. 3.1 and 3.2. In the first, a stably-stratified shear flow is confined between rigid horizontal boundaries at $z = 0$ and $z = H$. In the second, a stratified shear flow $U(z)$ in the region $0 \leq z \leq H$ underlies an infinitely-deep layer of a neutrally-stratified ($N \equiv 0$) uniform flow $U(z) \equiv U(H)$ in the region $z > H$. Such flow configurations, in which waves are confined in a particular direction (here the z-direction) are sometimes referred to as wave-guides. Note that in the latter example, vertical wave propagation cannot occur in the region $z > H$ as there is no stratification or shear in this region. Thus $l^2(z)$ is negative in (3.13) and solutions for $\tilde{w}$, and hence for other tilde wave quantities following from (3.9), must decay exponentially with height. This model is of some relevance to understanding the waves associated with the spectacular "Morning-Glory" clouds shown in Figs. 3.3 and 3.3. The morning glory phenomenon occurs regularly at certain times of the year in the Gulf of Carpentaria region of northern Australia (see e.g. Smith, 1988; Christie, 1992; Smith *et al.*, 1986).

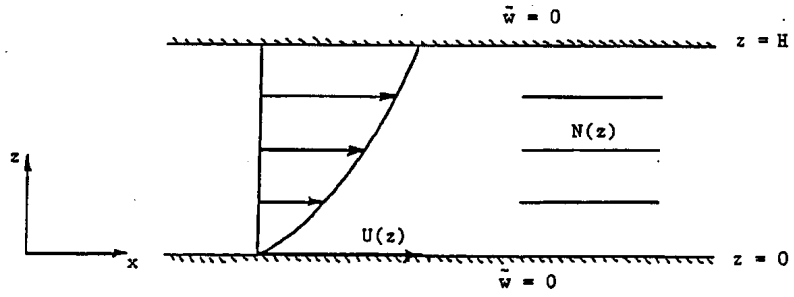

Figure 3.1: Stratified shear flow between rigid horizontal boundaries.

3.2 Forced waves

If the waves are being generated at a particular source level, the boundary conditions on Eq. (3.13) are inhomogeneous and a different type of mathematical problem arises. Examples are the flow detailed in Figs. 3.5 and

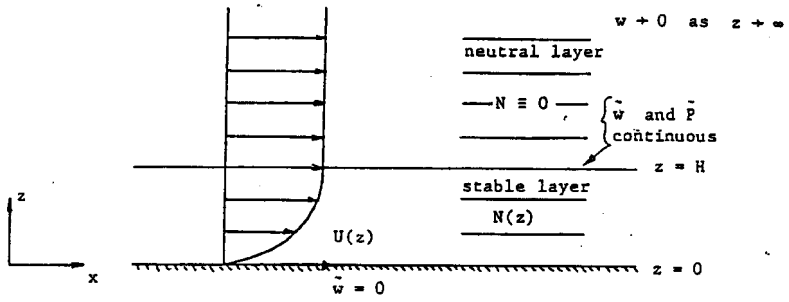

Figure 3.2: Wave-guide for waves on a surface-based stable layer underlying a deep neutrally-stratified layer. This configuration is an approximation to the wave-guide for 'morning-glory waves'.

Figure 3.3: A northeasterly Morning Glory cloud formation.

3.6. In the former, waves are generated at $z = 0$ by a moving boundary with small amplitude sinusoidal corrugations on it, and propagate upwards.

Assuming that there is no basic flow ($U \equiv 0$), that the Boussinesq approximation is valid ($1/H_s \equiv 0$), and that N and c are given constants, the vertical wavenumber m is determined by the dispersion relation,

$$m^2 = N^2/c^2 - k^2, \tag{3.15}$$

where k is the horizontal wavenumber (this equals the wavenumber of the corrugations) and c is the speed of the boundary. The group velocity of the waves is

Figure 3.4: A southerly Morning Glory.

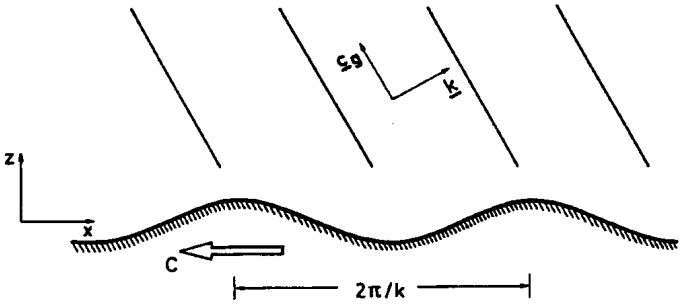

Figure 3.5: Waves produced by the motion of a (sinusoidal) corrugated boundary underlying a stably-stratified fluid at rest.

$$\mathbf{c}_g = \frac{c^3}{N^2}(m^2,\, -mk). \tag{3.16}$$

According to a result of problem 2.11, the vertical flux of mean wave energy is $\overline{pw}$, denoted by F, and this is equal to Ew_g, the mean wave energy density times the vertical component of the group velocity. In the problem under consideration, $c < 0$, and therefore $\mathrm{sgn}(w_g) = \mathrm{sgn}(mk)$. Thus those waves with their phase lines tilting with height in the negative x-direction (the direction of c) are those which propagate energy vertically.

In this problem, the solution of (3.13) for $\hat{w}(z)$ is determined by a condition at $z = 0$ relating $\hat{w}(0)$ to the amplitude of the corrugations and the speed of boundary motion (an inhomogeneous condition), together with a radiation condition as $z \to \infty$ which ensures that the direction of energy flux at large heights is away from the wave source, i.e., it is vertically upwards. This condition is applied by ensuring that only wave components with a positive group velocity (in this case there is only one) are contained in the solution. These two conditions determine the forced wave solution uniquely.

In the second example, the flow configuration is a Galilean transformation of the first; now the boundary is at rest and a uniform flow $u(> 0)$ moves over it. The two problems are clearly dynamically equivalent, but, as we shall see presently, they are not energetically equivalent. In particular, F can no longer be simply interpreted as the energy flux [2] and, without recognition of the dynamical equivalence with the former problem, it is not immediately clear how to choose an appropriate radiation condition.

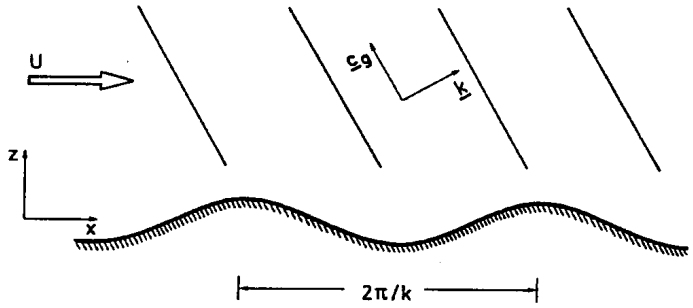

Figure 3.6: Waves produced by the flow of a stably-stratified fluid over a corrugated boundary.

3.3 Mountain waves

When a stably-stratified airstream crosses an isolated ridge or, more generally, a range of mountains, stationary wave oscillations are frequently observed over and to the lee of the ridge or range. These so-called mountain waves, or lee waves, may be marked by smooth lens-shaped clouds, known as lenticular clouds. The clouds occur in the crests of waves when a layer of air approaching the mountain is sufficiently moist; see Figs. 3.7. Photographs

[2]Indeed, the energy equation is not Galilean invariant.

of such clouds are shown in Figs. 3.8 - 3.10 The clouds are formed continuously on the upwind side of the crests as air rises, cools adiabatically, and becomes saturated so that condensation occurs. They are likewise eroded on the downwind side due to adiabatic heating and re-evaporation as the air descends into a wave trough. Sometimes, clouds marking many wave crests are observed downstream of the mountain ridge; they are usually more or less stationary, both in position and appearance, while the air blows through them. The smooth appearance of the clouds is indicative of low turbulence levels. In strong wind conditions, there may exist rotors in localized areas near the mountain. These are very turbulent regions with a closed mean circulation and may be marked by a ragged roll cloud. They are extremely hazardous for aircraft.

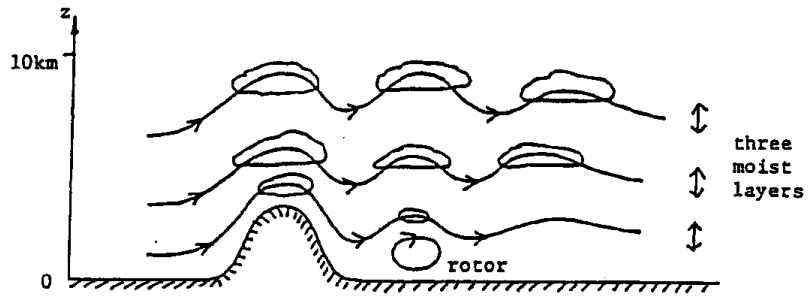

Figure 3.7: Formation of lenticular clouds in a series of mountain lee waves.

3.4 Linear Theory

With the foregoing discussion in mind, we consider now stationary solutions of (3.13) (i.e. solutions with $\omega = 0$, implying $c = 0$) within the framework of the Boussinesq approximation. Thus, for simplicity, we assume *inter alia* that $1/H_s \equiv 0$. It is instructive to begin by considering uniform flow U over sinusoidal topography $z = h(x) = h_m \, cos$ kx, bearing in mind that solutions for flow over other topographic shapes may be constructed as Fourier syntheses of those for sinusoidal terrain. The flow configuration is as shown in Fig. 3.6.

At the surface, the condition that the flow follows the terrain, or, in other words that the streamline slope equals the terrain slope, is

$$\frac{w}{U+u} = \frac{dh}{dx} \text{ on } z = h(x). \tag{3.17}$$

Figure 3.8: Lenticular mountain wave clouds over the European Alps.

Figure 3.9: Lenticular mountain wave clouds produced by the Australian southern Alps.

This condition is nonlinear, but for small-amplitude topography and disturbance velocity it can be linearized to give

$$w = U\frac{dh}{dx} \text{ at } z = 0. \tag{3.18}$$

Figure 3.10: Lenticular wave clouds near the Grampian Hills in Victoria, Australia.

Likewise, if $\zeta(x, z, t)$ is the vertical displacement of an air parcel from its level at a specified distance upstream, then $w = D\zeta/Dt$. This linearizes to $w \approx U\partial\zeta/\partial x$, so that

$$\hat{w} = ikU\hat{\zeta}. \tag{3.19}$$

When U is a constant, $\hat{\zeta}$ satisfies the same equation as $\hat{w}$, i.e.

$$\frac{d^2\hat{\zeta}}{dz^2} + \left(\frac{N^2}{U^2} - k^2\right)\hat{\zeta} = 0. \tag{3.20}$$

Here it is slightly more convenient[3] to work in terms of $\hat{\zeta}$ rather than $\hat{w}$.

The general solution of (3.20) is

$$\hat{\zeta}(z) = Ae^{imz} + Be^{-imz}, \tag{3.21}$$

where A and B are constants to be determined and

$$m^2 = N^2/U^2 - k^2. \tag{3.22}$$

The boundary condition at the ground, $\zeta(x, 0) = h_m \exp(\mathrm{ikx})$, gives

[3]One can also define a streamfunction ψ such that $u = \psi_z$, $w = -\psi_x$. Then $\hat{w} = -ik\hat{\psi}$ and hence $\hat{\psi}$ satisfies the same equation as $\hat{w}$. Moreover, from (3.19) it follows that $\hat{\psi} = U\hat{\zeta}$.

$$\hat{\zeta}(0) = h_m. \tag{3.23}$$

Evidently, the upper boundary condition and hence the solution depends on the sign of $N^2 - U^2k^2$ in (3.22). Let $l = N/U$.

Case $0 < |\mathbf{k}| < \mathbf{l}$

Then m is real and if m, $k > 0$, we must choose $B = 0$ to satisfy the radiation condition; this requires that the phase lines slope upstream with height (i.e. here $\text{sgn}(mk) > 0$) as discussed earlier in this chapter. Then the complete wave solution is

$$\zeta(x, z) = h_m e^{i(kx+mz)}, \tag{3.24}$$

the real part being implied, of course. The streamline patterns are shown in Fig. 3.11a. Since in this case the intrinsic frequency of the motion Uk is less than N, internal gravity waves are excited (this frequency is that experienced by a fluid parcel moving through the stationary wave pattern). These waves propagate vertically and thus the disturbance does not decay upwards. For very long waves, i.e., $|k| << l$, the vertical wavenumber of the disturbance is approximately equal to l; thus, it depends only on the characteristics of the airstream, not on k. Such motions are closely hydrostatic.

Case $\mathbf{l} < |\mathbf{k}|$

Then m is imaginary ($= im_0$ say) where m_0 is the positive root $(k^2 - l^2)^{1/2}$, and the expression for $\hat{\zeta}(z)$ is no longer wavelike. The appropriate upper boundary condition requires that $\hat{\zeta}(z)$ remains at least bounded as $z \to \infty$, i.e. $B = 0$. The complete solution is therefore

$$\zeta(x, z) = h_m e^{-(k^2-l^2)^{1/2}z+ikx}. \tag{3.25}$$

The streamlines for this solution are shown in Fig. 3.11b. As the intrinsic frequency is now greater than the buoyancy frequency, gravity waves are not excited and the flow is qualitatively similar to irrotational flow ($l = 0$) in that the phase lines are vertical and the disturbance decays with height. It may be helpful to think of this as the case of "closely spaced" topography, but not in absolute terms; only in relation to the airflow parameter l. Note that as $k^2 \to l^2$, the vertical penetration of the disturbance increases as buoyancy forces become more important.

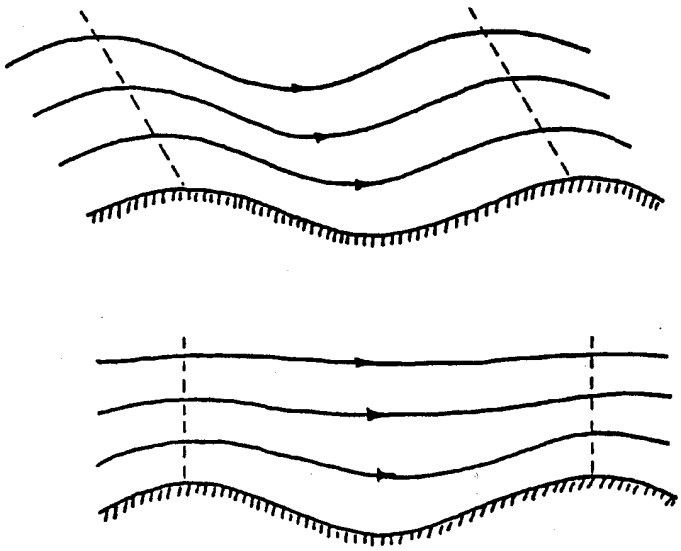

Figure 3.11: Streamline patterns for uniform flow over sinusoidal topograhy: (a) vertical propagation, $U|k| < N$, (b) vertical decay, $N < U|k|$.

3.5 Flow over isolated topography

We study now flow over an isolated ridge or mountain with shape $z = h(x) = h_m/[1 + (x/b)^2]$, sometimes referred to as the 'Witch of Agnesi' profile. The flow configuration is shown in Fig. 3.12. While the principal of the method to be described is quite general, the ridge shape chosen has a particular simple Fourier transform and this simplifies the calculations considerably. For this reason also, we assume as before a uniform basic flow, U = constant.

Since the ridge is symmetrical about $x = 0$, it may be expressed as a Fourier cosine integral, i.e.

$$h(x) = \int_0^\infty \overline{h} \cos kx \; dk = \mathrm{Re} \int_0^\infty \overline{h}\,(k) e^{ikx} dk, \tag{3.26}$$

where

$$\begin{aligned} \overline{h}(k) &= \frac{2}{\pi} \int_0^\infty h(x) \cos kx \; dx \\ &= \frac{2h_m}{\pi} \mathrm{Re} \int_0^\infty \frac{e^{ikx} dx}{1 + \left(\frac{x}{b}\right)^2} \end{aligned}$$

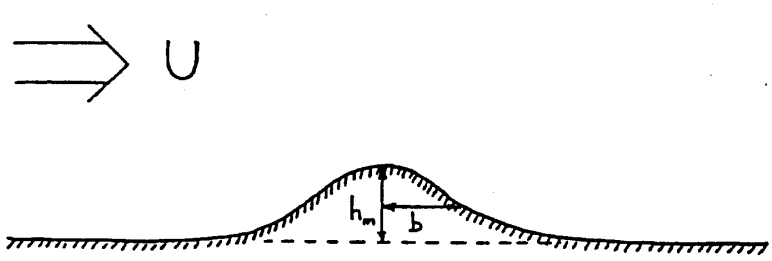

Figure 3.12: Schematic representation of flow over an isolated ridge with $h(x) = h_m/[1 + (x/b)^2]$; the maximum height of the ridge is h_m and its characteristic width, the width at which $h(x) = \frac{1}{2}h_m$, is b.

$$= \frac{2h_m b}{\pi} \int_0^\infty \frac{e^{ikbu} du}{1+u^2} = h_m b e^{-kb}. \tag{3.27}$$

But the solution $\zeta(x, z; k)$ for each Fourier component of the spectrum in (3.26) is simply that given by either (3.24) or (3.25); hence the solution for flow over the ridge is just the Fourier synthesis of these solutions, i.e.

$$\zeta(x,z) = \mathrm{Re}\left[\int_0^l \overline{h}(k) e^{i[kx+(l^2-k^2)^{1/2}z]}\, dk + \int_l^\infty \overline{h}(k)\, e^{ikx-(k^2-l^2)^{1/2}z} dk\right].$$

Using (3.27) and making the substitution $kb = u$, this becomes

$$\zeta(x,z) = I_1 + I_2,$$

where

$$I_1 = h_m \mathrm{Re} \int_{lb}^{lb} \exp\left[-u\left(1 - \frac{ix}{b}\right) + \left(l^2b^2 - u^2\right)^{1/2} \frac{z}{b}\right] du$$

and

$$I_2 = h_m \mathrm{Re} \int_{lb}^{lb} \exp\left[-u\left(1 - \frac{ix}{b}\right) - \left(u^2 - l^2b^2\right)^{1/2} \frac{z}{b}\right] du. \tag{3.28}$$

Before considering the full solution for $lb \sim 1$, we examine two limiting cases.

Narrow ridge, lb << 1

Then $I_1 << I_2$ and

$$\begin{aligned}\zeta(x,z) &\approx h_m \mathrm{Re} \int_0^\infty \exp\left[-u\left(1-\frac{ix}{b}+\frac{z}{b}\right)\right] du \\ &= \left(\frac{b}{b+z}\right) \frac{h_m}{[1+x^2/(b+z)^2]}. \end{aligned} \tag{3.29}$$

Written in this form, we see that each streamline has the same general shape as the ridge, but the width of the disturbed portion of a streamline increases linearly with z, whereas its maximum displacement decreases in proportion to $1/(1+z/b)$, becoming relatively small for heights a few times greater than the barrier width. Note that this limit corresponds with small Nb/U, i.e., with small static stability and/or high wind speeds, and gravity waves are not excited. Indeed, the flow is irrotational. As noted by Smith (1979, p101), the same flow field could have been constructed from potential flow theory by placing a doublet slightly below the ground. The streamline pattern is shown in Fig. 3.13.

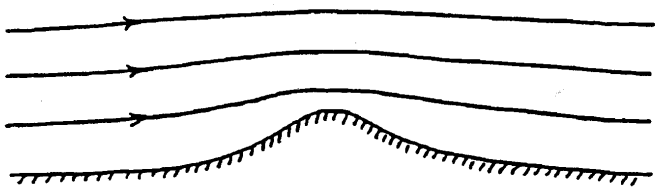

Figure 3.13: The steady flow of a homogeneous fluid over an isolated two-dimensional ridge, given by (3.29). From the spacing of the streamlines, it is evident that the highest wind speed and the lowest pressure occurs at the top of the ridge.

Broad ridge, lb >> 1

In this limit, $I_1 >> I_2$ and

$$\begin{aligned}\zeta(x,z) &\approx h_m \mathrm{Re}\left\{ e^{ilz} \int_0^\infty \exp\left[-u\left(1-ix/b\right)\right] du\right\} = h_m \mathrm{Re}\left[\frac{be^{ilz}}{b-ix}\right] \\ &= h_m \left[\frac{\cos\ lz - (x/b)\ \sin\ lz}{1+(x/b)^2}\right]. \end{aligned} \tag{3.30}$$

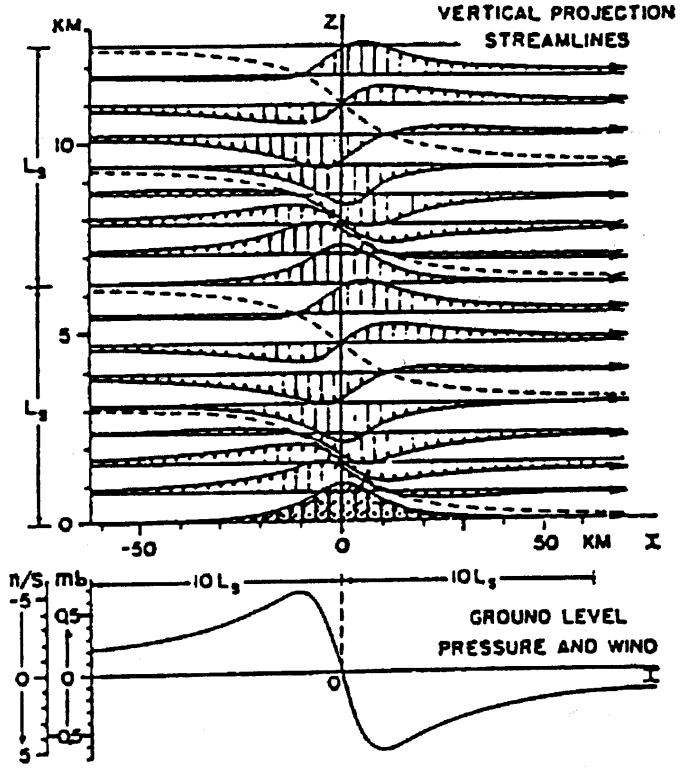

Figure 3.14: Buoyancy-dominated hydrostatic flow over an isolated-two-dimensional ridge, given by (3.30). The disturbance is composed of vertically-propagating, internal gravity waves of the sort shown in Fig. 3.11a. The evident upstream tilt of the phase lines indicates that disturbance energy is propagating upward away from the mountain. The maximum wind speed and minimum pressure occur on the leep slope of the ridge. The mountain height $h_m = 1$ km, the half-width $b = 10$ km, the mean wind speed $U = 10$ m/sec, the Brunt-Väisälä frequency $N = 0.01$/sec, and the vertical wavelength $L_s = 2\pi U/N = 6.28$ km. (After Queney, 1948 and taken from Smith, *op. cit.*.)

Now all Fourier components propagate vertically. A typical case is shown in Fig. 3.14. Note that the flow is periodic in the vertical, whereupon at $z = \pi/l$, the streamline shape looks like the ridge inverted and at $z = 2\pi/l$, the pattern is the ridge shape once again. The upstream tilt of the phase lines required of each Fourier component is still a prominent feature of the composite flow. Smith *op. cit.* (p103) notes that "This asymmetry to the

flow, which is associated with the vertical propagation of wave energy, has a number of implications. From the distance between the streamlines in Fig. 3.14 it is apparent that the wind speed is low on the windward slope of the ridge and faster on the leeward slope. From Bernoulli's equation, this requires a pressure difference across the ridge; higher pressure upwind and lower pressure downwind. The primary reason for the windward-side high pressure is the thickened layer of dense cool air just above the mountain, but this in turn is related to the radiation condition aloft." The pressure difference results in a net drag on the mountain. It can be computed either as the horizontal pressure force on the mountain

$$D = \int_{-\infty}^{\infty} p(x,0)\frac{dh}{dx}\, dx, \tag{3.31}$$

or, alternatively, as the vertical flux of horizontal momentum in the wave motion

$$D = -\rho_0(z)\int_{-\infty}^{\infty} uw\, dx, \tag{3.32}$$

where, of course, with the Boussinesq approximation, $\rho_0(z) = \rho*$. The increase in wind speed on the slope has been suggested as an explanation for severe downslope winds found occasionally in the lee of mountain ranges. Frequently the strong lee-side winds are warm and dry, replacing colder air, and are referred to as föhn-winds; in the US Rockies, the local name is "chinook" and in southern California, the term "Santa Ana" is used.

Moderate ridge, $lb \sim 1$

In the general case, the integrals in (3.28) are too difficult to evaluate analytically, but their asymptotic expansions at large distances from the mountain (compared with l^{-1}) are revealing. We consider first I_1. Let $u = lb\,\cos\,\alpha$, where $0 \le \alpha \le \pi/2$, and $x = r\,\cos\,\theta$, $z = rsin\theta$, where $0 \le \theta \le \pi$. Then

$$I_1 = h_m lb\,\mathrm{Re}\int_0^{\frac{\pi}{2}} (\sin\ \alpha\, e^{-lb\,\cos\,\alpha})\, e^{irl\,\cos(\theta-\alpha)}\, d\alpha, \tag{3.33}$$

which has the form,

$$I_1 = \mathrm{Re}\int_0^{\frac{\pi}{2}}\ h(\,\alpha\,)\, e^{irl\,g(\alpha)}\, d\alpha.$$

The asymptotic expansion of such integrals for large r may be obtained by the method of stationary phase (see e.g., Jeffreys and Jeffreys, Methods of Mathematical Physics, Chapter 17).

If $x > 0$ (i.e. $0 \leq \theta \leq \frac{\pi}{2}$), the phase $lr \cos(\alpha - \theta)$ is stationary for $\alpha = \theta$ and therefore the asymptotic value of the integral is $O((rl)^{-1/2})$, provided z is not too small, i.e. provided that $\alpha = \theta$ is not too close to the lower limit of the integral.

If $x < 0$ (i.e. $\frac{\pi}{2} < \theta \leq \pi$), the phase is monotonic because $0 < \alpha < \frac{\pi}{2}$ implies that $-\pi < \alpha - \theta < 0$. Thus $I_1 \sim (lr)^{-1}$, except in the vicinity of the zenith ($\theta = \frac{\pi}{2}$). In the latter case, the phase is stationary near $\alpha = \frac{\pi}{2}$, the upper limit of the integral, and $I_1 \sim (lr)^{-1/2}$. The behaviour is summarized in Fig. 3.15.

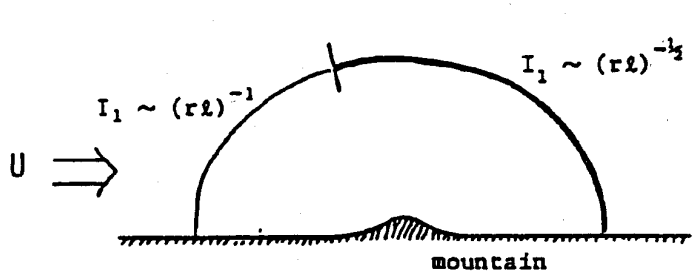

Figure 3.15: Asymptotic behaviour of I_1 (Eq. 3.33).

Now consider I_2. Since $(u^2 - l^2b^2)^{1/2} > u - lb$ for $u > lb$,

$$|I_2| \leq h_m \max_{lb \leq u \leq \infty} \left| \exp\left[-u\left(1 - \frac{ix}{b}\right)\right] \right| \int_{lb}^{\infty} e^{-(u-lb)z/b}\, du$$
$$= h_m b \exp(-lb)/z\,.$$

Hence I_2 is at most $O(hm/z)$ when z/h_m is large. Also, by the Riemann-Lebesgue theorem, I_2 is at most $O(b/x)$ for large $|x/b|$. Hence I_2 is at most $O(b/r)$ and, since $lb \sim O(1)$, $I_1 + I_2$ is always the same order as I_1. This is not surprising since I_1 contains all the vertically propagating wave components. Therefore, if we exclude the vicinities of $\theta = \pi/2$ and $\theta = 0$, the asymptotic expression for (3.28) is the same to leading order as that for (3.33) and hence

$$\zeta(x,z) \sim h_m lb \sin\theta e^{-lb\cos\theta} \left(\frac{2\pi}{lr}\right)^{1/2} \cos\left(lr - \frac{\pi}{4}\right) \qquad (3.34)$$

for $x > 0$ and θ not too close to 0 or π. It follows that successive extrema of ζ are located on circles $lr = (n + 1/4)\pi$, n being a positive integer. On a given circle,

$$\zeta(\theta)/h_m = lb \left[\frac{8}{4n+1}\right]^{\frac{1}{2}} e^{-lb\cos\theta} \sin\theta \tag{3.35}$$

Thus, $\zeta(\theta)/h_m$ is a maximum for $lb \sim 1$ and negligible for $lb << 1$ as well as $lb >> 1$ (because of the exponential factor). Hence the amplitude of the lee waves is appreciable when compared with the height of the mountain only if the width of the mountain is comparable with the (radial) wavelength $2\pi/l$ of the waves. The latter quantity depends only on the characteristics of the airstream, N and U. Note that the decay of wave amplitude away from the mountain is due to the dispersion of wave energy. An example of airflow over a ridge with $lb \sim 1$ is shown in Fig. 3.16.

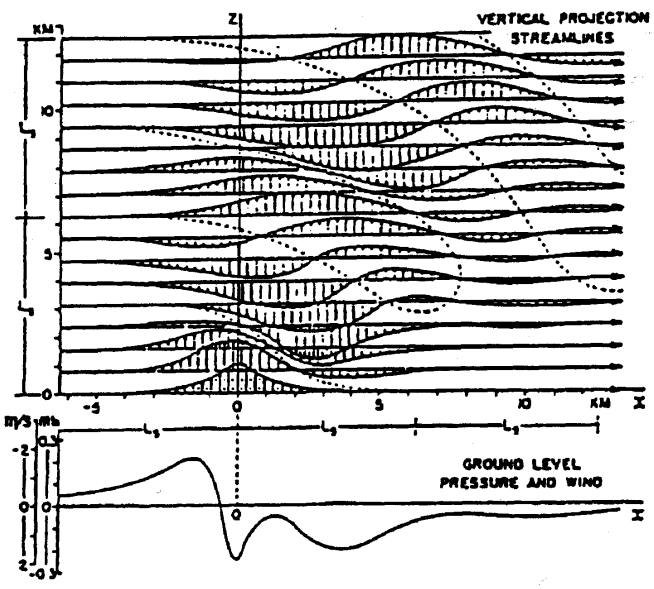

Figure 3.16: Lee waves in the case where $lb \sim 1$.

3.6 Trapped lee waves

It was pointed out by Scorer (1949) that, on occasion, a long train of lee waves may exist downstream of a mountain range, quite unlike the waves portrayed

in Figs. 3.14 and 3.16. Scorer showed that a long wave train is theoretically possible if the parameter $l^2(z)$ in (3.14) decreases sufficiently rapidly with height. Since eigensolutions of (3.13) are difficult to obtain when l^2 varies with z, Scorer studied situations in which l^2 is a different constant in each of two atmospheric layers, the difference being due to different static stabilities, U being the same constant value in each layer.

We denote quantities in the upper and lower layers by subscripts '*1*' and '*2*' respectively, and work in terms of the perturbation streamfunction ψ, defined in footnote 2 on p 38. In the Boussinesq approximation $\tilde{\psi}(z)$ satisfies the same differential equation as $\tilde{w}$, i.e.

$$\frac{d^2\tilde{\psi}}{dz^2} + (l^2 - k^2)\tilde{\psi} = 0, \tag{3.36}$$

assuming stationary wave solutions so that $c = 0$ where $l^2 = N^2/U^2$ as before. Hence $\tilde{\psi} \propto \exp(\mathrm{imz})$, where $m^2 = l^2 - k^2$. We assume that $m_2^2 > 0$, so that vertical wave propagation is possible in the lower layer.

Case (a): upper layer more stable ($l_1 > l_2$).

We consider an upward-propagating wave in the lower layer impinging on the discontinuity level as shown in Fig. 3.17. Since $m_l^2 > m_2^2$, vertical propagation is possible in the upper layer and we may anticipate that there will be a transmitted wave and a reflected wave. The streamfunctions for the transmitted wave ψ_1, and the incident plus reflected wave ψ_2, are given by

$$\psi_1 = \alpha e^{i(kx+m_1 z)}, \tag{3.37}$$

and

$$\psi_2 = a\, e^{i(kx+m_2 z)} + \beta e^{i(kx-m_2 z)}, \tag{3.38}$$

where a is the amplitude of the incident wave, assumed given, and α and β are the amplitudes of the transmitted and reflected waves to be found. It is assumed that m_1, $m_2 > 0$. The solutions are coupled by conditions expressing the continuity of interface displacement and pressure at $z = 0$. The former condition, $\hat{\zeta}_1 = \hat{\zeta}_2$ at $z = 0$, implies that $\hat{w}_1 = \hat{w}_2$ and $\hat{\psi}_1 = \hat{\psi}_2$ *provided*, as here, that $U_1 = U_2$. When the density is continuous across the interface, continuity of pressure implies that $\hat{\psi}_{1z} = \hat{\psi}_{2z}$ at $z = 0$ (see Ex. 3.6). Applying these conditions to (3.37) and (3.38), it follows readily that

$$\alpha = \frac{2m_2 a}{m_1 + m_2} \text{ and } \beta = \left(\frac{m_2 - m_1}{m_1 + m_2}\right) a. \tag{3.39}$$

The expression for α shows that there is always a transmitted wave and therefore trapped "resonant" solutions in the lower layer are impossible in this case. Note also that when $N_1 \cong N_2$, little energy is reflected.

Case (b): upper layer less stable ($l_1 < l_2$).

This situation is depicted in Fig. 3.18 assuming that $m_1^2 < 0$. Then the appropriate solution in the upper layer is the one which decays exponentially with height, i.e.

$$\psi_1 = \alpha e^{ikx - |m_1|z}. \tag{3.40}$$

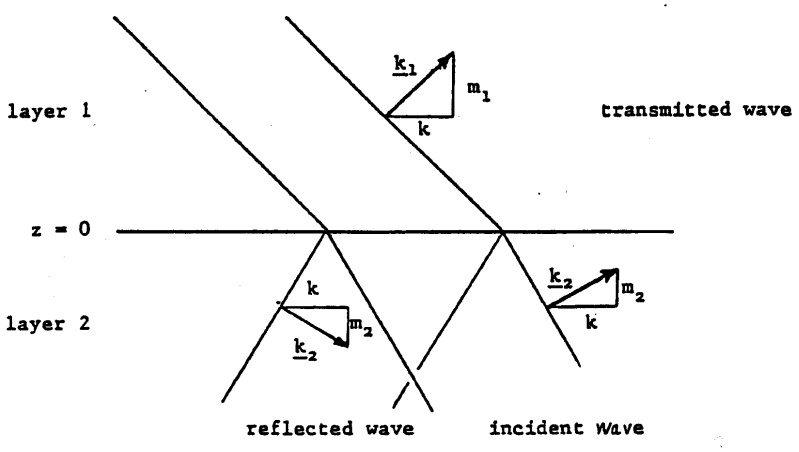

Figure 3.17: Wave transmission in the case $l_1 > l_2$.

For algebraic convenience we assume that α is given and obtain expressions for a and β in terms of this by requiring that $\hat{\psi}$ and $\hat{\psi}_z$ are continuous at $z = 0$ as before. After a little algebra, it follows that ψ_2 can be written in the form

$$\psi_1 = \alpha e^{ikx - |m_1|z}. \tag{3.41}$$

Observe that the x and z dependence are decoupled in (3.41) and hence the incident and reflected waves sum to give a horizontally-propagating wave. Such a wave is called trapped; it cannot propagate into the upper region, but decays therein on a scale $1/|m_1|$.

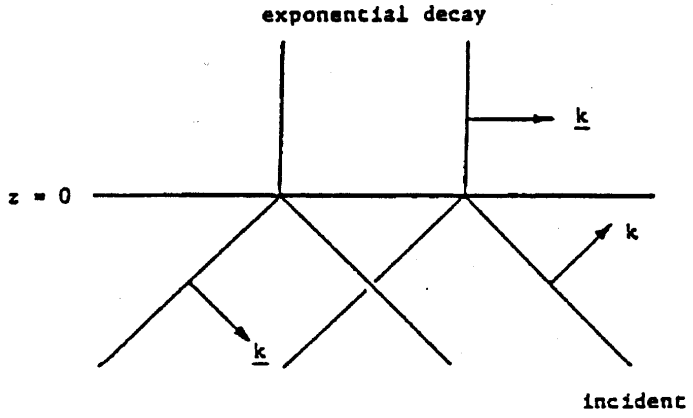

Figure 3.18: Total wave reflection in the case $l_1 < l_2$.

If the lower layer is bounded by a rigid boundary at $z = -h$, then $2\hat{w}(-h) = 0$, implying that $m_2(-h) = 0$. Thus from (3.41), m_2 must satisfy the condition

$$\tan\, m_2 h = -\frac{m_2 h}{|m_1|\, h}. \tag{3.42}$$

It follows that there is an infinite set of values for $m_2 h$ corresponding with the abscissa of points of intersection of the curves $y = \tan\theta$ with the line $y = -\theta/|m_1|h$. The smallest value is such that $\frac{\pi}{2} < m_2 h < \pi$, whence $l_2^2 - k^2 > \pi^2/4h^2$. Since it is assumed that $m_1^2 < 0$, $l_1^2 < k^2$ and therefore, for this mode,

$$l_1^2 < k^2 < l_2^2 - \pi^2/4h^2, \tag{3.43}$$

To illustrate the principles involved in obtaining solutions for trapped lee waves, we assume that the upper layer behaves as a rigid lid for some appropriate range of wavelengths; i.e. we take $\hat{w} = 0$ at the lid, which we now assume to be at $z = H$. A solution of (3.36) satisfying this condition is

$$\psi = Ae^{-ikx} \sin\, m(H - z), \tag{3.44}$$

where $m^2 = l^2 - k^2$ and A is a constant. The general solution may be expressed as a Fourier integral of (3.44):

$$\psi(x, z) = \frac{1}{\sqrt{2\pi}} \int_{-\infty}^{\infty} A(k) e^{-ikx} \sin\, m(H - z) dk. \tag{3.45}$$

Since $w = \psi_x$, the linearized surface condition (3.18) integrates to give $\psi = -Uh(x) + G(z)$, where $G(z)$ is an arbitrary function. But as $x \to -\infty$, $h \to 0$ and $\psi \to 0$ (i.e., the perturbation tends to zero) implying that $G(z) \equiv 0$. Hence, for the Witch-of-Agnesi ridge profile,

$$-\frac{Uh_m}{1+(x/b)^2} = \frac{1}{\sqrt{2\pi}} \int_{-\infty}^{\infty} A(k) e^{-ikx} \sin\, mH\, dk,$$

whereupon

$$A(k)\ \sin\ mH = -\frac{1}{\sqrt{2\pi}} \int_{-\infty}^{\infty} \frac{Uh_m}{1+(x/b)^2} e^{ikx}\, dx = -Uh_m b \left(\frac{\pi}{2}\right)^{1/2} e^{-|k|b},$$

and therefore

$$\psi(x,z) = -\tfrac{1}{2} Uh_m b \int_{-\infty}^{\infty} e^{-|\,k|b - ikx} \frac{\sin\ m(H-z)\ dk}{\sin\ mH}. \tag{3.46}$$

To evaluate this integral, consider

$$I = \int_C e^{-|\,k|b - ikx} \frac{\sin\ m(H-z)}{\sin\ mH} dk, \tag{3.47}$$

in the complex k-plane, where C is a semi-circular contour of radius R, see Fig. 3.19. The integrand has only simple pole singularities where $\sin mH = 0$, or $(l^2 - k^2)^{1/2} H = n\pi$, $(n = 1, 2, ...)$; i.e. where $k^2 = l^2 - (n\pi/H)^2 = k_n^2$, say. Of these, $2N$ lie on the real axis for $N\pi < lH < (N+1)\pi$, and the remainder lie on the imaginary axis. For $x > 0$, we choose the contour in the lower half k-plane so that the contribution from the semi-circular part of C tends to zero as $R \to \infty$, [see Ex. (3.11)], and for $x < 0$ we choose the contour in the upper half plane for the same reason. In each case, we deform the part of the contour along the real axis so that it passes above the poles on that axis and we regard these poles as lying wholly inside the lower contour for reasons discussed below.

The residue at the pole with $k = k_n$ is

$$e^{-|\,k_n|b - ik_n x} \frac{\sin\,(\,n\pi(1 - z/H)\,)}{H\ \cos(n\pi) \frac{1}{2} \left(l^2 - k_n^2\right)^{-1/2} (-2k_n)} = e^{-|\,k_n|b - ik_n x} \frac{n\pi\ \sin(n\pi z/H)}{H^2 k_n}.$$

When $k_n^2 > 0$, assume that $k_n > 0$ and when $k_n^2 < 0$, set $k_n = i$ with ${k_n}^* > 0$, then summing the residues, and remembering that the lower contour is taken clockwise, we obtain the solution:

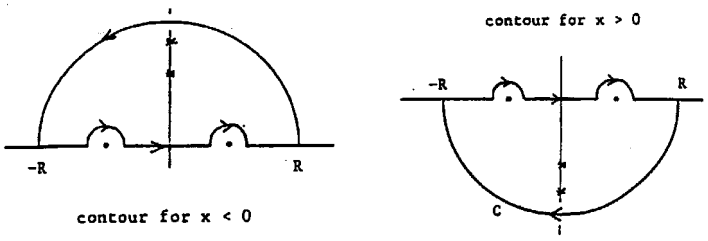

Figure 3.19: Contours for evaluating the integral in (3.47).

$$I = -\frac{4\pi^2}{H^2}\sum_{n=1}^{N} ne^{-k_n b}\frac{\sin k_n x}{k_n}\ \sin\frac{n\pi z}{H}$$

For $x \geq 0$

$$+\ \frac{2\pi^2}{H^2}\sum_{n=N+1}^{\infty} ne^{-k_n^*(b+x)}\frac{1}{k_n^*}\ \sin\frac{n\pi z}{H},$$

and

$$\text{for} \qquad x \leq 0 I = \frac{2\pi^2}{H^2}\sum_{n=N+1}^{\infty} ne^{-k_n^*(b-x)}\frac{1}{k_n^*}\ \sin\frac{n\pi z}{H}.$$

Hence, finally

$$\left.\begin{array}{ll}\psi(x,z) = \psi_1(x,z) + \psi_2(x,z) & \text{for } x \geq 0 \\ \psi(x,z) = \psi_2(x,z) & \text{for } x \leq 0\end{array}\right\} \tag{3.48}$$

where

$$\psi_1(x,z) = \frac{2Uh_m b\pi^2}{H^2}\sum_{n=1}^{N} ne^{-k_n b}\left[\frac{\sin\ k_n x}{k_n}\right]\ \sin\frac{n\pi z}{H},$$

and

$$\psi_2(x,z) = -\frac{Uh_m b\pi^2}{H^2}\sum_{n=N+1}^{\infty}\frac{ne^{-k_n^*(b+|x|)}}{k_n^*}\ \sin\frac{n\pi z}{H}.$$

It is evident from (3.48) that the solution downstream of the mountain consists of two parts: a wavy part represented by $\psi_1(x,z)$, and a part represented by $\psi_2(x,z)$ which decays downstream from mountain. The latter part describes essentially the local distortion of the airstream as it crosses

the mountain, whereas the former, which does not decay downstream, consists of a discrete spectrum of lee waves. As in the previous problem, the lee waves have significant amplitudes only if $k_n b \sim O(1)$. Upstream of the mountain, there is only a local distortion of the flow described by the term $\psi_2(x, z)$. Note that the lee waves arise from the residue contributions at the poles on the real axis and it emerges, therefore, why we chose the contours so as to exclude the contributions from these poles in the upper contour, but include them in the lower contour. Had we done the reverse, the lee wave would have appeared upstream of the mountain. The choice that they be positioned downstream is essentially a radiation condition appropriate for the present problem (see Ex. 3.12). That the Fourier transforms should be interpreted as they have been, with the contributions from the poles counting as if the poles were wholly inside the lower semi-circle and *not on the axis*, follows from a consideration of the slightly viscous problem. With a small amount of viscosity, the poles move off the axis a finite distance into the region Im(k) < 0. The inviscid solution (3.47) emerges as the correct limit to the viscous problem as the viscosity tends to zero.

Although the foregoing analysis applies to a Boussinesq fluid, accurate solutions for a deep atmosphere with the anelastic approximation are obtained simply by multiplying the Boussinesq solutions by $[\rho_o(0)/\rho_o(z)]^{1/2}$ as indicated on page 25.

Figure 3.20 shows an example of the flow over a ridge where the background wind speed and stability vary with height. High above the mountain, the disturbance is composed of vertically-propagating waves with tilted phase lines as in Fig. 3.16. In the lower atmosphere, trapped lee waves are evident extending well downstream. These waves have no phase line tilt. This figure is reproduced from Sawyer (1960).

An observational case study of large amplitude mountain waves over the Rocky mountains near Denver using research aircraft to determine the flow led to the construction of Fig. 3.21. This shows the cross-section of potential temperature normal to the mountain range. Since potential temperature is approximately conserved in the absence of moist processes, the isentropes should correspond with the streamlines, assuming that the flow is steady.

Exercises

(3.1) Obtain the possible phase speeds $c(k)$ and corresponding eigensolutions $\hat{w}(z)$ of Eq. (3.13) for the flow defined in Fig. 3.1 when U and N are constants and $1/H_s \equiv 0$.

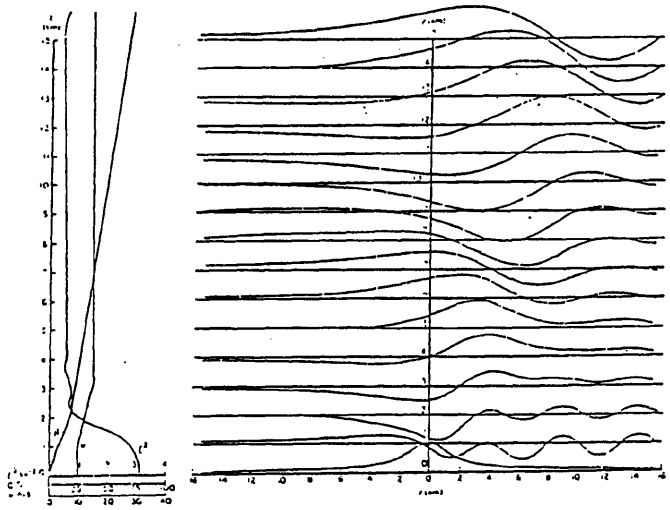

Figure 3.20: A solution showing trapped lee waves.

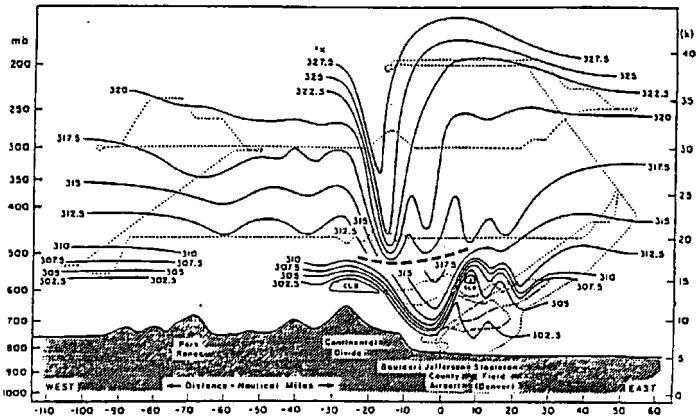

Figure 3.21: Cross-section of potential temperature field (K) during a severe downslope wind situation in the Colorado Rockies on 11 Januray 1972. Surface gusts exceeded 100 knots. The dotted lines are flight tracks. Heavy dashed lines separate measurements taken six hours apart. After Klemp and Lilly, 1975.

(3.2) Obtain the possible phase speeds and corresponding eigensolutions of Eq. (3.13) for the flow defined in Fig. 3.2 when $U \equiv 0$ and N is a constant for $0 \leq z \leq H$. Calculate the largest wave speed for a wave

of 10 km wavelength when $H = 600$ m and the buoyancy period is 5 min. [Hint: you will need to consider solutions to Eq. (3.13) in the subregions $0 \leq z \leq H$ and $H \leq z$ and match these using suitable boundary conditions].

(3.3) Show that when $U_z = 0$ and $H_s =$ constant, Eqs. (3.5) - (3.8) have solutions with $\hat{u}(z) \propto exp(z/2H_s) \times exp(imz)$ etc., which satisfy the dispersion relation $(\omega - Uk)^2 = N^2k^2/(k^2 + m^2 + 1/4H_s^2)$.

(3.4) Show that for a Boussinesq fluid (with $1/H_s = 0$), the energy equation obtained from Eqs. (3.1)-(3.4), analogous to Eq. (2.49), is

$$\frac{\partial E}{\partial t} = -\frac{\partial F}{\partial z} - \rho_* \overline{uw}\, U_z. \tag{3.49}$$

(3.5) Calculate the mean rate of working of pressure forces $\overline{pw}$ at the boundary $z = 0$ for the two solutions (3.24) and (3.25) and show that in the former case, the boundary exerts a drag on the airstream, whereas in the latter case it does not. Show also that, in the former case, there exists a mean downward flux of horizontal momentum $\overline{\rho uw}$ and that this is independent of height and equal to the drag exerted at the boundary.

(3.6) In a two-layer model, a homogeneous fluid with density ρ_1 and moving with uniform speed U_1 overlies a second homogeneous fluid with density ρ_2 and moving with uniform speed U_2. A small amplitude disturbance in the flow is associated with a sinusoidal displacement of the interface $\zeta(x,t) = Re\left[\hat{\zeta}e^{ik(x-ct)}\right]$, where $\hat{\zeta}$ is a constant. If the perturbation streamfunction has structure $\hat{\psi}(z)$, show that continuity of interface displacement and *total* pressure at the mean position of the interface $z = 0$ requires that $\hat{\psi}/(U-c)$ and $-\rho g\hat{\zeta} + \rho(c-U)\hat{\psi}_z$ both be continuous at $z = 0$.

(3.7) Obtain the relationship between a and β in (3.38) when the surface $z = 0$ is a rigid boundary. Hence show that the upper layer in the situation depicted in Fig. 3.18 behaves more and more like a rigid lid as $|m_1|/m_2$ increases.

(3.8) Taking Brunt-Väisälä periods $2\pi/N_1 = 10$ min, $2\pi/N_2 = 5$ min; $U = 20\ ms^{-1}$ and $h = 2$ km, find bounds on the wavelength of the lee wave satisfying the criterion (3.43).

(3.9) Show that the contribution to the integral (3.47) from the appropriate semi-circular part of the contour C tends to zero as the semi-circle radius R tends to infinity.

(3.10) The dispersion relation for internal gravity waves on a uniform flow $U(>0)$ in a Boussinesq Fluid is $(\omega - Uk)^2 = N^2k^2/(k^2+m^2)$. Calculate the x-component u_g of the group velocity, and show that for stationary waves, $u_g = U(kU/N)2$. Observe that for $k_2 > 0$, this is positive. It follows that energy is carried downstream by the waves.

(3.11) The linearized Boussinesq equations for stationary-wave motions in a fluid with Rayleigh friction (coefficient > 0) moving with uniform speed U in the x-direction are

$$Uu_x + P_x = -\mu u,$$

$$Uw_x + P_z = \sigma - \mu w,$$

$$U\sigma_x + N^2 w = 0,$$

$$u_x + w_z = 0.$$

Show that the streamfunction ψ satisfies the equation

$$\frac{\partial}{\partial x}\left[\nabla^2\psi + \frac{N^2}{U^2}\psi\right] = \frac{\mu}{U}\nabla^2\psi,$$

and repeat the analysis given above for trapped lee waves, showing that the solution (3.48) is recovered in the limit as $\mu \to 0$. Observe that, for finite μ, no radiation condition is required as the poles of the integral corresponding with (3.47) lie in the lower half k-plane.

Chapter 4

ENERGETICS OF WAVES ON STRATIFIED SHEAR FLOWS

For a shear flow $U(z)$ in a Boussinesq fluid, the wave-energy equation takes the form (see Ex. 3.4),

$$\frac{\partial E}{\partial t} = -\frac{\partial F}{\partial z} - \rho\overline{uw}\,U_z, \tag{4.1}$$

where E and F are the *mean wave energy density* and the *mean rate of working of the disturbance pressure force* $\overline{pw}$ in the vertical, respectively. In the case of a non-moving medium ($U \equiv 0$), F is interpreted as a *mean flux of wave energy* and equals Ew_g (Ex. 2.11). On account of this result, it is tempting to retain this interpretation of F for a moving fluid and to regard the term $-\rho\overline{uw}U_z$ in (4.1) as a 'source' of mean wave energy associated with the interaction of the wave with the basic shear, U_z. However, we shall see that this interpretation, which appears in the early literature, can be misleading. Accordingly, it is necessary to re-examine what is meant by 'energy flux' in a moving medium. The following discussion is based on unpublished lecture notes of M. E. McIntyre.

To see why $-\rho\overline{uw}U_z$ ought not to be interpreted as an energy source, we consider the equation for the mean flow to second-order in wave amplitude. The full horizontal momentum equation in flux form is[1]:

$$\rho\frac{\partial u^*}{\partial t} + \frac{\partial}{\partial x}\left(\rho u^{*2}\right) + \frac{\partial}{\partial z}\left(\rho u^* w\right) = -\frac{\partial p}{\partial x}, \tag{4.2}$$

where u^* represents here the *total* horizontal wind speed. If we replace u^*

[1]Using the continuity equation $(\rho u)_x + (\rho w)_z = 0$, this readily reduces to the more familiar form.

by $\overline{u}(z,t) + u(x,z,t)$, where u is now the *deviation* from the *mean wind*[2] $\overline{u}$, then (4.2) gives on substitution for u^* and averaging,

$$\rho\frac{\partial\overline{u}}{\partial t} + \frac{\partial}{\partial z}\left(\rho\overline{uw}\right) = 0$$

$$\rho\overline{u_t} + \left(\rho\overline{uw}\right)_z = 0. \tag{4.3}$$

This is the mean flow momentum equation. Assuming that the wave amplitude is sufficiently small, then $v = U(z)$ and $\overline{w} = 0$ and the interaction between the basic flow can be ignored. However, the waves have a second-order effect in amplitude on the mean flow governed by Eq. (4.3)[3]. The mean flow kinetic energy equation is obtained by taking $\overline{u}$ times (4.3) to get

$$\frac{\partial}{\partial t}\left(\tfrac{1}{2}\rho\overline{u}^2\right) = -\overline{u}\,\left(\rho\overline{uw}\right)_z. \tag{4.4}$$

It follows from (4.4) that local second-order changes in the mean flow are associated with nonzero values of the quantity and it is then appropriate that this term appears also as the "source term" in (4.1)[4]. This suggests that (4.1) should be written in the equivalent form

$$\frac{\partial E}{\partial t} = -\frac{\partial}{\partial z}\left(\overline{pw} + U\rho\overline{uw}\right) + U\left(\rho\overline{uw}\right)_z, \tag{4.5}$$

and that the quantity $F = \left(\overline{pw} + U\rho\overline{uw}\right)$ should be interpreted as the total "energy flux" in this problem. We shall refer to it here as the net energy flux, whilst retaining the term wave energy flux for F. Additional insight is obtained by combining (4.4) and (4.5) to give to $O(\varepsilon^2)$ (see footnote 3),

$$\frac{\partial}{\partial t}(E + \rho U\overline{u}_2) = -\frac{\partial}{\partial z}\left(\overline{p_1 w_1} + U\rho\overline{u_1 w_1}\right). \tag{4.6}$$

The term on the left hand side is the net rate of change of wave energy plus mean flow energy, the latter changing because of second-order wave-induced changes in the mean flow $\overline{u}_2$ (the change in mean flow energy being

[2]In problem (2.54), mean refers to an average over a wavelength; i.e. $(\,) = \frac{1}{\lambda}\int_0^\lambda (\,)\,dx$; in some circumstances, other definitions for mean quantities may be more appropriate; e.g. for an non-periodic disturbance which vanishes as $x \to \pm\infty$ we might define $(\,) = \int_{-\infty}^{\infty}(\,)\,dx$.

[3]If $u = \varepsilon u_1 + e^2 u_2 + ...$ etc., and $\overline{u} = U(z) + \varepsilon^{-2}u_2(z,t) + ...$, where $\varepsilon << 1$ and the u_i are $O(1)$, then the mean flow correction due to the presence of the waves satisfies $\rho\overline{u}2_t = -(\rho\overline{u_1 w_1}_z$, assuming that the wave induced mean vertical motion $i\overline{w}$ is zero to $O(\varepsilon^2)$.

[4]Recall that in this particular problem, there is no mean pressure gradient, i.e. $\overline{p}_x = 0$.

$\frac{1}{2}\rho(U+\varepsilon^2\overline{u}_2+\ldots)^2-\frac{1}{2}\rho U^2=\rho U\overline{u}_2$ to $O(\varepsilon^2)$). The second term on the right hand side of (4.6) is the divergence of the vertical advective flux of total kinetic energy, $\frac{1}{2}\rho(U+\varepsilon u_1)^2$ at $O(\varepsilon^2)$, i.e. the divergence of the first nonzero term in the expression $\frac{1}{2}\rho(U+\varepsilon u_1+\ldots)^2\varepsilon w_1$. Note that F is not invariant under Galilean coordinate transformation.

Exercises

(4.1) Show that the perturbation and mean flow equations (4.1) and (4.4) form an energetically closed system in the sense that, for a free wave with $F(0)=0$ and $F\to 0$ as $z\to\infty$,

$$\int_0^\infty \left(E+\tfrac{1}{2}\rho\overline{u}^2\right)dz \textit{ is a} \text{ constant}$$

(4.2) Verify that in the problem represented in Fig. 3.17, the fluxes of transmitted and reflected mean wave energy sum to equal the flux associated with the incident wave.

(4.3) Verify that in the problem represented in Fig. 3.18, the amplitude and hence the mean energy flux of the reflected wave is equal to that of the incident wave. Check directly by computing $\overline{w_1p_1}$ that the mean energy flux associated with the wave in the upper layer is identically zero at all heights.

The perturbation equations for waves in a Boussinesq fluid are:

$$u_t+Uu_x+wU_z=-P_x, \tag{4.7}$$

$$w_t+Uw_x=-P_z+\sigma, \tag{4.8}$$

$$\sigma_t+U\sigma_x+N^2w=0, \tag{4.9}$$

and

$$u_x+w_z=0. \tag{4.10}$$

We look for steady travelling wave solutions of the form

$$(u, w, P, \sigma) = \text{Re}\left[(\hat{u}(z), ...)\, e^{ik(x-ct)}\right]. \tag{4.11}$$

Then Eqs. (4.7)-(4.10) reduce to

$$ik(U-c)\hat{u} + U_z\hat{w} = -ik\hat{P}, \tag{4.12}$$

$$ik(U-c)\hat{w} = -\hat{P}_z + \hat{\sigma}, \tag{4.13}$$

$$ik(U-c)\hat{\sigma} + N^2\hat{w} = 0, \tag{4.14}$$

and

$$ik\hat{u} + \hat{w}_z = 0. \tag{4.15}$$

Setting $V = U - c$, then (4.12) and (4.15) give

$$\hat{P} = \frac{i}{k}(V\hat{w}_z - V_z\hat{w}), \tag{4.16}$$

Equation (4.14) gives

$$\hat{\sigma} = \frac{iN^2}{kV}\,\hat{w}, \tag{4.17}$$

and Eq. (4.13) then gives

$$\hat{P}_z = \left[-ikV + \frac{iN^2}{kV}\right]\,\hat{w}. \tag{4.18}$$

Finally, eliminating P from (4.16) and (4.18) gives

$$\hat{w}_{zz} + \left[\frac{N^2}{V^2} - \frac{V_{zz}}{V} - k^2\right]\,\hat{w} = 0. \tag{4.19}$$

This is identical with (3.13) when $H_s \to \infty$. Now, writing the components of (4.11) in the form

$$u = \frac{1}{2}\hat{u}(z)\, e^{ik(x-ct)} + (\ )^*,$$

where * denotes a complex conjugate, it follows that for any two quantities a and b, selected from the dependent variables,

$$\overline{ab} = \frac{1}{4}\left(\hat{a}\hat{b}^* + \hat{a}^*\hat{b}\right). \tag{4.20}$$

Multiplying (4.9a) by $\rho\hat{w}^*/ik$ and using (4.15) gives

$$(U-c)\,\rho\overline{uw} = -\overline{pw}. \tag{4.21}$$

Adding this equation to its complex conjugate and using (4.20) gives

$$(U-c)\rho\overline{uw} = -\overline{pw}. \tag{4.22}$$

Also, for wave perturbations such as (4.11)

$$F = \overline{pw} + U\rho\overline{uw} = \frac{cF}{c-U} = c\rho\overline{uw}. \tag{4.23}$$

Now, for a steady (in amplitude) sinusoidal wave, $\partial E/\partial t = 0$ and from (4.1) and (4.21),

$$\frac{\partial F}{\partial z} = -\rho\overline{uw}U_z, \tag{4.24}$$

and

$$(U-c)\rho\overline{uw} = -F. \tag{4.25}$$

Eliminating F, it follows that

$$(U-c)\frac{d}{dz}\,(\rho\overline{uw}) = 0,$$

and therefore

$$U = c \quad \text{or} \quad \frac{d}{dz}\,(\rho\overline{uw}) = 0. \tag{4.26}$$

In the latter circumstances, it follows from (4.23) that

$$\frac{dF}{dz} = 0,$$

and from (4.3) that the waves do not force any second-order acceleration of the mean flow. The last result is now known as the *nonacceleration theorem.* It was first obtained in a slightly less general form by Eliassen and Palm (1960) and has been shown to be a quite general result by Andrews and McIntyre (1978). The quantity F is the *total vertical flux of wave energy.* At this point we return to the problem of flow over sinusoidal topography depicted in Fig. 3.6. For waves that radiate vertically ($0 < |k| < l$), there exists a downward flux of mean horizontal momentum ($\rho\overline{uw} < 0$). This is independent of height (consistent with 4.26) and equal to the drag per unit

wavelength exerted by the boundary on the airstream (see Ex. 3.5), namely $-\rho U^2\, mk\, h_m^2$, where $\mathrm{sgn}(mk) > 0$ for upward propagation. Evidently, the momentum flux originates at infinity, where, presumably, the drag exerted by the boundary on the airstream acts. We return to this at first sight puzzling result shortly.

When a general airstream $U(z)$ flows over mountain ridge and produces upward radiating waves, a forward wave drag is exerted on the mountain; in other words, the mountain exerts a drag on the airstream. This raises the important question: how is the stress on the airstream distributed, or, put another way, at what level(s) does the drag act on the mean airstream? For steady waves, the nonacceleration theorem rules out the possibility of interaction except at a *critical level* where $U = c$, a level where the intrinsic frequency of the waves vanishes (see Eq. 3.4). In the case of stationary mountain waves, $c = 0$. Linear theory suggests that at such a level, the wave is almost completely absorbed, leading to a *deceleration* of the mean flow at that level. However, nonlinear and viscous effects may be important near the critical level. We shall not address the critical-layer problem in this course and for further details, the interested reader is referred to the important paper by Booker and Bretherton (1967).

For a propagating wave packet with a spectrum of horizontal phase speeds, there may be a range of critical levels. Then absorption by the mean flow takes place in a finite layer. However, for stationary mountain waves, $c = 0$ for all Fourier components.

4.1 Slowly varying wave trains or wave packets

The analysis of unsteady wave development and of wave propagation in arbitrary shear flows poses severe mathematical difficulties. For example, in the former case, Laplace transform techniques for initial-value problems usually lead to uninvertible transforms[5] and in the latter case, typical eigenvalue problems are analytically intractable, or at best, very complicated. However some analytical progress and further physical insight may be obtained by studying slowly-modulated wavetrains or wave packets, in which the waves are locally plane, with wavelength and amplitude varying significantly only over a space scale of many wavelengths. We sketch here a calculation of

[5] An example given by Booker and Bretherton (1967).

this type[6] performed by Acheson (1976, pp 452 - 455). Acheson investigates waves whose frequency ω and horizontal wavenumber k are constant, but whose amplitude varies with height and time on scales very long compared with one wavelength and one period, respectively. Accordingly, he introduces the 'slow' variables

$$Z \equiv az \text{ and } T \equiv \alpha t,$$

where $\alpha << 1$ is a dimensionless measure of how slowly the wavetrain is modulated in the sense that at any given height/time its amplitude varies by a factor $O(1)$ over a height/time scale of $O(\alpha^{-1})$ wavelengths/periods. His analysis is for a basic shear $(U(Z), 0, 0)$ in a Boussinesq fluid with N constant. Acheson considers linear wave perturbations with streamfunction

$$\psi = \psi_1 + \alpha\psi_2 + \ldots, \tag{4.27}$$

where

$$\psi_n = \text{Re}\left[\hat{\psi}_n(Z,T)e^{i(kx+\theta(z)-\omega t)}\right]. \tag{4.28}$$

Similar expansions are taken for other flow quantities. A local vertical wavenumber defined in terms of the phase function $\theta(z)$ is

$$m(Z) = \frac{d\theta}{dz}. \tag{4.29}$$

The multiple-scaling technique applied to the present problem involves replacing time and height derivatives by $\partial/\partial t + \alpha\partial/\partial T$ and $\partial/\partial z + \alpha\partial/\partial Z$, respectively, whereupon Eqs. (4.7) - (4.10) become

$$u_t + Uu_x + P_x = -\alpha(u_T + wU_Z), \tag{4.30}$$

$$w_t + Uw_x + P_z - \sigma = -\sigma(w_T + P_Z), \tag{4.31}$$

$$\sigma t + U\sigma_x + N^2 w = -\alpha\sigma T, \tag{4.32}$$

$$u_x + w_z = -\alpha w_Z. \tag{4.33}$$

Note that the term describing the effect of vertical shear appears only at order α. As expected, substitution of the expansions for $u,\ w,\ P,\ \sigma$ in Eqs.

[6]Acheson's calculations are for mixed hydromagnetic-gravity waves, but setting the electrodynamical quantities f and h equal to zero gives the result for pure internal gravity waves.

(4.30)- (4.33) gives to $O(\alpha^0)$ a locally-plane wave solution, identical with that which would be obtained if U were a constant. For this solution, it follows readily that

$$\omega^{\star 2} = \frac{N^2 k^2}{k^2 + m^2}, \tag{4.34}$$

where the intrinsic frequency, given by

$$w^\star(Z) = w - kU(Z), \tag{4.35}$$

is a function of Z by virtue of its dependence on $m(Z)$ and $U(Z)$.

At $O(\alpha)$ in the expansion, the equations for subscript '2' quantities become[7]

$$i(w^\star \hat{u}_2 - k\hat{P}_2) = \hat{u}_{1T} + U_Z \hat{w}_1, \tag{4.36}$$

$$i(w^\star \hat{w}_2 - m\hat{P}_2) + \hat{\sigma}_2 = \hat{w}_{1T} + \hat{P}_{1Z}, \tag{4.37}$$

$$i\omega\hat{\sigma}_2 - N^2\hat{w}_2 = \hat{\sigma}_{1T}, \tag{4.38}$$

$$i(k\hat{u}_2 + m\hat{w}_2) = -\hat{w}_{1T}. \tag{4.39}$$

Eliminating $\hat{u}_2$, $\hat{P}_2$, $\hat{\sigma}_2$, say, we obtain an expression of the form

$$\begin{aligned}(\quad)\hat{w}_2 \quad &= \text{expression involving } T \text{ and } Z \text{ derivatives of} \\ &\qquad \text{subscript '1' quantities,}\end{aligned} \tag{4.40}$$

where using (4.34), the coefficient of $\hat{w}_z$ is zero. Thus, the expression on the right-hand-side of (4.40), when set equal to zero, gives a solvability condition for the $O(\alpha)$ problem. After some algebraic manipulation (see Appendix), the solvability condition may be written in the form

$$\frac{\partial A}{\partial T} + \frac{\partial}{\partial Z}(w_g A) = 0 \tag{4.41}$$

where

$$A = E/\omega^*, \tag{4.42}$$

[7]This 4×4 set of linear equations has the general form $Ax = b$, where A is a 4×4 matrix with $\det A = 0$ and x and b are column vectors. It has a nonunique solution, but only if b is orthogonal to the solution y of the adjoint homogenous problem $A'y = 0$.

$$w_g = \frac{\partial \omega}{\partial m}, \tag{4.43}$$

and

$$E = \tfrac{1}{2}(\rho_0(1 + m^2/k^2)\,|\hat{w}_1|^2\,. \tag{4.44}$$

The quantity A is called the *wave action* and, of course, $w_g(Z)$ is simply the *local* vertical component of the group velocity. Thus (4.41) expresses the *conservation of wave action.*

Exercise

(4.4) Assuming that the mean second-order perturbation to the basic flow forced by the foregoing slowly-varying wave varies only with Z and T, the mean horizontal momentum equation (corresponding with (4.3)) may be written (c/f Acheson, 1976, p.455)

$$\alpha\,(\partial \overline{u}_2/\partial t + U_Z \overline{w}) = -\,(\overline{u_1 w_1})_z\,, \tag{4.45}$$

where, from continuity (4.33),

$$\overline{w}_z = 0. \tag{4.46}$$

Show that

$$\rho \frac{\partial \overline{u}_2}{\partial T} = -k \frac{\partial}{\partial Z}(w_g A). \tag{4.47}$$

Moreover, using (4.41), show that if $\overline{u}_2 = 0$ in the absence of waves (i.e., when $A = 0$), then

$$p\overline{u}_2 = \frac{E}{c - U}. \tag{4.48}$$

From (4.41), when the amplitude of the wave is independent of time, it follows that Aw_g is independent of height, and using the result of Ex. (4.2), this means that is independent of height. We have seen already that this is true when the amplitude is steady (c/f 4.19 with 4.25), even when no restriction is placed on how fast U varies over a vertical wavelength. Following Acheson we consider now a wave train of the above type set up by the horizontal translation with speed c of a corrugated boundary at $z = 0$.

The corrugations are assumed to increase gradually in amplitude (from zero at time $t = 0$) on the slow time scale T as governed by the formula

$$z(x, t; T) = A(T) \cos k(x - ct). \tag{4.49}$$

It follows readily from (4.49) that $\overline{w} = 0$ at $z = 0$, whence, by (4.33), $\overline{w} \equiv 0$. As the slowly-modulated wave train propagates upwards past any given level, the local wave energy density, E, will slowly increase to a maximum and (in the absence of dissipation) then diminish again to zero as the wave train passes. According (4.48) the local modification $|\overline{u}_2|$ to the mean flow varies similarly, the mean flow being accelerated (decelerated) if $c > U (c < U)$.

Acheson notes that if the forcing (4.49) slowly attains a constant amplitude A_0 on the time scale T and persists at that amplitude thereafter, the wavetrain will consist of a precursor (which contains $O(\alpha^{-1})$ wavelengths and whose amplitude increases with depth from effectively zero to that amplitude A_0 which the source ultimately attains) and a lower part of constant amplitude A_0 extending all the way down to the source. When U is a constant, so are m and w_g and (4.41) simply reduces to the statement that amplitude modulations propagate upwards at the group velocity; in particular, what we call for convenience the 'front' of the wave train (i.e. the tolerably well-defined highest point at which the amplitude is A_0) moves upwards at this speed. The above situation is depicted in Fig. 4.1.

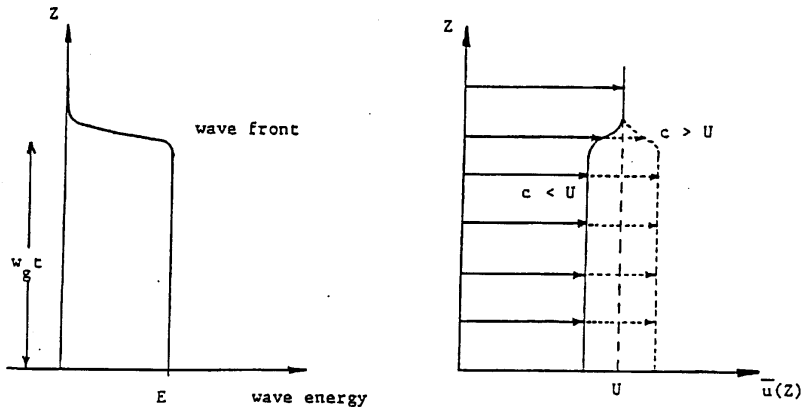

Figure 4.1: Wave energy density as a function of height for a wave source switched on at $z = 0$ at time $t = 0$ (left panel). The mean flow changes are indicated in the right panel. See text for discussion.

We are now in a position to understand the result outlined in the second paragraph on page 54 that for steady flow over sinusoidal topography there is

a downward flux of mean horizontal momentum *from infinity*. If we imagine such a flow to be established by the gradual evolution of the topography as described by (4.49) with $c = 0$, it is evident from the foregoing discussion that the source of the downward momentum flux in the steady wave regime (i.e. at heights below $z = w_g t$) is the deceleration of the mean flow in the region constituting the front of the wave train. At no finite time is there a momentum flux at infinity.

Chapter 5

SHEARING INSTABILITY

In Chapter 3 we studied stable gravity waves, including those modified by shear. The relative effects of stratification and shear are characterized by the Scorer parameter $l(z)$ given by

$$l^2(z) = \frac{N^2}{(U-c)^2} - \left[\frac{d^2U}{dz^2} + \frac{1}{H_s}\frac{dU}{dz}\right]\frac{1}{(U-c)} - \frac{1}{4H_s^2}. \tag{5.1}$$

We consider now the other extreme of sheared motion, possibly modified by stratification. Again, for simplicity, we make the Boussinesq approximation. Cross-differentiating (3.1) and (3.2) and introducing a streamfunction y such that the horizontal vorticity component, $u_z - w_x = \nabla^2\psi$, gives

$$\left[\frac{\partial}{\partial t} + U\frac{\partial}{\partial x}\right]\nabla^2\psi - \frac{\partial\psi}{\partial x}\frac{d^2U}{dz^2} = -\frac{\partial\sigma}{\partial x}. \tag{5.2}$$

5.1 Helmholtz instability

To begin with let us assume that buoyancy effects are unimportant ($\sigma \approx 0$) and suppose that $U(z)$ changes from one relatively uniform value to another in a small height interval. This situation may be idealized by the uniform flow of inviscid fluid with speed U_1 above $z = 0$ past fluid of the same density moving uniformly at speed U_2 below $z = 0$, as shown in Fig. 5.1. The interface $z = 0$ may be regarded as a vortex sheet. We consider small-amplitude perturbations to this basic flow of the form

$$\psi = \hat{\psi}(z)e^{ik(x-ct)}, \tag{5.3}$$

where $\hat{\psi}$ and c are constants. The quantity c is determined as a function of k from an eigenvalue problem and turns out to be complex. Thus, the phase

speed of the wave is $Re[c]$. Substitution of (5.3) into the vorticity Eq. (5.2) gives

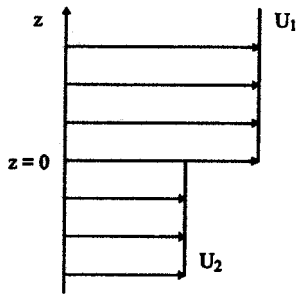

Figure 5.1: Vortex sheet model for Helmholtz instability.

$$\frac{\partial^2 \hat{\psi}}{\partial x^2} - k^2 \hat{\psi} = 0, \tag{5.4}$$

except at $z = 0$ where Uzz is unbounded. Bounded solutions of (5.4) in the two regions $z > 0$ and $z < 0$ are:

$$\begin{aligned} \hat{\psi}_1 &= A_1 e^{-kz} \quad z > 0, \\ \hat{\psi}_2 &= A_2 e^{kz}, \quad z < 0. \end{aligned} \tag{5.5}$$

These are related at $z = 0$ by boundary conditions expressing the requirements that the pressure along the vortex sheet and displacement of the sheet, $z = \xi(x, t)$, are continuous (as usual the condition is linearized to $z = 0$). It follows from the result of Ex. (3.6) that $\psi/(c - U)$ and $(c - U)d\psi/dz$ must be continuous at $z = 0$. From these conditions it is easily deduced that

$$c = \tfrac{1}{2}(U_1 + U_2) \pm \tfrac{1}{2}(U_1 - U_2). \tag{5.6}$$

Thus, from (5.3) we see that a perturbation of wavelength $2\pi/k$ travels with the average flow speed $\frac{1}{2}(U_1 + U_2)$ and grows (or decays) exponentially with time. The growth rate kc_i is proportional to $k(U_1 - U_2)$, i.e. short waves grow faster than long waves and that the degree of instability increases as $|U_1 - U_2|$ increases. In practice, viscosity inhibits rapid growth of the very short waves and there exists a finite wavelength at which the growth rate is a maximum.

5.2 Kelvin-Helmholtz instability

It happens frequently in the atmosphere that the region of strong shear coincides with a sharp, stable density gradient. We model this situation by supposing that the fluid densities in Fig. 5.1 are ρ_1 and ρ_2 with $\rho_1 < \rho_2$, a statically-stable configuration.

Exercise

(5.1) Using the interfacial boundary condition in Ex. (3.6), show that the complex phase speed in the case of Kelvin-Helmholz perturbations is

$$c = \frac{\rho_1 U_1 + \rho_2 U_2}{\rho_1 + \rho_2} \pm \left[c_0^2 - \rho_1 \rho_2 \left[\frac{U_1 - U_2}{\rho_1 + \rho_2} \right]^2 \right]^{\frac{1}{2}}, \tag{5.7}$$

where

$$c_0^2 = \frac{g}{k} \left[\frac{\rho_2 - \rho_1}{\rho_2 + \rho_1} \right] \tag{5.8}$$

is the speed of interfacial waves in the absence of mean currents (i.e. when U_1 and U_2 are both zero).

It is evident from (5.7) that Kelvin-Helmholz flow is unstable to small-amplitude perturbations [with $Im(c) > 0$] when

$$\rho_1 \rho_2 \left[\frac{U_1 - U_2}{\rho_1 + \rho_2} \right]^2 > c_0^2. \tag{5.9}$$

The occurrence of Helmholtz- and Kelvin-Helmholz instability may be attributed to a redistribution of vorticity in the vortex sheet by the disturbance. Let us view the perturbation in the frame of reference in which it is stationary. Then, assuming that $(\rho_2 - \rho_1) << (\rho_2 + \rho_1)$, the upper and lower fluids move in opposite directions with equal magnitude U. Suppose the vortex sheet is instantaneously distorted into a sinusoidal shape without there being a change in vorticity distribution in the x-direction (Fig. 5.2). Consider the velocities induced at various places on the sheet, indicated by straight arrows. Note that the vorticity, indicated by curved arrows, is everywhere clockwise. At a wave crest (e.g. at B) there is no component of induced velocity in the z-direction (by symmetry), but there is a net component in the x-direction, arising from the induced effects of neighbouring elements. Similarly at a wave trough (e.g. at D), there is a net component in the negative x-direction. Now a positive net component of induced x-velocity

in the parts of the sheet for which the vertical displacement is upward results in a drift of vorticity to the right while the reverse is true for parts of the sheet displaced downwards; see Fig. 5.3. The vorticity redistribution induces continued displacements of the troughs and ridges in a "runaway process" as illustrated.

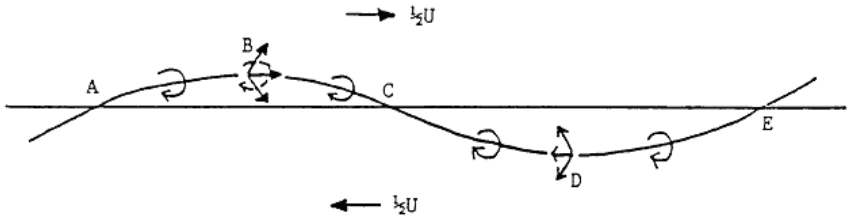

Figure 5.2: Vortex-sheet model illustrating Helmholtz and Kelvin-Helmholtz instability. See text for discussion.

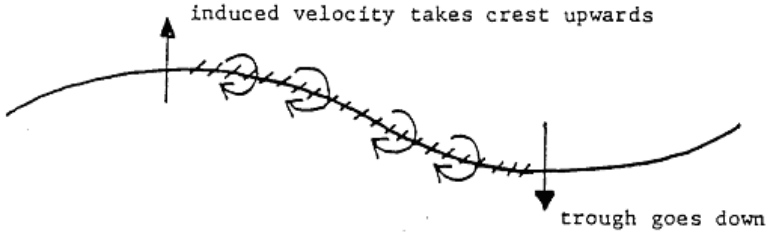

Figure 5.3: Vorticity evolution in Helmholtz and Kelvin-Helmholtz instability.

The existence of a regime of stable wavelengths in the case of Kelvin-Helmholtz (KH-) instability, as implied by (5.9) with (5.8), can be attributed to the stabilizing effect of the density contrast. An alternative interpretation of this instability which incorporates the role of static stability is as follows (see Fig. 5.4). We may regard the stability criterion (5.9) as a measure of the pressure suction or Bernoulli effect (the second term in brackets in Eq.(5.7)), compared with the gravitational restoring effect (the first term in brackets in Eq.(5.7)). When the former exceeds the latter, a stable gravity wave is not possible. Note that c_o^2 increases with decreasing wavenumber (increasing wavelength) and so, therefore, must the effective gravitational stability. Hence there is a long wave "cut-off", a wavelength above which all waves are stable. Of course, this follows from (5.8) and (5.9).

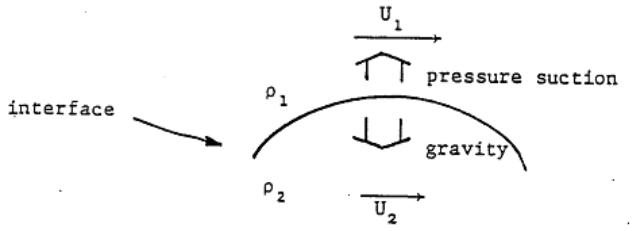

Figure 5.4: Force balance in Kelvin-Helmholz instability.

A sequence of diagrams illustrating the development of a Kelvin-Helmholz wave to *finite amplitude* is shown in Fig. 5.6. The figure is adapted from Scorer's book *Clouds of the World* (see especially Chapter 6 therein), which contains also some fine photographs of atmospheric manifestations of Kelvin-Helmholz instability as well as photographs of related laboratory experiments by Thorpe (1971). As described in Scorer *op cit.*, the Kelvin-Helmholz mechanism is probably the reason for the occurrence of 'billow clouds' in the atmosphere and is thought to be an important mechanism for the generation of clear air turbulence (CAT) in the middle and upper troposphere (see Bretherton, 1971). Figure 5.5 shows an example of clouds associated with Kelvin-Helmholz instability.

Figure 5.5: Clouds associated with Kelvin-Helmholz instability.

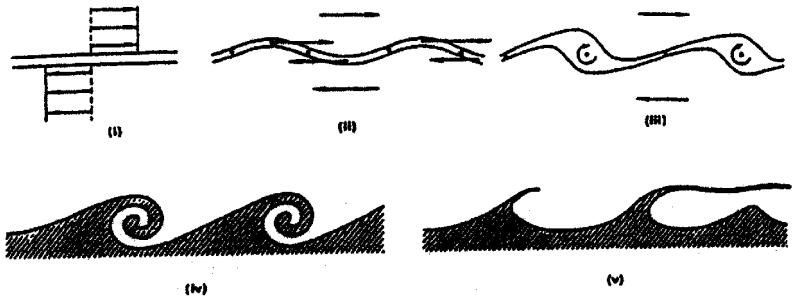

Figure 5.6: Sequence illustrating the growth of finite amplitude Kelvin-Helmholz waves. The following commentary is adapted from Scorer. (i) When the layer is undisturbed the upper and lower layers move in opposite directions with uniform speeds. (ii) The crests and troughs of any transverse corrugations are transported in the direction of the layer into which they penetrate. (iii) The vorticity is accumulated by the thickening of the layer at alternate nodes of the original wave form. The layer is thinned at the other nodes. (iv) The layer becomes rolled up into traverse billows. If the bottom fluid only is visible the appearance is rather like 'breaking' waves (but the mechanism is actually quite different from the breaking of waves on a sloping beach). (v) If the instability is checked by a reduction in the velocity difference between the fluids, the vortex layer does not roll up, but may have cusped waves on it from which thin filaments of the lower layer are carried embedded in the upper layer. These waves are not symmetrical and no material of the upper layer penetrates into the lower. For this to happen the upper fluid must usually be mixed up by turbulence while the flow in the lower fluid is laminar.

5.3 The Richardson number criterion for Kelvin-Helmholz instability

To better understand the criterion (5.9) for instability, suppose that the vortex sheet and density contrast have a finite depth scale h (Fig. 5.7). Then the velocity shear $U' = (U_1 - U_2)/h$, the density gradient $\rho' = (\rho_2 - \rho_1)/h$, and the static stability parameter analogous to N^2 is $-g(\rho_1 - \rho_2)/h$, where is the mean density $(\rho_2 + \rho_1)$. Assuming $(\rho_2 - \rho_1)$, the criterion (5.9) takes the form

$$\tfrac{1}{4}(U_1 - U_2)^2 > \tfrac{1}{2}g(\rho_2 - \rho_1)/\overline{\rho}k,$$

or

$$Ri = \frac{N^2}{U'^2} < \frac{1}{2}kh. \tag{5.10}$$

The nondimensional quantity Ri is called the *Richardson number*. It is a measure of the stabilizing effect of the stratification compared with the destabilizing effect of the shear.

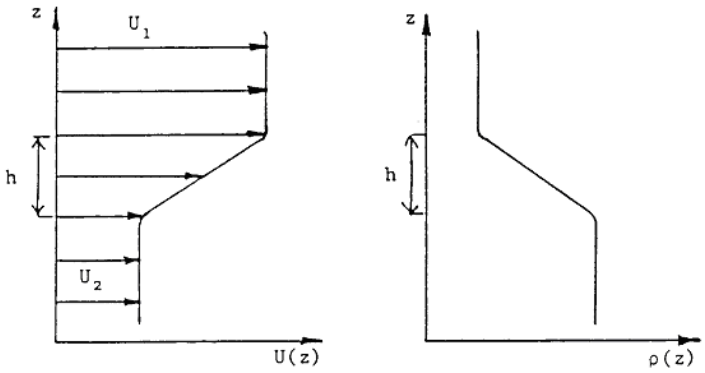

Figure 5.7: A uniform shear-layer model for Kelvin-Helmholz instability.

Exercise

(5.2) Show that the phase speed c for small-amplitude Helmholtz waves with wavenumber k on the finite shear layer with

$$U(z) = \begin{cases} U_1\,, & h \le z\,, \\ U_2 + (U_1 - U_2)z/h, & 0 \le z \le h\,, \\ U_2\,, & z \le 0\,, \end{cases}$$

where U_1, U_2, and h are constants, is given by

$$\left[c - \frac{1}{2}\left(U_1 + U_2\right)\right]^2 = \frac{\left(U_1 - U_2\right)^2}{4k^2h^2}\left[(1-kh)^2 - e^{-2kh}\right].$$

Show that the threshold for instability occurs when kh is about 1.3.

With the threshold value of 1.3 for kh as obtained in problem (5.3) for the case of no stratification, the Richardson number criterion (5.10) gives $Ri < 0.65$ for instability.

5.4 An energy criterion

Consider a shallow layer of fluid of depth $2H$ in which the shear and static stability may be assumed to be constant (see Fig. 5.8). We suppose that the layer is completely mixed by some process and pose the question: does the total energy (kinetic + potential) increase or decrease? Assume that no net work is done by the pressure field as a consequence of the mixing process. Then the momentum and sensible energy must be the same as before the mixing, whereupon $U = 0$ and $\theta = \Theta$ in the final state. It follows that:

$$\begin{aligned} \text{Change in } KE &= \Delta KE = \int_{-H}^{H} \tfrac{1}{2}\overline{\rho}\left[U^2 - (U+\alpha z)^2\right] dz = -\tfrac{1}{3}\overline{\rho}\, H^3\alpha^2 \\ \text{Change in } PE &= \Delta PE = \int_{-H}^{H} g(\rho_F - \rho_I) z dz, \end{aligned}$$

where ρ_I and ρ_F are the initial and final densities. At a given height z, there is no pressure change (to lowest order) so that

$$\frac{\Delta\rho}{\rho} = (1-\kappa)\frac{\Delta p}{p} - \frac{\Delta\theta}{\theta} \quad \text{or} \quad \frac{\Delta\rho}{\rho} = \frac{\rho_F - \rho_I}{\overline{\rho}} = \frac{\theta_I - \theta_F}{\Theta} = \frac{\beta z}{\Theta}$$

whereupon $\Delta PE = (\bar{\rho} g\beta/\Theta)\int_{-H}^{H} z^2 dz = \frac{2}{3}\overline{\rho} g\beta H^3/\Theta$. Hence, the total energy is decreased if $\Delta\,(KE + PE) < 0$, i.e. if $\frac{1}{3}\overline{\rho} H^3\,(2g\beta/\Theta - \alpha^2) < 0$, implying that $Ri < \frac{1}{2}$.

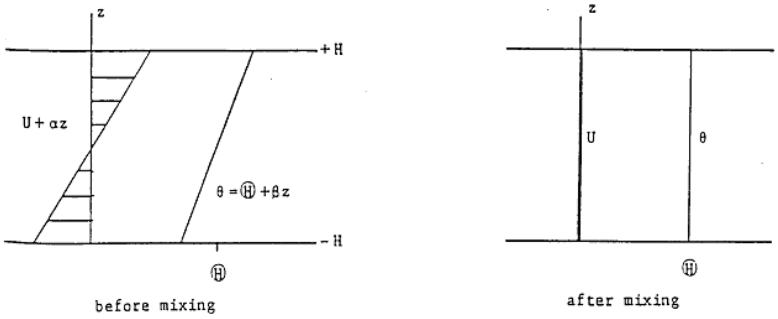

Figure 5.8: Before and after states in the complete mixing of a uniform shear layer with a uniform potential-temperature gradient.

Most analytic investigations suggest that $Ri = \frac{1}{4}$ is the critical Richardson number for instability (see below). According to J.S.A. Green (*unpublished*

lecture notes), the discrepancy between this value and the value obtained from energy arguments may be associated with the fact that such theories assume laminar flow; in these, momentum is transferred ('mixed') by pressure forces, but potential temperature is not.

5.5 Instability of stratified shear flows

The starting point for the inviscid theory is the Boussinesq system of Eqs. (4.7) - (4.10). We introduce the quantity $h(x, z, t)$ to represent the vertical displacement of a fluid parcel. Then, for small displacements, h satisfies the linearized equation

$$\frac{\partial \eta}{\partial t} + U\frac{\partial \eta}{\partial x} = w. \tag{5.11}$$

Assuming, as before, a disturbance of the form

$$\eta(x, z, t) = \hat{\eta}(z)e^{ik(x-ct)}, \text{etc}\ldots, \tag{5.12}$$

Eq. (5.11) gives

$$\hat{w} = ikV\hat{\eta}. \tag{5.13}$$

Substitution (5.13) into (4.19) gives, after a little algebra,

$$\frac{d}{dz}\left[V^2\frac{d\hat{\eta}}{dz}\right] + [N^2 - k^2V^2]\hat{\eta} = 0. \tag{5.14}$$

Let us consider a flow between horizontal rigid boundaries at $z = 0$ and $z = d$. Then

$$\hat{\eta}(0) = \hat{\eta}(d) = 0. \tag{5.15}$$

Alternative boundary conditions for a free surface or interface are easily formulated. We shall prove the following result:

Miles Theorem

If the Richardson number $Ri = \frac{N^2}{(dU/dz)^2} \geq \frac{1}{4}$ everywhere, then the flow is stable.

Proof

Put $G(z) = V^{1/2}(z)$. Then $V^{1/2}(d\hat{\eta}/dz) = dG/dz - (1/2V)(dV/dz)G$. Now Eq. (5.14) may be manipulated to give

$$V^{1/2}(d/dz)[V^{3/2}d\hat{\eta}/dz] + \tfrac{1}{2}(dV/dz)/V^{1/2})[V^{3/2}\hat{\eta}] + [N^2 - k^2V^2]\hat{\eta} = 0,$$

and substitution for $d\hat{\eta}/dz$ and $\hat{\eta}$ gives, with a little more algebra,

$$\frac{d}{dz}\left[V\frac{dG}{dz}\right] - \left[\frac{1}{2}\frac{d^2U}{dz^2} + k^2V + \frac{1}{V}\left(\frac{1}{4}\left(\frac{dU}{dz}\right)^2 - N^2\right)\right]G = 0. \qquad (5.16)$$

Multiply this equation by the complex conjugate G^* of G and integrate with respect to z from 0 to d, noting that

$$\int_0^d G^*\frac{d}{dz}\left|V\frac{dG}{dz}\right|dz = \int_0^d G^* d\left|\left(V\frac{dG}{dz}\right)\right| - \int_0^d V\frac{dG}{dz}\frac{dG^*}{dz}\,dz \text{ using 5.15.}$$

Then

$$\int_0^d [V\left(\left|\frac{dG}{dz}\right|^2 + k^2\left|G\right|^2\right) + \tfrac{1}{2}\frac{G}{V}\frac{d^2U}{dz^2}\left|G\right|^2 + \left[\frac{1}{4}\left(\frac{dU}{dz}\right)^2 - N^2\right]V^*\left|\frac{G}{V}\right|^2 dz = 0. \qquad (5.17)$$

If $c_i \neq 0$, the imaginary part of (5.17) gives

$$\int_0^d \left(\left|\frac{dG}{dz}\right|^2 + k^2\left|G\right|^2\right)dz + \int_0^d \left[N^2 - \frac{1}{4}\left(\frac{dU}{dz}\right)^2\right]\left|\frac{G}{V}\right|^2 dz = 0. \qquad (5.18)$$

If $N^2 > \frac{1}{4}(dU/dz)^2$ i.e. if $Ri > \frac{1}{4}$, Eq. (5.18) implies that k and dG/dz are identically zero. This, in turn, implies that G = constant = 0 using (5.15) or (5.18). Hence, if $Ri \geq \frac{1}{4}$ everywhere, the flow is stable. **q.e.d**.

5.6 Howard's semi-circle theorem

The complex wave speed c of any unstable mode must lie inside the semi-circle in the upper half of the c-plane with the range of U as its diameter.

Proof

Assume that $c_i \neq 0$, multiply (5.14) by $\hat{\eta}\star$ and integrate, using (5.15), to obtain

$$\int_0^d (U-c)^2 \left(\left| \frac{d\hat{\eta}}{dz} \right|^2 + k^2 \left| \hat{\eta} \right|^2 \right) dz = \int_0^d N^2 \left| \hat{\eta} \right|^2 dz. \tag{5.19}$$

With $Q = |d\hat{\eta}/dz|^2 + k^2|\hat{\eta}|^2$, the real part of this equation gives

$$\int_0^d (U-c_r)^2 - c_i^2]Q dz = \int_0^d (N^2|\hat{\eta}|^2 dz, \tag{5.20}$$

and the imaginary part gives

$$\int_0^d UQ dz = c_r \int_0^d Q dz. \tag{5.21}$$

Using (5.21), Eq. (5.20) gives

$$\int_0^d [U^2 - (c_r^2 + c_i^2)]Q \; dz - \int_0^d N^2 \left| \hat{\eta} \right| dz = 0 \tag{5.22}$$

Now

$$\begin{aligned} 0 &\geq \int_0^d (U - U_{\min})(U - U_{\max})\, Q\, dz \\ &= \int_0^d [U^2 - U)(U_{\min} + U_{\max}) U_{\min} U_{\max}]\, Q\, dz \\ &= \int_0^d [c_r^2 + c_i^2 - (U_{\min} + U_{\max})\, c_r + U_{\min} U_{\max}]\, Q\, dz + \underbrace{\int_0^d N^2 |\hat{\eta}|^2 dz}_{\text{positive definite}} \end{aligned}$$

It follows that

$$c_r^2 + c_i^2 - (U_{min} + U_{max}) c_r + U_{min} U_{max} \leq 0,$$

or

$$[c_r - \tfrac{1}{2}(U_{min} + U_{max})]^2 + c_i^2 \leq [\tfrac{1}{2}(U_{max} - U_{min})]^2. \tag{5.23}$$

Hence in the complex plane, a point representing c lies in the circle with diameter along the real axis, extending from $(U_{min}, 0)$ to $(U_{max}, 0)$. Only

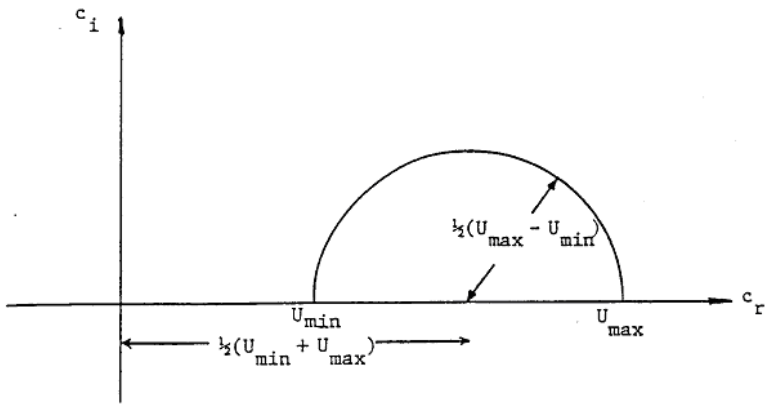

Figure 5.9: Semi-circle in Howard's theorem.

values $c_i > 0$ are significant. Hence all eigenvalues c of unstable modes lie in the semi-circle (see Fig. 5.9).

From (5.18) we can obtain a bound on the growth rate of an unstable wave. Since $|U - c_r - ic_i|^2 \geq c_i^2$, $|V|^{-2} \leq c_i^{-2}$ and hence from (5.18),

$$\begin{aligned} k^2 \int_0^d |G|^2 dz &= \int_0^d (\tfrac{1}{4}U_z^2 - N^2)|G/V|^2 dz - \int_0^d |G_z|^2 dz \\ &\leq c_i^{-2} \max(\tfrac{1}{4}U_z^2 - N^2) \int_0^d |G|^2 dz \\ k^2 c_i^2 &\leq \max(\tfrac{1}{4}U_z^2 - N^2) \end{aligned}$$

Note that this result contains Miles' theorem for if $N^2 > \frac{1}{4}U_z^2$, $k^2 c_i^2 \leq 0$ and the flow is stable.

Chapter 6

QUASI-GEOSTROPHIC WAVES

Both here and in DM we have studied a variety of wave motions in rotating and/or stratified fluid system. Table 6 summarizes the important types.

In this chapter we shall be concerned with quasi-geostrophic waves, of which 'extra-tropical' Rossby waves are a special type. The culmination of the chapter is a unified treatment of baroclinic instability. The chapter is based on unpublished lecture notes kindly provided by M. McIntyre.

The quasi-geostrophic equations for a Boussinesq fluid with constant Brunt-Väisälä frequency (DM, Chapter 8) may be written as

$$\left(\frac{\partial}{\partial t} + u \cdot \nabla\right) q = 0, \tag{6.1}$$

and

$$\left(\frac{\partial}{\partial t} + u \cdot \nabla\right) \frac{\partial \psi}{\partial z} + \frac{N^2}{f} w = 0, \tag{6.2}$$

Table 6.1: Types of wave motion in the atmosphere and oceans

balanced state	elastostatic (compressible)	hydrostatic	geostrophic	Sverdrup
result of disturbing it	acoustic oscillations	inertial gravity waves $w >> f$	inertia or inertia-gravity waves $w \sim f$	Rossby waves $w << f$

where

$$\mathbf{u} = \mathbf{k} \wedge \nabla\psi, \tag{6.3}$$

and

$$q = \nabla^2\psi + f + f^2\frac{\partial}{\partial z}\left(\frac{1}{N^2}\frac{\partial\psi}{\partial z}\right). \tag{6.4}$$

Here $\mathbf{u}$ is the horizontal velocity vector, $\boldsymbol{\psi}$ is the geostrophic streamfunction (proportional to the pressure), w the vertical velocity component, q the *quasi-geostrophic potential vorticity*, N the Brunt-Väisälä frequency and $f = f_0 + \beta y$ is the Coriolis parameter.

Equation (6.1) expresses the conservation of q for parcels moving with the geostrophic wind $\mathbf{u}$, while Eq. (6.2) relates the buoyancy changes following a parcel due to its vertical motion in the presence of density stratification, characterized by N. Henceforth we shall take N^2 to be a constant and define $\varepsilon = f^2/N^2$.

Recall (DM, Chapter 8) that an important scaling assumption in the derivation of (6.1) and (6.2) is that the Burger number, $B = f^2L^2/N^2H^2$, is of order unity, H and L being vertical and horizontal length scales for the motion. Indeed, it can be shown that this ratio characterizes the relative magnitude of the final term in (6.2) compared with the advective term. Thus $B \sim 1$ implies that there is significant coupling between the buoyancy field and the vertical motion field. A further implication is that $L \sim L_R = NH/f$, the Rossby radius of deformation.

The principle behind the method of solution of the quasi-geostrophic equations is outlined in DM, Chapter 8. The steps are briefly as follows:

1. Calculate q and $\mathbf{u}$ from (6.4) and (6.3), respectively, from initial data on ψ at time t.

2. Predict q at time $t + \delta t$ using (6.1).

3. Solve for ψ at time $t + \delta t$ using (6.4).

4. Solve for $\mathbf{u}$ at time $t + \delta t$ using (6.3).

Equation (6.2) can be used to evaluate w, and to provide a horizontal boundary condition on ψ. The latter is required when (6.4) is solved as a Poisson equation for ψ, given q. An example of the use of (6.2) is provided by the Eady baroclinic instability calculation in DM, Chapter 9; see Eq. (9.6). The ability to calculate ψ from (6.4) from a knowledge of q (step 3)

is sometimes referred to as the *invertibility principle*. The foregoing steps will be invoked in the discussion that follows shortly. We shall show that *perturbations of a horizontal basic potential vorticity gradient lead to waves.*

We study only quasi-geostrophic perturbations described by (6.1) - (6.4); these should not be confused with the much more rapidly oscillating inertia-gravity waves that result from disturbing the geostrophic-hydrostatic balance. This balance is built into the quasi-geostrophic theory; in other words, inertia-gravity waves are filtered out by the quasi-geostrophic approximation.

Consider a perturbation to the basic zonal flow $\overline{u}(y,z)$. The perturbation forms of (6.1) and (6.2) may be written as

$$(\partial_t + \overline{u}(y,z)\partial_x)q + \overline{q}_y\psi_x = 0, \tag{6.5}$$

and

$$(\partial_t + \overline{u}(y,z)\partial_x)\psi_z - \overline{u}_z\psi_x + (f/\varepsilon)w = 0, \tag{6.6}$$

where q and ψ represent perturbation quantities and ∂_t, ∂_x are a shorthand notation for $\partial/\partial t$ and $\partial/\partial x$, respectively. Assuming that N is constant, q and ψ are governed by the diagnostic equation:

$$\psi_{xx} + \psi_{yy} + \varepsilon\psi_{zz} = q, \tag{6.7}$$

and the basic potential vorticity gradient in (6.5) is given by

$$\overline{q}_y(y,z) = \beta - \overline{u}_{yy} - \varepsilon\overline{u}_{zz}. \tag{6.8}$$

Example 1. Rossby waves [let $\overline{u} \equiv 0$, $\overline{q}_y = \beta(> 0)$].

The physical picture is based on the conservation of total potential vorticity (here $\overline{q} + q$) for each particle, expressed by Eq. (6.5); c/f the discussion in DM, Chapter 6. Then $\overline{q}_y > 0$ implies that for a positive northwards displacement $\xi > 0$, $q < 0$; and for a southwards displacement $\xi < 0$, $q > 0$.

As in DM, we consider for simplicity motions for which $\partial_x >> \partial_y$, ∂_z, although the arguments can be extended more generally. Then (6.7) becomes

$$\psi_{xx} = q. \tag{6.9}$$

This is, in effect, a one-dimensional Poisson equation, and the structure of solution can be deduced by using the stretched string analogy [the lateral

displacement ψ of a stretched string in equilibrium under the lateral force distribution $-q(x)$ is solved by (6.9); see Exercise (6.1).]

Suppose each string of particles along lines of latitude (y = constant) is given a sinusoidal meridional (north-south) displacement $\xi(x)$, as shown in Fig, 6.1a. Then the corresponding perturbation in potential vorticity for each string, $q(x)$, is as shown in Fig. 6.1b. From this, and using the string analogy (keeping in mind that a positive force is analogous to a negative q) we deduce the streamfunction distribution shown in Fig. 6.1c and finally, using the second component of (6.3), $v = \psi_x$, we infer the meridional velocity component to have the variation shown in Fig. 6.1d. Comparison of the meridional displacement (Fig. 6.1a) with the meridional velocity (Fig, 6.1d) shows that:

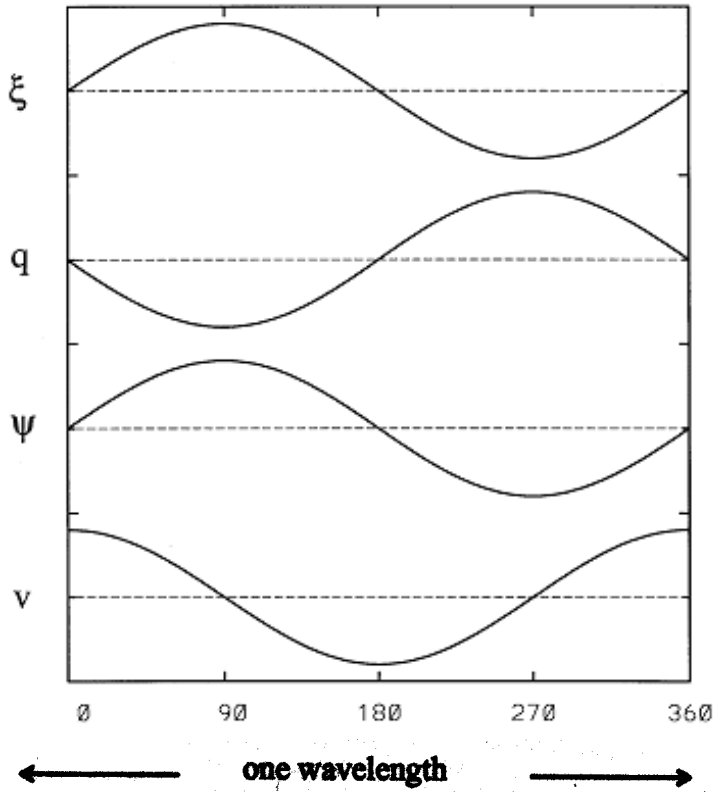

Figure 6.1:

(i) that the disturbance propagates westwards, and

(ii) since the longitudes of displacement maxima are places of zero velocity,

the wave amplitude does not vary with time; in particular, the wave is stable.

Example 2. Topographic waves $\overline{u} \equiv 0$; $\overline{q}_y = \beta = 0$ (but see later!).

.

We assume now a slightly sloping lower boundary. The configuration is sketched in Fig. 6.2. Equation (6.5) reduces in this case to

$$\partial_t q = 0. \tag{6.10}$$

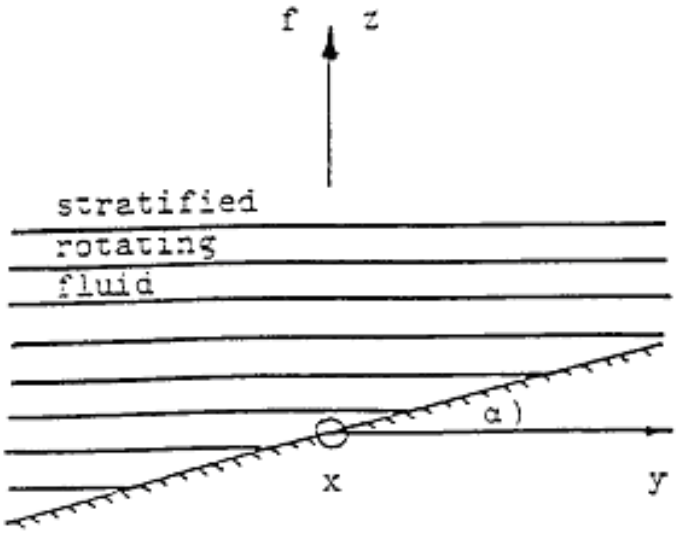

Figure 6.2:

The boundary condition at the (lower) sloping boundary is

$$w = \tan \alpha \psi_x \quad \text{at} \quad z = \alpha y.$$

Now α must be no larger than $O(RoH/L)$, otherwise the implied w for a given v would be too large to be accommodated within quasi-geostrophic theory. But if $\alpha << 1$ we can approximate $\tan \alpha$ by α and can apply the foregoing boundary condition at $z = 0$ with sufficient accuracy; i.e.,

$$w = \alpha \psi_x \quad \text{at} \quad z = 0. \tag{6.11}$$

It may be easily verified that there exist plane wave solutions for ψ of the form

$$\psi = a \ \exp \ \left[i(kx + ly - \omega t) - (N/f)(k^2 + l^2)^{1/2} z \right], \tag{6.12}$$

where, to satisfy (6.6)together with (6.11),

$$\omega = \frac{-\alpha \ Nk}{(k^2 + l^2)^{1/2}}. \tag{6.13}$$

This is the *dispersion relation*. It follows that the wave propagates to the left of upslope (towards negative x). Note that ω does not depend on f. This does not mean that f is unimportant; in fact for a horizontal wavelength $2\pi/\kappa$, where $\kappa^2 = k^2 + l^2$, the e-folding vertical scale of the wave is $f/(Nk)$ as can be seen from (6.12).

In this example, changes in *relative vorticity* ξ arise from stretching and shrinking of vortex lines at the rate fw_z, associated with the differences between the slope of the boundary and those of the density isopleths. Above the boundary, $\overline{q}_y \equiv 0$, but we can say that there is a potential vorticity gradient *at the boundary* if we make the following generalization of the notion of potential vorticity. The foregoing problem can be written as

$$\partial(\psi_{xx} + \psi_{yy} + \varepsilon\psi_{zz}) = 0, \tag{6.14}$$

with

$$(f/N^2)\psi_{zt} + \alpha\psi_x = 0 \quad \text{at } z = 0. \tag{6.15}$$

It is mathematically equivalent to the problem:

$$\partial_t(\psi_{xx} + \psi_{yy} + \varepsilon\psi_{zz}) + \overline{q}_y\psi_x = 0 \tag{6.16}$$

with

$$\overline{q}_y = f\alpha\delta(z), \tag{6.17}$$

and

$$\psi_z = 0, \ \text{continuous } at \ z = 0-, \tag{6.18}$$

where $\delta(z)$ is the Dirac delta function. This is because $\delta(z) \equiv 0$ for $z > 0$; hence (6.14) and (6.16) are identical for $z > 0$. Moreover, integrating (6.16)

with respect to z from $0-$ to $0+$ (i.e., taking $\int_{-\tau}^{\tau}(\ )$ and letting $\tau \to 0$, we obtain[1] (6.15).

The alternative formulation expressed by Eqs. (6.16) - (6.18) involves a potential vorticity gradient $\overline{q}_y$ confined to a "sheet" at $z = 0$, and the wave motion can be attributed to this. Note that it is of no formal consequence in the quasi-geostrophic theory whether the boundary is considered to be exactly at $z = 0$, or only approximately at $z = 0$. What matters dynamically is the slope of the isopleths relative to the boundary.

Example 3. Waves on vertical shear

Let $\beta = 0$ and $\overline{u} = \Lambda_z$, Λ constant. Then again $\overline{q}_y \equiv 0$, but now we assume a horizontal lower boundary.

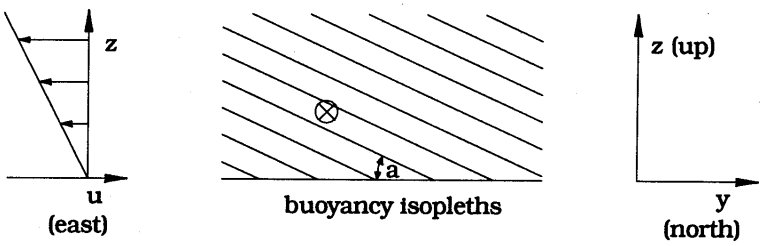

Figure 6.3:

In the case $\Lambda < 0$, the slopes of the density isopleths relative to the boundary are the same as in Example 2; see Fig. 6.3. Since $\overline{q}_y = 0$ for $z > 0$, the dynamics is the same as before within the quasi-geostrophic theory. Equation (6.5) gives

$$(\partial_t + \overline{u}\partial_x)q = 0 \quad \text{for} \quad z > 0, \tag{6.19}$$

and $q = 0$ is a solution thereof as in Example 2. Thus one has the same solution as in Example 2 if α is identified with $-f\Lambda/N^2$, since the slope of the density isopleths is a

[1]
$$\underbrace{\int_{-\tau}^{\tau} \partial_t \left[\psi_{xx} + \psi_{yy}\right]}_{\substack{\leq 2\tau \max_{-\tau<z<\tau}(\psi_{xxt}+\psi_{yyt}) \\ \to 0 \text{ as } \tau\to 0}} + \underbrace{\epsilon\psi_{zz}]\, dz}_{\substack{[\epsilon\psi_{zt}]_{-\tau}^{\tau} \\ \to \tau\psi_{zt}|_{z=0+}}} + \underbrace{\int_{-\tau}^{\tau} f\alpha\delta(z)\psi_x dz = 0}_{\substack{f\alpha\psi_x|_{z=0} \\ \text{as } \tau\to 0 \text{ using (6.18)}}}$$

$$\alpha = \frac{\rho_y}{\rho_z} = \frac{(g/\overline{\rho})\,\rho_y}{(g/\overline{\rho})\,\rho_z} = \frac{\sigma_y}{N^2} = -\frac{f\overline{u}_z}{N^2} = -\frac{f\Lambda}{N^2}, \text{in the usual notation.}$$

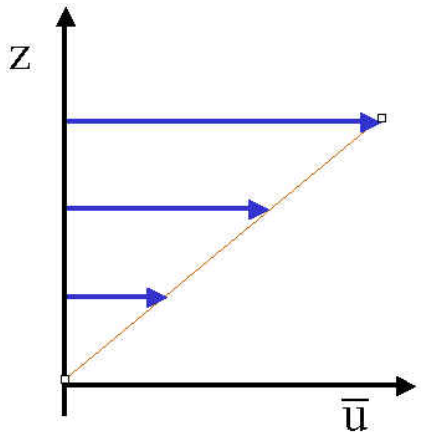

Figure 6.4:

Example 4. Waves at a boundary of discontinuous vertical shear

$\beta = 0$, $\overline{u} = \Lambda z H(z)$ where $H(z) = 1$ for $z > 0$, $H(z) = 0$ for $z < 0$, and the flow unbounded above and below; see Fig. 6.4.

In this case[2] ,

$$\begin{aligned} \overline{u}_z &= \Lambda z\delta(z) + \Lambda H(z), \\ \overline{u}_{zz} &= \Lambda\delta(z), \quad \text{whereupon} \\ \overline{q}_y &= -\Lambda(f^2/N^2)\delta(z) \end{aligned} \tag{6.20}$$

Hence there is a thin layer of negative $\overline{q}_y$ concentrated at $z = 0$. The boundary conditions are $\psi \to 0$ as $z \to \pm\infty$ and ψ continuous at $z = 0$, the latter implying continuity of pressure.

Again, $\lim_{\tau\to 0} \int_{-\tau}^{\tau}$ (Eq.(6.5))dz gives

[2]Note that $(d/dz)H(z) = \delta(z)$ and $z\delta(z) = 0$. For these and other results on δ-functions, see e.g., Friedmann, Principles and Techniques of Applied Mathematics, Chapter III.

$$\lim_{\tau\to 0}\int_{-\tau}^{\tau}[(\partial_t+\Lambda zH(z)\partial_x)(\psi_{xx}+\psi_{yy}+\varepsilon\psi_{zz})-\Lambda(\varepsilon)\delta(z)\psi_x]dz=0,$$

which reduces as before to

$$[\varepsilon\psi_{zt}]_{0-}^{0+}=2\Lambda\varepsilon\psi_x\mid_{z=0} \tag{6.21}$$

By inspection, the solution of the perturbation vorticity equation

$$(\partial_t+\Lambda zH(z)\partial_x)q-\Lambda\varepsilon\delta(z)\psi_x=0,$$

subject to $\psi\to 0$ as $z\to\pm\infty$ together with (6.21) is

$$\psi=a\exp[i(kx+ly-\omega t)-z\mathrm{sgn}(z)(N/f)(k^2+l^2)^{1/2}], \tag{6.22}$$

where

$$\omega=\tfrac{1}{2}k\Lambda f/N/(k^2+l^2)^{1/2}. \tag{6.23}$$

The dispersion relation (6.23) should be compared with that in Example 3. Note that the wave is stable and has the vertical scale given again by $f/(kN)$. McIntyre (1972) extends this analysis to the case where a beta effect is included and where allowance is made for the effect of variable density with height. Then

$$\begin{aligned}\overline{q}_y &= \beta-f_0^2\rho_0(z)^{-1}\partial_z(\rho_0(z)\overline{u}_z/N^2)\\ &= \beta+(f_0^2/N^2)[(\Lambda/H_s)H(z)-\Lambda\delta(z)],\end{aligned}$$

where $H_s=[-\rho_0(z)^{-1}(d/dz)\rho_0(z)]^{-1}$, and f_0 is the value of f at $y=0$. Interest centres on parameter regimes in which $\overline{q}_y$ changes sign in the flow region. McIntyre shows that unstable modes are then possible, for reasons which will transpire in the following section, but growth rates are insufficient to explain the breakdown of the polar night jet in the stratosphere, the problem which motivated his study. A further reference on the polar night jet is Simmons (1974).

Exercises

(6.1) Show that the lateral displacement $\xi(x)$ of a stretched string in equilibrium under the lateral force distribution $F(x)$ per unit length is governed by the differential equation

$$\xi_{xx} = -F/T, \tag{6.24}$$

where T is the tension in the string. Assume that the displacement is small in the sense that $|d\xi/dx| << 1$.

(6.2) Show that the Green's function for Eq.(6.24) on the interval $(0, 1)$ and satisfying boundary conditions $G(0) = 0$, $G(1) = 0$ is:

$$G(x; x') = \begin{cases} x(1-x') & 0 \le x < x' \\ x'(1-x) & x' < x \le 1\,. \end{cases} \tag{6.25}$$

[Hint: the Green's function satisfies the equation $G_{xx} = \delta(x - x')$, which reduces to $G_{xx} = 0$ for $0 \le x < x'$ and $x' < x \le 1$]. You will need to obtain a "jump condition" on G_x at $x = x'$ by integrating the differential equation across the discontinuity.

(6.3) Use the Green's function to find the solution of (6.24) for the function

$$F(x) = \begin{cases} 0, & 0 < x < \frac{1}{2} - a\,, \\ F_0\left(\frac{1}{2} - x\right)\left(\frac{1}{2} + x\right), & \frac{1}{2} - a < x < \frac{1}{2} + a\,, \\ 0, & \frac{1}{2} + a < x < 1\,. \end{cases}$$

Show that for fixed F_0, the maximum value of ξ, $\xi\left(\frac{1}{2}\right)$, increases with a and interpret this result in terms of the string analogy.

(6.4) Verify that (6.12) is a solution of (6.10) satisfying the boundary condition (6.11), provided that w satisfies (6.13). Show that in this problem, the parcel trajectories lie in a plane parallel to the boundary, irrespective of their distance from the boundary.

(6.5) Solve the problem in Example 3 directly using the appropriate linearized forms of (6.1) - (6.4). Assume that $\Lambda > 0$. Show that the steering level for these waves, $z_c = Nk/f$. Show that the slope of the particle trajectories in the $y - z$ plane is less than the slope of the basic isentropes for $z < z_c$ and steeper for $z > z_c$.

6.1 A Unified Theory

The generalization of the definition of potential vorticity gradient to include isolated sheets of $\overline{q}_y$, either internal or at a boundary, enable a unified description of "potential vorticity gradient waves" to be given. The description

is similar to that given for Example 1, but requires the motion to be viewed in two planes; a horizontal $x - y$ plane and a vertical $x - z$ plane. To be specific, consider the $\overline{q}_y$ defined by the shear flow $\overline{u}(z)$ shown in Fig. 6.5. The curvature of the velocity profile, and hence $\overline{q}_y$, are non-zero only in the

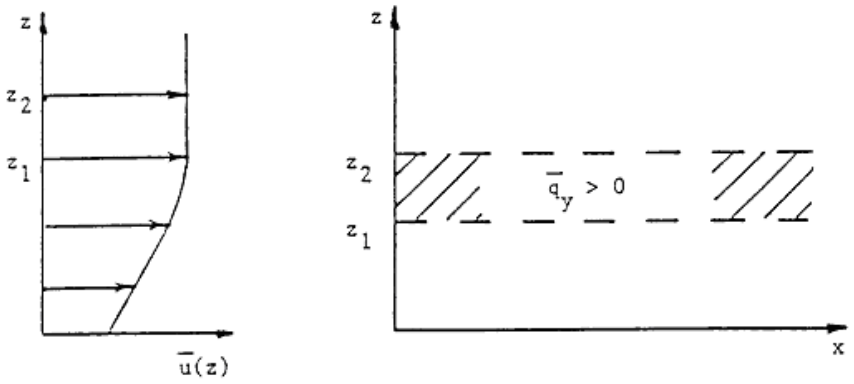

Figure 6.5: A curved profile of vertical velocity $\overline{u}(z)$ (left) and the corresponding distribution of potential vorticity gradient $\overline{q}_y$ (right).

height range (z_1, z_2). Consider now a perturbation in the form of a sinusoidal displacement in the north-south direction. This leads to a potential vorticity perturbation in horizontal planes as shown in Fig. 6.6. The description parallels that in Example 1, but now the q perturbation is confined to the height range (z_1, z_2). The membrane analogy (see Appendix to Chapter 6) allows us to infer the distribution of $\psi(x, y)$ in the $x - z$ plane sketched in Fig. 6.6(b). It does not matter whether the boundary condition is $\psi \to 0$ as $z \to \infty$ and/or $-\infty$ in an unbounded fluid, or $\psi_z = 0$ at a particular horizontal boundary. From this distribution of ψ we can infer the meridional velocity $v = \psi_x$ and note that, as in Example 1, this is exactly $\pi/2$ out of phase with η. Thus the whole pattern is a propagating one; to the left (west) if $\overline{q}_y > 0$ as in the picture, or to the east if $\overline{q}_y < 0$.

6.2 The baroclinic instability mechanism

The foregoing ideas may be extended to provide a qualitative description of the baroclinic instability mechanism. We shall use the fact that a velocity field *in phase* with a displacement field corresponds to *growth of amplitude*, just as quadrature corresponds to *phase propagation*. Suppose that the displacement of a particle is

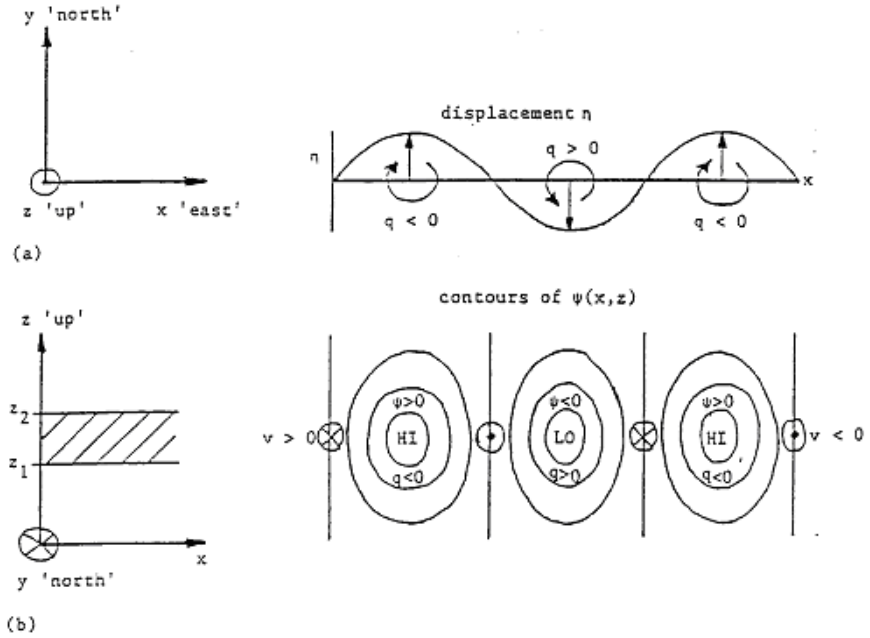

Figure 6.6: Upper panel: Horizontal view of the PV distribution associated with a sinusoidal displacement of fluid parcels in the meridional direction with the layer of positive PV gradient shown in Fig 6.5. Lower panel: Contours of perturbation streamfunctions in the vertical plane corresponding with the sinusoidal disturbance.

$$\eta = A(t)\,\sin\, nt \qquad\qquad (A,\ n > 0),$$

and that we know (by some independent means) that the velocity of the particle is

$$v = B(t)(\cos\, nt + \mu\, \sin\, nt).$$

It follows that

$$B = nA \quad \text{and} \quad \frac{1}{A}\frac{dA}{dt} = \mu n.$$

In particular, if $\mu > 0$ (i.e., the phase lag between the velocity and displacement is less than $\pi/2$) then the amplitude must be growing. In other words, the velocity perturbation is positive when the displacement is a maximum. Let us consider now a 'double-decker' distribution of $\overline{q}_y$ as shown in Fig. 6.7.

We shall try to describe the most important parts of what the equations say using similar ideas to those employed earlier, together with the criterion for growth just presented. The entire dynamics (as opposed to kinematics) is expressed in the simple relationship between displacement and disturbance potential vorticity q that holds at each level where $\overline{q}_y \neq 0$.

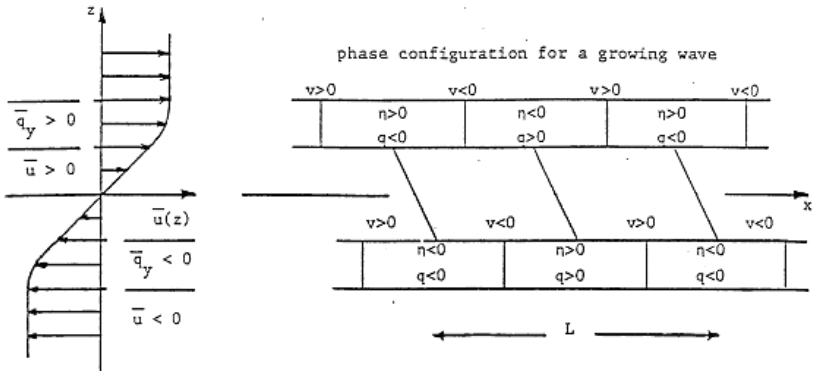

Figure 6.7:

It is plausible from the examples studied so far that we can choose a wavelength L, and a frame of reference, such that a perturbation to the flow, like that illustrated in Fig. 6.5, can be stationary. The perturbation is assumed to be sinusoidal in x. Note that the sign of $\overline{q}_y$ in the top part is such as to make the pattern tend to propagate to the left, against the local stream; likewise the bottom part of the pattern tends to propagate to the right, also against the local stream. If L is small, the phase velocities are small (see e.g. Example 1-4) and the stream will win; if L is large enough, the propagation will win; therefore there ought to be some intermediate value of L such that each pattern is held stationary in some reference frame.

Now suppose not only that this value of L exists, but also that it is such that

$$H < fL/N.$$

Then the perturbation velocities v attributable to the bottom q-distribution are noticeable at the top, and vice versa; see Fig. 6.8. This configuration has three consequences:

1. In as much as the q patterns are nearly in phase, each half 'helps' the other to propagate against the local stream. That is, the contributions to v attributable to each q pattern are of such a sign as to reinforce each

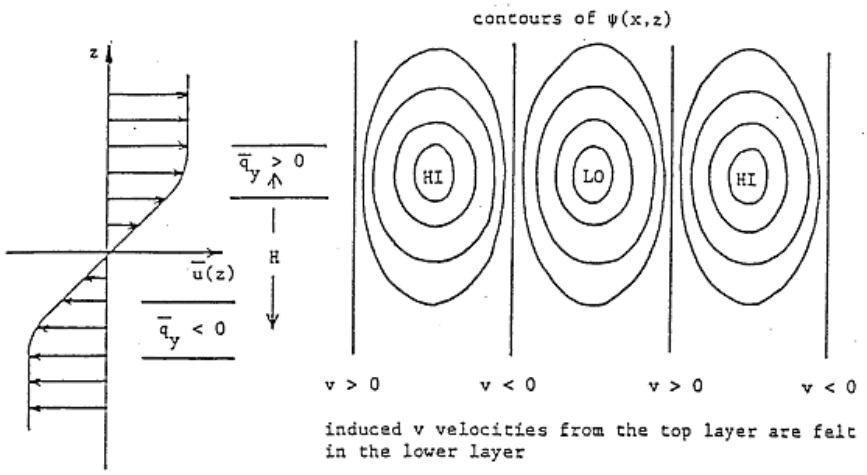

Figure 6.8:

other almost everywhere. This means that the local stream, against which each pattern is holding itself stationary, must actually be faster than would be the case if the other pattern were not present.

2. If the bottom q pattern were shifted to the left so as to be *more* nearly in phase with the top, then each half would help the other propagate even more strongly against the stream: this would move the patterns back towards their original relative position. If the bottom pattern were shifted to the right, the basic flow advection would become stronger than the propagation and shift the pattern back. That is, granted that the pattern shown above can be stationary at all, the relative phase will tend to stay 'locked in' if $H < fL/N$.

3. Now, as we have shown, the contribution to v from the bottom q pattern is exactly $\frac{1}{2}\pi$ out of phase with the bottom η pattern. But it must therefore be less than $\frac{1}{2}\pi$ out of phase with the top η pattern and hence the top pattern must consequently be growing in amplitude. Likewise, the induced v from the top q distribution causes the bottom displacements to increase. See Fig. 6.8.

It is now plausible that the growth rates of the top and the bottom displacements will become equal, since neither can grow without the other. The whole pattern then has a single growth rate proportional to its amplitude; the growth rate is therefore exponential.

The main gap in the foregoing is its lack of attention to what happens at the critical level z_c at which $\overline{u}(z) = 0$ in the frame of reference in which

the wave pattern is stationary. If $\overline{q}_y = 0$ near $z = z_c$, no further discussion is required. However, if $\overline{q}_y \neq 0$ near $z = z_c$, the resulting q distribution can be important if the growth rate predicted without considering it is small. Then the particle displacements near $z = z_c$ are much larger than at the top and bottom, so that q can become significant even if $\overline{q}_y$ at $z = z_c$ is small compared to $\overline{q}_y$ at top and bottom. However the pattern can often adjust itself so that it still grows exponentially - see Bretherton (1966).

A few examples of stable and unstable flow configurations are shown in Fig. 6.9. Examples (a) and (b) follow from the corresponding Rayleigh problems for homogeneous non-rotating shear instability; the eigenvalue problem happens to be the same, although the physical meaning of the variables is different. Example (c) has the original model solved by Charney in the 'forties' as its prototype; it has no finite vertical distance H separating the regions of positive and negative $\overline{q}_y$ and remains unstable, but with decreasing growth rate as the wavelength tends to zero. Example (d) is similar. Instability can be demonstrated mathematically for (c) and (d) for general forms of $\overline{u}(y, z)$ and $\overline{q}_y(y, z)$ ($v\overline{q}_y > 0$), provided that $LN\overline{q}_y/f\overline{u}_z$ is sufficiently small, using perturbation theory about the Eady problem (McIntyre, 1970).

The stability of examples (a) and (b) is due to lack of sign change in $\overline{q}_y$ (including boundary delta-function contributions) in the flow domain (see a very general theorem by Blumen, 1968).

6.3 Perturbation energy equation for quasi-geostrophic waves

An energy equation for quasi-geostrophic wave perturbations can be obtained by multiplying Eq. (6.5) by the perturbation streamfunction ψ to obtain

$$\psi(\partial_t + \overline{u}\partial_x)(\psi_{xx} + \psi_{yy} + \varepsilon\psi_{zz}) + \overline{q}_y\psi\psi_x = 0. \tag{6.26}$$

Note that, for example,

$$\begin{aligned} \psi\partial_t\psi_{xx} = \psi\partial_x(\psi_{xt}) &= \partial_x(\psi\psi_{xt}) - \psi_x\psi_{xt} \\ &= \partial_x(\psi\psi_{xt}) - \partial_t(\tfrac{1}{2}\psi_x^2). \end{aligned} \tag{6.27}$$

We define the zonal average of any quantity by $\overline{(\quad)} = \frac{1}{\lambda}\int_0^\lambda (\,)\,dx$, where λ denotes the zonal wavelength. It follows immediately that for any zonally-periodic quantity, $\overline{\partial_x(\quad)} = 0$. Now we take the zonal average of (6.26),

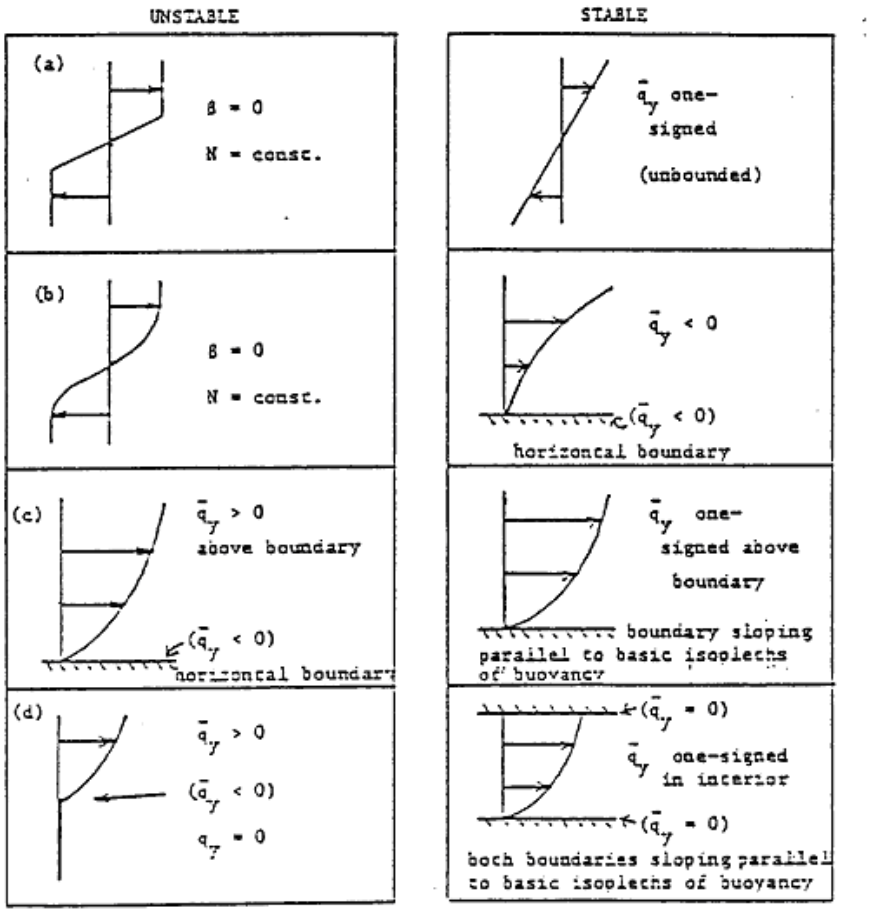

Figure 6.9:

making use of (6.27) and similar expressions when x is replaced by y or z and/or t is replaced by x. After a few lines of algebra we obtain

$$\begin{aligned} \partial_t[\tfrac{1}{2}\overline{(\psi_x^2+\psi_y^2+\varepsilon\psi_z^2)}] &= \partial_y\overline{(\psi\psi_{yt})}+\overline{u}\,\partial_y\overline{(\psi\psi_{yx})} \\ +\,\varepsilon(\partial_z\overline{(\psi\psi_{zt})} &+ \overline{u}\,\partial_z\overline{(\psi\psi_{zx})})\,. \end{aligned} \tag{6.28}$$

The second term on the right hand side of (6.28) may be written $\partial_y[\overline{u}\,\overline{(\psi\psi_{xy})}]-\overline{u}_y[\overline{\partial_x(\psi\psi_y)}-\overline{\psi_x\psi_y}]$. Note that $\overline{\psi\psi_{xy}}=[\overline{\partial_x(\psi\psi_y)}-\overline{\psi_x\psi_y}]$ and $\overline{\partial_x(\psi\psi_y)}$ is zero. The term in ε in (6.28) may be written $\partial_z[\overline{\psi(\partial_t+\overline{u}\partial_x)\psi_z}]-\overline{u}_z[\overline{\partial_x(\psi\psi_z)}-\overline{\psi_x\psi_z}]$. The first term of this may be reduced to $\partial_z[\overline{u}_z\overline{\psi\psi_x}-(f/\varepsilon)\,\overline{\psi w}]$, the first

term of which is zero. Using these results, we now take the double integral $\int_{y_1}^{y_2} dy \int_0^H dz$ of (6.28) and obtain

$$\begin{aligned}\frac{dE}{dt} &= \int_0^H \left[\overline{\psi\psi_{yt}}\right]_{y_1}^{y_2} dz - \int_0^H \left[\overline{u}\,\overline{(\psi_x\psi_y)}\right]_{y_1}^{y_2} dz \\ &+ \int_0^H \int_{y_1}^{y_2} \overline{u}_y \left(\overline{\psi_x\psi_y}\right)\, dy\, dz - f \int_{y_1}^{y_2} \left[\overline{\psi w}\right]_0^H dy \\ &+ \varepsilon \int_0^H \int_{y_1}^{y_2} \overline{u}_z \overline{\psi_x\psi_z}\, dy\, dz,\end{aligned}$$

where

$$E = \tfrac{1}{2} \int_0^H \int_{y_1}^{y_2} \overline{(\psi_x^2 + \psi_y^2 + \varepsilon\psi_z^2)}\, dy\, dz \tag{6.29}$$

is the total perturbation wave energy. With the assumption of channel boundary conditions $v = 0$ at $y = y_1, y_2$ (or less restrictively, that the Reynold's stress $\overline{uv} = 0$ at these boundaries) and that $w = 0$ at $z = 0, H$, this expression may be written

$$\begin{aligned}\frac{dE}{dt} &= \frac{\varepsilon}{f} \int_0^H \int_{y_1}^{y_2} \overline{u}_z \overline{v\sigma}\, dy\, dz - \int_0^H \int_{y_1}^{y_2} \overline{u}_y \left(\overline{uv}\right)\, dy\, dz \\ &+ \int_0^H \left[\overline{\psi\psi_{yt}}\right]_{y_1}^{y_2} dz\ . \end{aligned} \tag{6.30}$$

This is the perturbation wave-energy equation. The term on the left-hand side is simply the rate-of-change of total wave energy. The first term on the right-hand side represents the conversion of basic state available potential energy, characterized by the vertical shear, to perturbation energy when the poleward eddy heat flux $\overline{v\sigma}$ has the same sign as $\overline{u}_z$ (i.e. the opposite sign to the meridional temperature gradient). The third term represents the conversion of basic state kinetic energy to perturbation energy when the Reynold's stress term $-\overline{uv}$ has the same sign as the horizontal shear $\overline{u}_y$; otherwise it represents a loss of energy to the basic state. The last term on the right-hand side is proportional to $-\int_0^H [\overline{pu_t}]_{y_1}^{y_2} dz$. If $\psi_x = 0$ at $y = y_1, y_2$, then ψ is a function only of y, z and t at these boundaries, whereupon $\overline{\psi\psi_{yt}}$ equals $\overline{\psi}\,\overline{\psi_{yt}}$, which is proportional to $-\overline{pu}_t$. This term is zero as long as $\overline{u}_t$ can be regarded as zero at the meridional boundaries. In linear problems, $\overline{u}$ is assumed to be independent of t, but in nonlinear problems, if $\overline{u}_t$ is nonzero, the foregoing term may represent an energy source or sink (see e.g. Smith, 1974; 1977).

Exercises

(6.6) Define the pseudo-potential vorticity for quasi-geostrophic motion on a beta plane in a compressible atmosphere with density $\rho_0(z)$ and Brunt-Väisälä frequency $N^2(z)$ as

$$q = f_0 + \beta y + \frac{\partial^2\psi}{\partial x^2} + \frac{\partial^2\psi}{\partial y^2} + \frac{f_0^2}{\rho_0(z)}\frac{\partial}{\partial z}\left[\frac{\rho_0(z)}{N^2}\frac{\partial\psi}{\partial z}\right].$$

Show that

$$\begin{aligned}\rho_0 q\frac{\partial\psi}{\partial x} &= \frac{\partial}{\partial y}\left\{\rho_0\frac{\partial\psi}{\partial y}\frac{\partial\psi}{\partial x}\right\} + \frac{\partial}{\partial z}\left[\frac{f_0^2}{N^2}\rho_0\frac{\partial\psi}{\partial x}\frac{\partial\psi}{\partial y}\right] \\ &+ \frac{\partial}{\partial x}\left[\rho_0\left\{(f_0+\beta y)\psi + \tfrac{1}{2}\left(\frac{\partial\psi}{\partial x}\right)^2 - \tfrac{1}{2}\left(\frac{\partial\psi}{\partial y}\right)^2 - \frac{f_0^2}{N^2}\left(\frac{\partial\psi}{\partial z}\right)^2\right\}\right].\end{aligned}$$

Show further that, if $\frac{\partial\psi}{\partial x} = 0$ on $y = y_1, y_2$ and $\frac{\partial\psi}{\partial x}$ = constant on $z = 0, h$, then

$$\int_0^h\int_{y_1}^{y_2}\overline{\rho_0 q\frac{\partial\psi}{\partial x}}\,dy\,dz = 0, \tag{6.31}$$

where $\overline{(\quad)}$ denotes a zonal mean such that $\overline{\partial(\quad)/\partial x} = 0$.

(6.7) Under the same boundary conditions used to derive Eq.(6.31), show that

$$\int_0^h\int_{y_1}^{y_2} E\,dy\,dz = -\int_0^h\int_{y_1}^{y_2}\overline{q\psi}\,dy\,dz,$$

where ψ is the perturbation stream function. Equation (6.31) states *that the mean northward geostrophic eddy flux of potential vorticity integrated over the whole volume of fluid vanishes.* This important result is due to Charney and Stern (1962); see also Bretherton (1966).

6.4 The omega equation in terms of PV

Equation (6.4) can be written

$$q = f + L\psi \tag{6.32}$$

where L is the elliptic operator

$$\mathrm{L} = \nabla_h^2 + \varepsilon \frac{\partial^2}{\partial z^2}. \tag{6.33}$$

Then (6.1) can be written

$$L\left(\frac{\partial \psi}{\partial t}\right) = -\mathbf{u} \cdot \nabla q. \tag{6.34}$$

The thermodynamic equation (6.2) can be written alternatively as

$$f\frac{\partial}{\partial z}\left(\frac{\partial \psi}{\partial t}\right) = -\mathbf{u} \cdot \nabla \sigma - N^2 w. \tag{6.35}$$

Taking $f(\partial/\partial z)$ (6.34) - L (6.35) gives

$$L\left[w + \frac{u \cdot \nabla \sigma}{N^2}\right] = \frac{f}{N^2}\frac{\partial}{\partial z}\left(\mathbf{u} \cdot \nabla q\right). \tag{6.36}$$

This is an alternative form of the omega equation [DM, Eq.(10.6)], which can be solved diagnostically for the vertical velocity w given suitable boundary conditions on it.

Let us write $w = w_1 + w_2$ such that

$$Lw_1 = \frac{f}{N^2}\frac{\partial}{\partial z}\left(\mathbf{u} \cdot \nabla q\right), \tag{6.37}$$

with boundary conditions $w_1 = 0$ everywhere, and

$$L\left[w_2 + \frac{\mathbf{u} \cdot \nabla \sigma}{N^2}\right] = 0, \tag{6.38}$$

with the same boundary conditions relevant to (6.36). It follows that w_1 is the contribution to w forced by the vertical gradient of potential vorticity advection, while w_2 is forced by temperature advection.

Chapter 7

FRONTOGENESIS, SEMI-GEOSTROPHIC THEORY

7.1 Frontogenesis in a horizontal deformation field.

We consider now a specific problem in which a pure horizontal deformation field $\overline{u} = -\alpha x$, $\overline{V} = \alpha y$, acts on an initially diffuse potential temperature field $\theta_i(x)$. By 'initially diffuse' is meant that the thermal wind component associated with $\partial\theta_i/\partial x$ can be ignored. We assume that α is a constant and that geostrophic balance exists the x-direction, an assumption that is not strictly valid for large $|x|$. The flow configuration is sketched Fig. 7.1.

We follow Hoskins and Bretherton (1972) and use the 'pseudo-height' coordinate system with $z = [1 - (p/p_o)^{(\gamma-1)/\gamma}]\gamma H_s/(\gamma - 1)$, where $H_s = p_o/(\rho_o g)$ and the subscript $'o'$ denotes surface values. The pseudo-height is equal to physical height in an adiabatic atmosphere, but differs only slightly from it in the troposphere for typical $\theta(z)$ profiles. In this coordinate system, the so-called semi-geostrophic equations, DM (14.27) - (14.31), take the form

$$-fv = -\frac{\partial\phi}{\partial x}, \tag{7.1}$$

$$\frac{Dv}{Dt} + fu = -\frac{\partial\phi}{\partial y}, \tag{7.2}$$

$$0 = -\frac{\partial\phi}{\partial z} + g\frac{\theta}{\theta_0}, \tag{7.3}$$

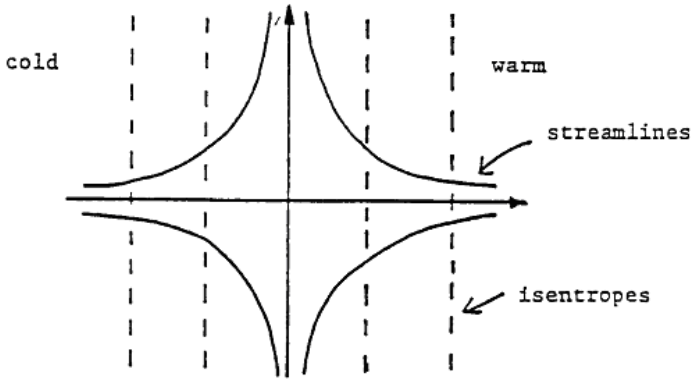

Figure 7.1: Frontogenesis in a pure horizontal deformation field.

$$\frac{D\theta}{Dt} = 0, \tag{7.4}$$

and

$$\frac{\partial u}{\partial x} + \frac{\partial v}{\partial y} + \frac{\partial w}{\partial z} = 0. \tag{7.5}$$

Here, ϕ is the geopotential (analogous to P) and $w = Dz/Dt$ is the 'pseudo-vertical velocity', which we shall refer to as the 'vertical velocity'. We express now the total flow as the basic initial flow plus a deviation therefrom; i.e.,

$$u = -\alpha x + u'(x, y, t), \tag{7.6}$$

$$v = \alpha y + v'(x, y, t), \tag{7.7}$$

$$w = w(x, y, t), \tag{7.8}$$

$$\phi = f\alpha xy - \tfrac{1}{2}\alpha^2 y^2 + \phi'(x, y, z), \tag{7.9}$$

and

$$\theta = \theta(x, y, t). \tag{7.10}$$

Substitution of Eqs. (7.6) - (7.10) into (7.1) - (7.5) gives

$$fv' = \frac{\partial \phi'}{\partial x}, \tag{7.11}$$

$$\frac{\partial v'}{\partial t} + (-\alpha x + u')\frac{\partial v'}{\partial x} + w\frac{\partial v'}{\partial z} + fu' + \alpha v' = 0, \tag{7.12}$$

$$g\frac{\theta}{\theta_0} = \frac{\partial \phi'}{\partial z}, \tag{7.13}$$

$$\frac{\partial \theta}{\partial t} + (-\alpha x + u')\frac{\partial \theta}{\partial x} + w\frac{\partial \theta}{\partial z} = 0, \tag{7.14}$$

and

$$\frac{\partial u'}{\partial x} + \frac{\partial w}{\partial z} = 0. \tag{7.15}$$

Equations (7.11) - (7.15) include conservation of potential temperature, and of a form of Ertel's potential vorticity:

$$q = \frac{g}{\theta_0}\left[-\frac{\partial v'}{\partial z}\,\frac{\partial \theta}{\partial x} + \left(f + \frac{\partial v'}{\partial x}\right)\,\frac{\partial \theta}{\partial z}\right]. \tag{7.16}$$

The latter follows from the result of Exercise (14.5) in DM since g/θ_0 is a constant. Note the slightly different definition for q used in (7.16). A third conservation property can be obtained as follows. Let $X = x + v'/f$. Then

$$\begin{aligned} \frac{DX}{Dt} &= \frac{Dx}{Dt} + \frac{1}{f}\frac{Dv'}{Dt} \\ &= u + \frac{1}{f}\left[-fu' - \alpha v'\right], \text{ using (7.12)} \\ &= -\alpha X. \end{aligned} \tag{7.17}$$

Hence, following a fluid parcel, $X = X_o e^{-\alpha t}$, where X_o is the value of X for the parcel at the initial instant. Thus the quantity $Xe^{\alpha t}$ is conserved following fluid parcels. Note that conservation of this quantity is equivalent to the conservation of absolute momentum fX, and is a direct result of Eq. (7.12).

Further progress towards a solution of Eqs. (7.11) - (7.15) is facilitated by a transformation of coordinates to so-called *geostrophic coordinates*:

$$(X, Z, T) = (x + v'/f, z, t). \tag{7.18}$$

Exercises

(7.1) Show that the Jacobian, J, of the transformation (7.18) can be written variously as

$$J = \frac{\partial\,(X,Z)}{\partial(x,z)} = 1 + \frac{1}{f}\frac{\partial v'}{\partial x} = \frac{\zeta_a}{f} = \left[1 - \frac{1}{f}\frac{\partial v'}{\partial X}\right]^{-1}, \tag{7.19}$$

where ζ_a is the absolute vorticity.

(7.2) Establish the following results, based on the transformation of Eqs. (7.11) - (7.14):

$$q = \frac{g}{\theta_o}\frac{\partial\,(fX,\theta)}{\partial(x,z)} = f\,J\frac{g}{\theta_o}\frac{\partial\theta}{\partial Z}, \tag{7.20}$$

$$\left(fv',\ \frac{g\theta}{\theta_0}\right) = \left(\frac{\partial\phi'}{\partial x}, \frac{\partial\phi'}{\partial z}\right) = \left(\frac{\partial\phi}{\partial X}, \frac{\partial\phi}{\partial Z}\right), \tag{7.21}$$

where

$$\phi = \phi' + \tfrac{1}{2}v'^2, \tag{7.22}$$

$$q = f\frac{\partial^2\phi}{\partial Z^2}\left(1 - \frac{1}{f^2}\frac{\partial^2\phi}{\partial X^2}\right)^{-1}, \tag{7.23}$$

$$\frac{D}{Dt} \equiv \frac{\partial}{\partial t} + u\frac{\partial}{\partial x} + w\frac{\partial}{\partial z} \equiv \frac{\partial}{\partial T} - \alpha X\frac{\partial}{\partial X} + w\frac{\partial}{\partial Z}. \tag{7.24}$$

From Eq. (7.23) it follows at once that

$$\frac{1}{f^2}\frac{\partial^2\phi}{\partial X^2} + \frac{f}{q}\frac{\partial^2\phi}{\partial Z^2} = 1. \tag{7.25}$$

7.2 Uniform potential vorticity model, q = constant.

Suppose that:

- $q/f = N^2$, a constant;
- the fluid is contained between horizontal boundaries at $z = 0, H$,

- $\theta = \theta_i(x)$ ($i = 1$, 2 for $z = 0, H$) is specified initially on these boundaries.
- at zero time, the temperature gradient is everywhere weak enough so that $x \approx X$ (i.e. $v'/(xf) << 1$, for all x).

Then $q/f = N^2$ everywhere for all t and (7.25) gives

$$\frac{1}{f^2}\frac{\partial^2\phi}{\partial X^2} + \frac{1}{N^2}\frac{\partial^2\phi}{\partial Z^2} = 1. \tag{7.26}$$

On the boundaries $z = Z = 0, H$,

$$\frac{\partial\phi}{\partial Z} = \frac{g}{\theta_o}\theta_i\left(X_o\right) = \frac{g}{\theta_o}\theta_i\left(Xe^{\alpha T}\right). \tag{7.27}$$

With suitable boundary conditions on f for large $|X|$, the mathematical problem for ϕ is easily solved at any time T. Then v' and θ can be obtained from Eq. (7.21). Note that T occurs only as a parameter through (7.27).

The meridional circulation is found in a similar way to that described earlier. The form of the continuity equation (7.15) permits the introduction of a streamfunction ψ for the ageostrophic circulation, i.e.

$$u' = \frac{\partial\psi}{\partial z}, \qquad w = -\frac{\partial\psi}{\partial x} \tag{7.28}$$

or in transformed form,

$$u' = \frac{1}{f}J\frac{\partial v'}{\partial Z}\frac{\partial\psi}{\partial X} + \frac{\partial\psi}{\partial Z}, \qquad w = -J\frac{\partial\psi}{\partial X}. \tag{7.29}$$

Using (7.24) and (7.29), the transformed forms of (7.12) and (7.14) are

$$\frac{\partial v'}{\partial T} - \alpha X\frac{\partial v'}{\partial X} + w\frac{\partial v'}{\partial Z} + f\frac{\partial\psi}{\partial Z} + \alpha v' = 0, \tag{7.30}$$

and

$$\frac{\partial\theta}{\partial T} - \alpha X\frac{\partial\theta}{\partial X} + w\frac{\partial\theta}{\partial Z} = 0. \tag{7.31}$$

Then, taking $f(/Z)$ (7.30) $-$ $(g/\theta_o)(\partial\partial/X)$ (7.31) and using cross-front thermal wind balance expressed by $f(\partial v'/\partial Z) = (g/\theta_o)(\theta/X)$, we obtain,

$$f^2\frac{\partial^2\psi}{\partial Z^2} + \frac{\partial}{\partial X}\left[\frac{q}{f}\frac{\partial\psi}{\partial X}\right] = -Q, \tag{7.32}$$

where

$$Q = 2\alpha \frac{g}{\theta_o} \frac{\partial \theta}{\partial X}. \tag{7.33}$$

This should be compared with DM Eq. (14.42); remember that here, $q/f = N^2 =$ constant. Suitable boundary conditions would be, for example, that $w \to 0$ for large $|X|$ and $w = 0$ at $Z = 0, H$.

Evidently, the solution of the transformed semi-geostrophic equations leads to the same mathematical problem as that which arises in solving the analogous quasi-geostrophic problem. The difference between the diagnosed circulation lies in the transformation back to physical space required in the semi-geostrophic case. This transformation is easily performed when the solution for $v'(X, Z, T)$ has been obtained.

7.3 Zero potential vorticity model, $q \equiv 0$.

Much can be learned from the special case in which the static stability is initially zero (i.e. $\partial\theta/\partial z \equiv 0$ at $t = 0$). This simple problem exhibits many features of frontogenesis and can be solved analytically. Equation (7.25) reduces in this case to $\partial^2\phi/\partial Z^2 = 0$, implying that ϕ is a linear function of Z. Suppose that at $t = 0$, $\theta_1(x) = \theta_2(x) = \overline{\theta}(X_o)$[1]. Then at later times, $\theta = \theta(Xe^{\alpha T}) = \theta(X, T)$ say.

It follows from (7.21) that

$$\frac{\partial \phi}{\partial Z} = \frac{g\theta}{\theta_o}, \quad \phi = \frac{g\theta}{\theta_o} Z + F(X), \quad v' = \frac{g\theta_X}{f\theta_o} Z + F'(X), \tag{7.34}$$

where $F(X)$ is an arbitrary function of X to be determined. Now the slope of a line $X(x, z) =$ constant is

$$\begin{aligned} -\frac{(\partial X/\partial x)}{(\partial X/\partial z)} &= -\left[1 + \frac{1}{f}\frac{\partial v'}{\partial x}\right] / \left[\frac{1}{f}\frac{\partial v'}{\partial z}\right] = -J/\left[\frac{1}{f} J \frac{\partial v'}{\partial Z}\right] \\ &= -\frac{f^2\theta_o}{g}\theta_X^{-1} = \text{ constant.} \end{aligned}$$

Hence, in physical space, θ is a constant on the straight line

$$x = X - \frac{g}{f^2\theta_0}\theta_X z - \frac{F'(X)}{f}$$

This line represents also the position of particles which were initially vertical as indicated in Fig. 7.2. In the Boussinesq formulation, conservation of mass

[1]Note that $N^2 = 0 \Rightarrow \theta_1(x, 0, 0) = \theta_2(x, H, 0)$ for consistency.

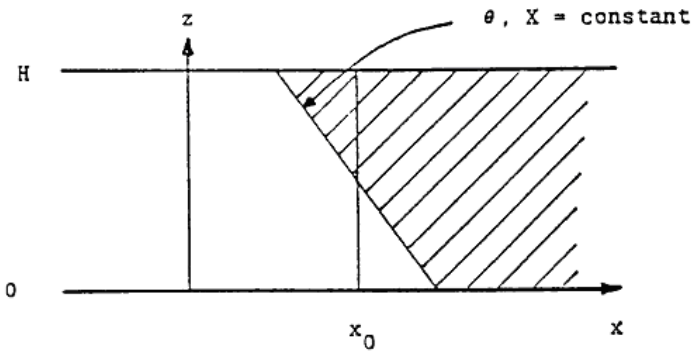

Figure 7.2:

implies conservation of volume, which in turn implies that the line of particles move in such a way that the displacement is zero at $z = \frac{1}{2}H$. It follows that $F'(X) = -gH\theta_X/(2f\theta_o)$, whereupon

$$x = X - \frac{g}{f^2\theta_o}\theta_X z', \tag{7.35}$$

where $z' = z - \frac{1}{2}H$. On such a line,

$$x = X - \frac{g}{f^2\theta_o}\theta_X z', \tag{7.36}$$

and

$$\zeta_a = \frac{\partial X}{\partial x} = f\left[1 - \frac{g}{f^2\theta_o}\theta_{XX} z'\right]^{-1}. \tag{7.37}$$

Exercise

(7.3) Starting from $u = \frac{\mathrm{Dx}}{\mathrm{Dt}} = \frac{\mathrm{DX}}{\mathrm{Dt}} - \frac{1}{f}\frac{\mathrm{Dv'}}{\mathrm{Dt}}$, show that

$$\mathrm{u} = -\alpha\mathrm{X} - \frac{g}{f^2\theta_o}\left(\alpha\mathrm{z'}+\mathrm{w}\right)\theta_X, \tag{7.38}$$

and using the continuity equation, show that

$$w = -\frac{\alpha g}{f^2\theta_o}\theta_{XX}\frac{1/4\ H^2 - z'^2}{1-(g/f^2\theta_o)\theta_{XX}z'}. \tag{7.39}$$

Hint: first show that $J = 1/(1-aZ')$ where $a = (g/f^2\theta_o)\theta_{XX}$ and $Z' = z'$; then show that w satisfies the equation $\frac{\partial w}{\partial Z'} - aJw = -\alpha\left[1 - J(1+aZ')\right]$.

Some features of the solution are as follows:

(i) The frontogenesis problem of determining v' and θ at time t has separated from the problem of finding u and w.

(ii) Consider the initial distribution of $\overline{\theta}$ sketched in Fig. 7.3. The corresponding values of $\overline{\theta}_x$ and $\overline{\theta}_{xx}$ are shown also. Since $\overline{\theta}_{xx} \propto e^{2\alpha t}$, it follows from (7.37) that infinite vorticity and associated discontinuities in velocity and temperature in Fig. 7.3 occur in a finite time. This "collapse" of the solution occurs first on the boundaries: at $z = 0$, where θ_{XX} is most negative, and at $z = H$, where θ_{XX} is most positive. The singularities do not occur in the problem as viewed using X, Z, but in the transformation $X = X(x, z)$.

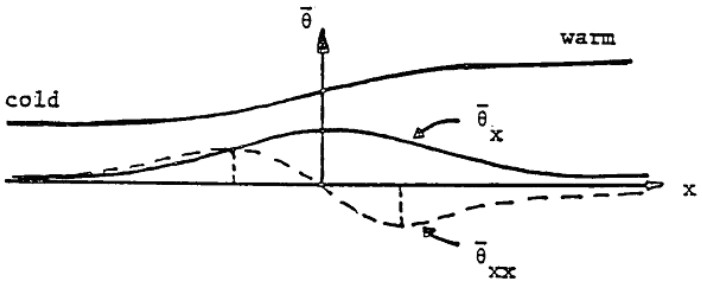

Figure 7.3: For discussion, see text.

(iii) Below $z = \frac{1}{2}H$, the largest vertical velocity at any time is on the line on which $\partial^2\theta/\partial X^2$ is a minimum; this is the line on which $\partial^2\overline{\theta}/\partial x^2$ is a minimum. However note that the surface position of $(\theta_x)_{max}$ and ζ_{max} are not the same.

(iv) There is upward motion when $\partial^2\theta/\partial X^2$ is negative and downward motion when it is positive.

(v) Frontogenesis tends to occur on the lower boundary towards the warm side of a temperature contrast.

(vi) At a boundary, (7.38) may be rewritten as

$$u = -\alpha x - 2\alpha\partial v'/\partial x,$$

which on differentiation becomes

$$-\partial u/\partial x = \alpha + 2\alpha\, \partial v'/\partial x$$

The first term on the right-hand side is the basic horizontal deformation, while the second is the vertical circulation associated with the induced ageostrophic circulation. For vertical vorticities large compared with f, the latter dominates. Moreover, the position of maximum horizontal convergence $(-u_x)_{max}$ is coincident with that of the maximum relative vorticity.

Figure 7.4 shows a typical solution for the zero potential vorticity model, for a case in which the initial potential temperature distribution is proportional to $\tan^{-1}x$. Notice the surface jet in the along-front velocity component with maximum speed on the cold side of the surface front

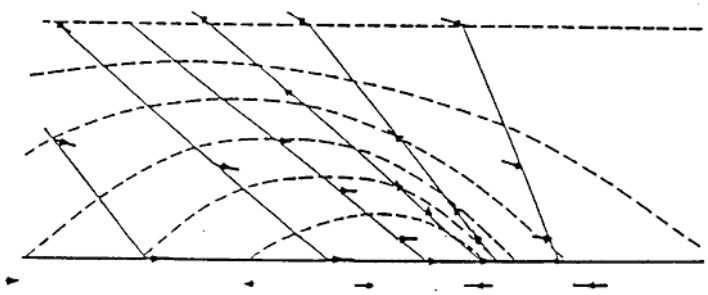

Figure 7.4: Deformation model with zero potential vorticity (lower half domain). Continuous and broken lines are isolines of potential temperature and along-front velocity, respectively. Arrowed lines are the velocity vectors drawn on the same scale as the basic deformation velocity shown beneath the lower surface. (From Hoskins and Bretherton, 1972).

7.4 The geostrophic momentum approximation

A generalization of the quasi-geostrophic system of equations may be made on the assumption that the *Lagrangian time* scale t, i.e., the time scale for changes following a fluid parcel, is much larger than f^{-1} (≈ 3 hours). It may often happen that this is the case, even when the *Eulerian time scale*, i.e., the time scale for changes at a fixed point in space, is not much less than f.

Now the horizontal momentum equation in a rotating fluid may be written

$$\mathbf{u} = \mathbf{u}_g + k \wedge \frac{1}{f}\frac{D\mathbf{u}}{Dt}, \tag{7.40}$$

where D/Dt is the total derivative following a fluid parcel. Then[2]

$$\begin{aligned} \mathbf{u} &= \mathbf{u}_g + k \wedge \frac{1}{f}\frac{D}{Dt}\left[\mathbf{u}_g + k \wedge \frac{1}{f}\frac{D\mathbf{u}}{Dt}\right] \\ &= \mathbf{u}_g + k \wedge \frac{1}{f}\frac{D\mathbf{u}_g}{Dt} - \frac{1}{f^2}\frac{D^2\mathbf{u}}{Dt^2}. \end{aligned} \tag{7.41}$$

Let $t = \tau t^*$, and define the Lagrangian Rossby number to be $Ro = 1/(ft)$. Then (7.41) becomes

$$\mathbf{u} = \mathbf{u}_g + Ro\mathbf{k} \wedge \frac{D\mathbf{u}_g}{Dt^*} - Ro^2\frac{D^2\mathbf{u}}{Dt^{*2}}.$$

Neglecting the term of order Ro^2 and taking $\mathbf{k}\wedge$ gives, in dimensional form,

$$\frac{D\mathbf{u}_g}{Dt} + f\mathbf{k} \wedge \mathbf{u} = f\mathbf{k} \wedge \mathbf{u}_g. \tag{7.42}$$

This is called the *geostrophic momentum approximation* because the momentum $\mathbf{u}$ in $D\mathbf{u}/Dt$ is computed geostrophically. Further insight into this approximation comes from writing the horizontal momentum equation in natural coordinates (ξ, η): see Fig. 7.5. In these coordinates, the velocity vector is $(V, 0)$; i.e., $\mathbf{u} = V\ \cos\ \chi\mathbf{i} + V \sin\chi\mathbf{j}$. Then

$$\frac{\partial\mathbf{u}}{\partial t} = \frac{\partial V}{\partial t}\left(\cos\ \chi\mathbf{i} + \ \sin\ \chi\mathbf{j}\right) + V\frac{\partial\chi}{\partial t}\left(-\sin\chi\mathbf{i} + \ \cos\ \chi\mathbf{j}\ \right).$$

It follows readily that $(\partial\mathbf{u}/\partial t)\cdot\mathbf{i}' = \partial V/\partial t$ and $(\partial\mathbf{u}/\partial t)\cdot\mathbf{j}' = V\partial\chi/\partial t$, and similarly for the x and y derivatives, so that in (ξ, η) coordinates, the acceleration vector is:

$$\frac{D\mathbf{u}}{Dt} = \left(\frac{DV}{Dt},\ V\frac{D\chi}{Dt},\ 0\right),$$

and the momentum equations take the form

$$\frac{DV}{Dt} = -\frac{\partial\phi}{\partial\xi} \quad \text{and} \quad V\frac{D\chi}{Dt} + fV = -\frac{\partial\phi}{\partial\eta}. \tag{7.43}$$

[2] $\mathbf{k} \wedge D(\mathbf{k} \wedge D\mathbf{u}) = (\mathbf{k}\cdot D^2\mathbf{u})\mathbf{k} - (\mathbf{k}\cdot\mathbf{k})D^2\mathbf{u} = 0.$

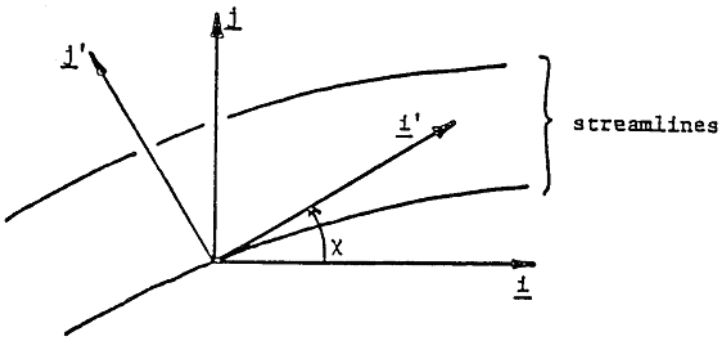

Figure 7.5:

Now V can be computed geostrophically from ϕ_η if $D\chi/Dt << f$. If, in addition, $DV/Dt << fV$, i.e., the Lagrangian time scale for V is large compared with f, then $|\partial\phi/\partial\xi| << fV$ and the geostrophic momentum vector $\mathbf{V}_g = (-f^{-1}\phi_\eta, f^{-1}\phi_\xi)$ is a good approximation to the momentum vector $(V, 0)$. Hence the geostrophic momentum approximation requires that the magnitude of the acceleration, DV/Dt, is $<< fV$ *and* that the rate-of-change of the direction of V with time is $<< f$. The full hydrostatic system of equations in rectangular coordinates with the geostrophic momentum approximation included is,

$$\frac{Du_g}{Dt} - fv = -\frac{\partial\phi}{\partial x}, \tag{7.44}$$

$$\frac{Dv_g}{Dt} + fu = -\frac{\partial\phi}{\partial y}, \tag{7.45}$$

$$0 = -\frac{\partial\phi}{\partial z} + g\frac{\theta}{\theta_0}, \tag{7.46}$$

$$\frac{D\theta}{Dt} = 0, \tag{7.47}$$

and

$$\nabla \cdot \mathbf{u} = 0, \tag{7.48}$$

where

$$(fu_g, fv_g) = (-\phi_y, \phi_x) \tag{7.49}$$

and

$$\frac{D}{Dt} \equiv \frac{\partial}{\partial t} + u\frac{\partial}{\partial x} + v\frac{\partial}{\partial y} + w\frac{\partial}{\partial z}; \tag{7.50}$$

i.e. advection is by the unapproximated velocity vector. Hoskins (1975) shows that, like the full Boussinesq equations, the approximated set (7.44)-(7.50) has a full energy equation, a three-dimensional vorticity equation, and an Ertel potential vorticity conservation equation. The equations form a balanced system which excludes gravity waves and can describe regions of large shear vorticity such as jet streams and fronts, provided that the curvature vorticity is small compared with the Coriolis parameter.

For these equations, the "vorticity" has the form

$$\begin{aligned}\boldsymbol{\omega} = &\left(-\frac{\partial v_g}{\partial z},\ \frac{\partial u_g}{\partial z},\ f + \frac{\partial v_g}{\partial x} - \frac{\partial u_g}{\partial y}\right) + \\ &\frac{1}{f}\left(\frac{\partial(u_g,\, v_g)}{\partial(y,z)}, \frac{\partial(u_g,\, v_g)}{\partial(z,x)}, \frac{\partial(u_g,\, v_g)}{\partial(x,y)}\right),\end{aligned} \tag{7.51}$$

and the vorticity equation is

$$\frac{D\boldsymbol{\omega}}{Dt} = (\boldsymbol{\omega}\cdot\nabla)\,\mathbf{u} - \mathbf{k}\wedge(g/\theta_0)\nabla\theta. \tag{7.52}$$

It is usually the case that the nonlinear term in the expression for vorticity in (7.51) is small. The *potential vorticity* is defined as

$$q = \boldsymbol{\omega}\cdot\nabla\theta, \tag{7.53}$$

where

$$\frac{Dq}{Dt} = 0. \tag{7.54}$$

Exercises

(7.4) Verify that the third component of (7.51) is satisfied. [Hint: take $\mathbf{k}\wedge$ Eq. 7.42 and take $\mathbf{k}\cdot\nabla\wedge$ of the result.]

(7.5) Show that (7.54) follows from (7.47) and (7.52). [Hint: use tensor notation.]

Equations (7.44)-(7.50) are difficult to solve as they stand because the ageostrophic motion is not *predicted*, but needs to be diagnosed. As in the

frontogenesis problem studied earlier, the solution is facilitated by a transformation of coordinates. Thus we set

$$(X, Y, Z, T) = (x + v_g/f, y - u_g/f, z, t). \tag{7.55}$$

Then, assuming that f is constant,

$$\frac{DX}{Dt} = \frac{Dx}{Dt} + \frac{1}{f}\frac{Dv_g}{Dt} = u + \frac{1}{f}(\mathrm{fu_g} - \mathrm{fu}) = \mathrm{u_g},$$

using (7.45). Similarly, $DY/Dt = v_g$. Thus X, Y are the horizontal positions a fluid parcel would have if it moved with the geostrophic velocity $\mathbf{u}_g = (u_g, v_g, 0)$. The mathematical details of the transformation proceed in the same way as described earlier. The material derivative (7.50) transforms to

$$\frac{D}{Dt} = \frac{\partial}{\partial T} + \mathbf{u_g} \cdot \nabla_X + w\frac{\partial}{\partial Z}, \tag{7.56}$$

while the Jacobian of the transformation reduces to

$$\begin{aligned} J &= \frac{\partial(X, Y)}{\partial(x, y)} \\ &= \frac{\partial}{\partial x}\left(x + \frac{v_g}{f}\right)\frac{\partial}{\partial y}\left(y - \frac{u_g}{f}\right) - \frac{\partial}{\partial x}\left(y - \frac{u_g}{f}\right)\frac{\partial}{\partial y}\left(x + \frac{v_g}{f}\right) \\ &= \frac{1}{f}\left[f + \frac{\partial v_g}{\partial x} - \frac{\partial u_g}{\partial y}\right] + \frac{1}{f^2}\left[\frac{\partial u_g}{\partial x}\frac{\partial v_g}{\partial y} - \frac{\partial v_g}{\partial x}\frac{\partial u_g}{\partial y}\right] \\ &= \frac{1}{f}\mathbf{k} \cdot \boldsymbol{\omega}\,. \end{aligned} \tag{7.57}$$

Thus the transformation is valid provided that $0 < J < \infty$.

Exercises

(7.6) Obtain the matrix A such that $\partial_{\mathbf{x}} = A\partial_{\mathbf{X}}$, for the transformation (7.55), where $\partial_{\mathbf{x}}$ denotes the vector operator $(\partial/\partial x,\ \partial/\partial y,\ \partial/\partial z)$. Verify that $det\ A = J$ and find A^{-1}. Hence show that

$$J\frac{\partial}{\partial Z} = \frac{1}{f}\boldsymbol{\omega} \cdot \nabla. \tag{7.58}$$

(7.7) From the expression for A^{-1} obtained in Exercise (7.6), show that

$$J\left(1-\frac{1}{f}\frac{\partial v_g}{\partial X}\right)=1-\frac{1}{f}\frac{\partial u_g}{\partial y},\quad J\left(1+\frac{1}{f}\frac{\partial u_g}{\partial Y}\right)=1+\frac{1}{f}\frac{\partial v_g}{\partial x},$$

and

$$J\frac{\partial u_g}{\partial X}=-\frac{\partial u_g}{\partial x}=-J\frac{\partial v_g}{\partial Y}.$$

Hence, using (7.57), show that

$$J^{-1}=1-\frac{1}{f^2}(\phi_{XX}+\phi_{YY})+\frac{1}{f^4}(\phi_{XX}\,\phi_{YY}-\phi_{XY}^2), \tag{7.59}$$

where ϕ is defined below.

It follows from (7.58) that,

$$J\frac{\partial\theta}{\partial Z}=\frac{1}{f}\boldsymbol{\omega}\cdot\nabla\theta=\frac{q}{f}. \tag{7.60}$$

Hence the static stability is proportional to the potential vorticity. Indeed, geostrophic coordinates, the potential vorticity plays the role of static stability. If we define now

$$\phi=\phi'+\tfrac{1}{2}(u_g^2+v_g^2), \tag{7.61}$$

Eqs. (7.46 and 7.49) become

$$\left(\frac{\partial\phi'}{\partial X},\ \frac{\partial\phi'}{\partial Y},\ \frac{\partial\phi'}{\partial Z}\right)=\left(\frac{\partial\phi}{\partial x},\ \frac{\partial\phi}{\partial y},\ \frac{\partial\phi}{\partial z}\right)=\left(fv_g,\ -fu_g,\ g\frac{\theta}{\theta_0}\right), \tag{7.62}$$

and from (7.59, 7.60 and 7.62) it follows easily that

$$q=\frac{f\frac{\theta_0}{g}\frac{\partial^2\phi'}{\partial Z^2}}{1-\frac{1}{f^2}\left(\frac{\partial^2\phi'}{\partial X^2}+\frac{\partial^2\phi'}{\partial Y^2}\right)+\frac{1}{f^4}\left[\frac{\partial^2\phi'}{\partial X^2}\frac{\partial^2\phi'}{\partial Y^2}-\left(\frac{\partial^2\phi'}{\partial X\partial Y}\right)^2\right]}, \tag{7.63}$$

where, as it turns out, the nonlinear term in the denominator is normally small. Equations (7.62) and (7.63), the transformed versions of (7.47) and (7.54) express the conservation of potential temperature and potential vorticity, respectively. These, together with the continuity equation (7.48) constitute the semi-geostrophic equations. Thus the semi-geostrophic system is the geostrophic momentum approximation in transformed space.

Suitable boundary conditions on ϕ at a horizontal boundary are provided by setting $w = 0$ in (7.47).

Hoskins and Draghici (1977) show that to within the level of approximation of the geostrophic momentum approximation, the nonlinear terms in (7.57) and (7.63) can be neglected (see Appendix). Hence the third component of vorticity is

$$f\,J = f + \frac{\partial v_g}{\partial x} - \frac{\partial u_g}{\partial y} = \frac{f^2}{f - \frac{\partial v_g}{\partial X} + \frac{\partial u_g}{\partial Y}}, \tag{7.64}$$

and ϕ' satisfies

$$\frac{1}{f^2}\left[\phi'_{XX} + \phi'_{YY}\right] + \frac{1}{q_g}\phi'_{ZZ} = 1, \tag{7.65}$$

where

$$q_g = \frac{gq}{f\theta_o} = \frac{g}{f\theta_o}(\omega \cdot \nabla\theta), \tag{7.66}$$

is the square of the buoyancy frequency that the fluid would have if the geostrophic velocity were negligible; i.e., q_g plays the analogous role in transformed space that the Brunt-Väisälä frequency squared plays in physical space.

7.5 The Eady problem in semi-geostrophic theory.

The Eady problem of baroclinic instability considers the stability of a zonal flow with uniform vertical shear in thermal wind balance with a linear meridional temperature field (DM, Chapter 9), i.e., the basic flow is defined by

$$(u_g, v_g) = \left(\frac{Uz}{H},\ 0\right),$$

and

$$\theta = \theta_0 + \frac{N^2}{g}\theta_0 z - f\frac{\theta_0}{g}\frac{Uy}{H}$$

where N is constant. The reader should check that this basic state is such that

$$f\frac{\partial u_g}{\partial z} = f\frac{U}{H} = -\frac{g}{\theta_0}\frac{\partial\theta}{\partial y},\ \text{and}\ \ \frac{g}{\theta_0}\frac{\partial\theta}{\partial z} = N^2.$$

The geostrophic coordinate transformation is

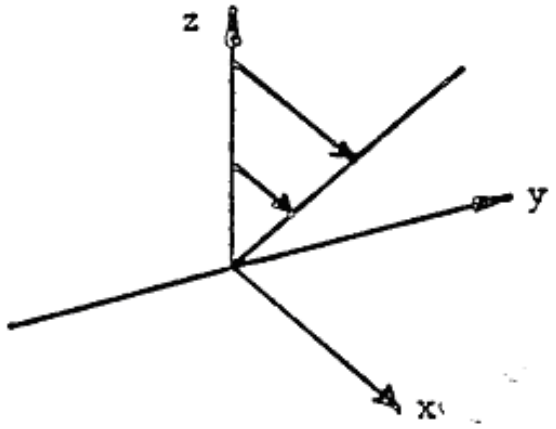

Figure 7.6: The Eady-model basic state.

$$X = x,\ Y = y - u_g/f = y - Uz/(fH),\ Z = z,$$

so that in physical space, lines $Y =$ constant have the equation $z = (fH/U)(y - Y)$. These lines slope towards the pole as shown in Fig. 7.7. For typical values: $U = 30\ ms^{-1}$, $|f| = 10^{-4}\ s^{-1}$, $H = 10$ km, the poleward displacement of the line $Y =$ constant between $z = 0$ and H is 300 km and the angle α shown is $\tan^{-1}(1/30) = 2°$.

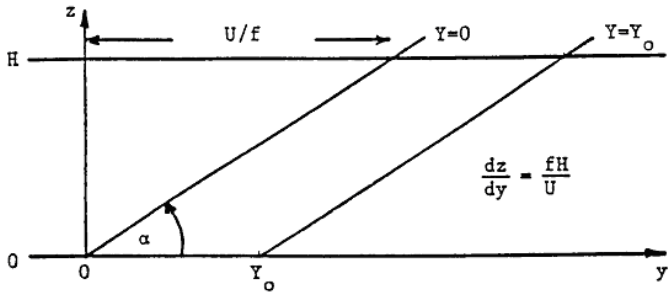

Figure 7.7: Lines $Y =$ constant in physical space (x, y).

In transformed space, the basic flow is characterized by

$$u_g = \frac{UZ}{H}\frac{\theta_0}{g},\quad \theta = \theta_0 + \frac{\theta_0}{g}\left[N^2 - \frac{U^2}{H^2}\right] Z - f\frac{\theta_0}{g}\frac{UY}{H},$$

$$\phi = gZ + \tfrac{1}{2}(N^2 - (U/H)^2)Z^2 - (fU/H)YZ, \tag{7.67}$$

and

$$q_g = N^2 - (U/H)^2. \tag{7.68}$$

Using (7.65), and (7.47) in transformed space, the perturbation to the basic flow characterized by ϕ' satisfies

$$\frac{1}{f^2}(\phi'_{XX} + \phi'_{YY}) + \frac{1}{q_g}\phi'_{ZZ} = 0, \tag{7.69}$$

with

$$\left[\frac{\partial}{\partial T} + \frac{UZ}{H}\frac{\partial}{\partial X}\right]\frac{\partial \phi'}{\partial z} - \frac{U}{H}\frac{\partial \phi'}{\partial X} = 0 \text{ at } Z = 0, 1. \tag{7.70}$$

Equation (7.69) with the boundary condition (7.70) leads to the same eigenvalue problem as for the quasi-geostrophic Eady problem in physical space, except that N^2 is replaced now by $q_g = N^2(1-(U/NH)^2)$. For $N = 10^{-2}s^{-1}$ and the above values of U and H, $q_g = 0.91N^2$.

The solution of (7.69) and (7.70) analogous to (9.18) in DM is

$$\phi'(X, Z, T) = A(Z')e^{ke_iT}\cos[k(X - \tfrac{1}{2}UT) - \gamma(Z')], \tag{7.71}$$

where $Z' = Z - \frac{1}{2}H = z - \frac{1}{2}H$. For this, $u'_g = -f^{-1}\phi'_Y = 0$ and $v' = v'_g + f^{-1}Du'_g/Dt = v'_g$. The structure in physical space becomes distorted since $x = X - v'_g/f = X - (\partial\phi'/\partial X)/f^2$, although $y = Y - u'_g/f = Y$. Thus the region of cyclonic vorticity $\phi_x = \phi_X > 0$ is reduced and the region of anticyclonic vorticity is increased. Of course, for the linear solution, v' is small and $x \approx X$ so that the distortion would be hardly noticeable. However, this is not the case when the wave grows to finite amplitude as shown by a calculation for the fully nonlinear problem after five days (Fig. 7.8). As in the quasi-geostrophic case, the fastest growing wave perturbation has half-wavelength $\pi_R/1.6$ and growth rate $kc_i|_{max} = 0.31u/L_R$, where now $L_R = (H\sqrt{q_g}/f)$. Thus the wavelength is slightly reduced and the growth rate slightly increased (since $q_g < N^2$) in comparison with the quasi-geostrophic case.

In the absence of lateral boundaries, both the quasi-geostrophic and semi-geostrophic equations admit three-dimensional solutions, the former periodic in y, the latter in Y. In the former case, such solutions satisfy boundary conditions appropriate to a zonal channel flow (i.e., $v = 0$ at $y = y_0$, y_1, say), but in the latter case they do not, since the periodicity is in transformed space

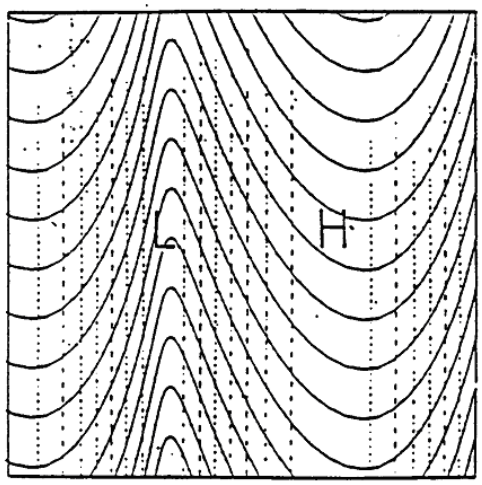

Figure 7.8: Surface map for the Eady wave independent of $y(\mu = 0)$ at day 5. Contours of height field f are dashed and drawn every 75 m ($\sim$ 9 mb) and those of surface (potential) temperature are continuous and drawn every 6 K. Height field lows and highs are indicated. The domain is 5623 km in both horizontal directions. This is approximately 1.25 wavelengths in the zonal direction (from Hoskins and West, 1979).

rather than physical space. In essence, the semi-geostrophic solution includes a factor cos mY in (7.71) and, as in the quasi-geostrophic case, the stability criterion is modified by the contribution of m to the total wavelength (DM, page 133, Eq. (9.20)). Of major significance now is the fact that the patterns of pressure, geostrophic velocity, and potential temperature are distributed along lines $Y =$ constant; i.e., $y - (Uz/fH) =$ constant. These are parallel with the absolute vorticity vector and slope upward and poleward as shown in Fig. 7.7. Hoskins and West (1979, p1670) argue that the cyclic boundary condition may, in fact, be rather better than the imposition of $v = 0$ at latitudinal walls. They studied the growth of baroclinic wave disturbances to finite amplitude by integrating the semi-geostrophic equations numerically. In particular they have studied the growth of fronts in such waves. They consider the instability of basic zonal jet flows of the type shown in Fig. 7.9, for which $q_g =$ constant. These flows have the form

$$u = \frac{U}{H}Z - \frac{1}{2}\mu\left[\frac{Z}{H} + \frac{\sinh\,\ell Z}{\sinh\,\ell H}\,\cos\,mY\right], \tag{7.72}$$

where $\ell/m = H\sqrt{q_g}/f$, the Rossby radius of deformation. They are periodic

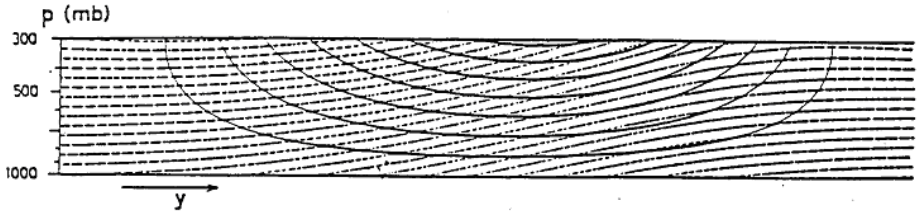

Figure 7.9: The zonal flow given by (7.53) with $\mu = 1$. Dashed lines are potential temperature contours and continuous lines contours of zonal velocity. Using the dimensional values specified in the text, the contour intervals are 2. 5 K and 4 m s^{-1}, respectively (from Hoskins and West 1979).

in Y with half-wavelength π/m and tend to the Eady basic flow as $\mu \to 0$. Since q_g is a constant initially, it will remain constant for all time according to (7.54). Then the diagnostic equation (7.65) has constant coefficients and (7.54) is not needed further. Figure 7.10 shows the normal mode perturbation

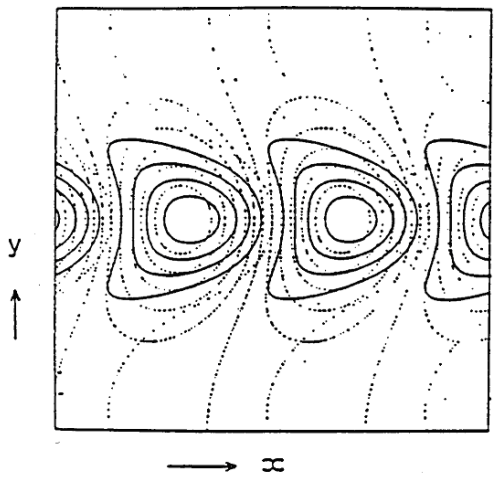

Figure 7.10: Normal mode perturbation fields of height field ϕ and vertical component of relative vorticity ζ at $z = 0$ for the most unstable mode for $\mu = 1$. Contours of ϕ are dashed and those of ζ continuous except for the zero contour which is dotted. A distance $2\pi/\ell$ is shown in x, this being more than one wavelength (from Hoskins and West 1979).

height field f and vertical component of relative vorticity ζ at $z = 0$ for the most unstable mode when $\mu = 1$. This solution, obtained by solving the

linear eigenvalue problem numerically, is used as the initial condition for a full nonlinear solution of the semi-geostrophic equations.

Chapter 8

SYMMETRIC BAROCLINIC INSTABILITY

We consider further the stability of a basic zonal flow $U(y, z)$ in the x direction in thermal wind balance with the basic state potential temperature field $\theta(y, z)$ - see Fig. 8.1. Here z is Hoskins' pseudo-height coordinate used earlier. Unlike the classical baroclinic instability problem, we consider disturbances with only meridional structure; i.e. roll perturbations, independent of x.

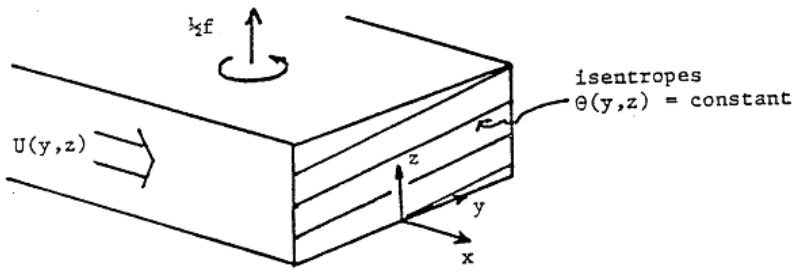

Figure 8.1: Zonal flow $U(y, z)$ in thermal wind balance with the isentropes $\theta(y, z)$.

An important application of the theory is to the stability of pre- and post-frontal jets (see e.g. Fig. 8.2), while the analogous axisymmetric problem is relevant to tropical cyclones. Thermal wind balance of $U(y, z)$ and $\theta(y, z)$ implies that

$$f\frac{\partial U}{\partial z} = -\frac{g}{\theta_0}\frac{\partial \theta}{\partial y}, \tag{8.1}$$

We define the basic frequencies N, S and F by

$$N^2 = \frac{g}{\theta_0}\frac{\partial\theta}{\partial z}, \quad S^2 = -\frac{g}{\theta_0}\frac{\partial\theta}{\partial y} = f\frac{\partial U}{\partial z}, \quad F^2 = f\left(f - \frac{\partial U}{\partial y}\right), \tag{8.2}$$

all taken to be positive. Typically, $N \sim 10^{-2}s^{-1}$, $S \sim 5 \times 10^{-4}s^{-1}$ and $F \sim 10^{-4}s^{-1}$.

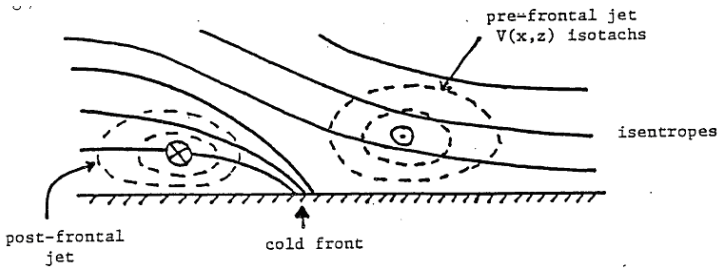

Figure 8.2: A cold front with pre- and post-frontal along-front jets.

The classical work on symmetric instability was carried out under the name of the stability of a baroclinic vortex. (Fjortoft, 1950; Eliassen, 1957). We pursue here the normal mode approach of Ooyama (1966) and Hoskins (1974). We make the Boussinesq approximation, but allow for motions to be non-hydrostatic. The equation are as formulated by Hoskins and Bretherton (1972).

The linearized equations for perturbations independent of x are:

$$\frac{\partial u'}{\partial t} + v'\frac{\partial U}{\partial y} + w'\frac{\partial U}{\partial z} - fv' = 0, \tag{8.3}$$

$$\frac{\partial v'}{\partial t} + fu' + \frac{\partial \phi'}{\partial y} = 0, \tag{8.4}$$

$$\frac{\partial w'}{\partial t} - g\frac{\theta'}{\theta_0} + \frac{\partial \phi'}{\partial z} = 0, \tag{8.5}$$

and

$$\frac{\partial v'}{\partial y} + \frac{\partial w'}{\partial z} = 0. \tag{8.6}$$

It is convenient to introduce a new dependent variable $M = -fy + U$, which loosely may be called the *absolute velocity*. Then (8.3) takes the form

$$\frac{\partial u'}{\partial t} + v'\frac{\partial M}{\partial y} + w'\frac{\partial M}{\partial z} = 0, \tag{8.7}$$

and

$$F^2 = -f\frac{\partial M}{\partial y}. \tag{8.8}$$

One then observes a symmetry between the pairs of variables (u', v') and (w', q'), assuming that N^2, S^2, F^2 and θ_0 are constants:

$$\frac{\partial u'}{\partial t} + v'\frac{\partial M}{\partial y} + w'\frac{\partial M}{\partial z} = 0, \quad \frac{\partial \theta'}{\partial t} + v'\frac{\partial \theta}{\partial y} + w'\frac{\partial \theta}{\partial z} = 0$$
$$\frac{\partial v'}{\partial t} + fu' + \frac{\partial \phi'}{\partial y} = 0, \quad \frac{\partial w'}{\partial t} - g\frac{\theta'}{\theta_0} + \frac{\partial \phi'}{\partial z} = 0.$$

When U is proportional to $z, \partial\theta/\partial y =$ constant, and if $\partial\theta/\partial z =$ constant, $\nabla\theta$ and ∇M are constant vectors; i.e.,

$$\nabla\theta = \left(0,\ \frac{\partial\theta}{\partial y},\ \frac{\partial\theta}{\partial z}\right) \quad \text{and} \quad \nabla M = \left(0,\ -f + \frac{\partial U}{\partial y},\ \frac{\partial U}{\partial z}\right),$$

$$\text{typically} < 0,\ > 0 \qquad \text{typically} < 0,\ > 0$$

and the isentropes and isopleths of M are as shown in Fig. 8.3. Typically,

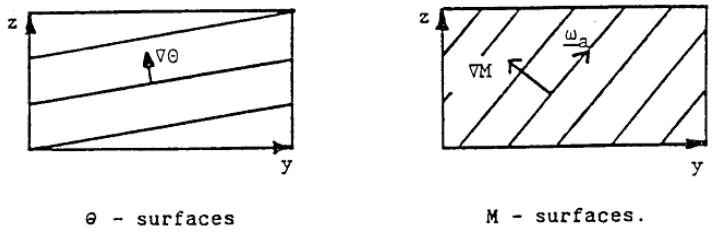

Figure 8.3: A cold front with pre- and post-frontal along-front jets.

$\partial U/\partial z \sim 20/10^4 = 2 \times 10^{-3} s^{-1}$ and $f \sim 10^{-4} s^{-1} > |\partial U/\partial y|$, so that M surfaces normally have a slope $<< \frac{\pi}{4}$. Note that, the curl of $M\mathbf{i}$ is $\boldsymbol{\omega}_a = (0,\ \partial U/\partial z,\ f - \partial U/\partial y)$, which defines the *absolute vorticity vector*. Therefore, since $\boldsymbol{\omega}_a \cdot \nabla M = 0$, M-surfaces lie along the absolute vorticity vector.

Exercises

(8.1) Show that M surfaces have slope χ given by $\tan\chi = F^2/S^2$, while θ surfaces have slope Λ given by $\tan\Lambda = S^2/N^2$. Hence show that $\partial u'/\partial t$ and $\partial\theta'/\partial t$ are proportional respectively to $\sin(\chi-\alpha)$ and $\sin(\Lambda-\alpha)$, where α is the trajectory slope ($\tan\alpha = w'/v'$), and find the constant of proportionality. A consequence is that the generation of u' depends on the slope of trajectories compared with that of M-surfaces, while the generation of θ' depends on the slope of trajectories compared with that of θ surfaces.

(8.2) Derive the zonal component of the perturbation vorticity $\xi(=\partial w'/\partial y - \partial v'/\partial z)$; i.e.,

$$\frac{\partial\xi}{\partial t} = \frac{g}{\theta_0}\frac{\partial\theta'}{\partial y} + f\frac{\partial u'}{\partial z}, \tag{8.9}$$

and observe that circulation in a meridional plane is generated by the thermal wind imbalance of the perturbation.

(8.3) Assuming that S^2, N^2 and F^2 are constants (in other words, that length scales for the variation of basic flow variables are much larger than perturbation length scales), deduce from (8.9) that

$$\frac{\partial^2\xi}{\partial t^2} = -N^2\frac{\partial w'}{\partial y} + S^2\left(\frac{\partial v'}{\partial y} - \frac{\partial w'}{\partial z}\right) + f^2\frac{\partial v'}{\partial z}, \tag{8.10}$$

If we introduce a stream function y for the meridional motion such that

$$v' = -\frac{\partial\psi}{\partial z},\ w' = \frac{\partial\psi}{\partial y}, \tag{8.11}$$

then (8.6) is automatically satisfied; $\xi = \nabla^2\psi$; and (8.10) becomes

$$\frac{\partial^2}{\partial t^2}\left[\frac{\partial^2\psi}{\partial y^2} + \frac{\partial^2\psi}{\partial z^2}\right] = -N^2\frac{\partial^2\psi}{\partial y^2} - F^2\frac{\partial^2\psi}{\partial z^2} - 2S^2\frac{\partial^2\psi}{\partial y\partial z}. \tag{8.12}$$

In an unbounded domain we may seek solutions of the form

$$\psi = \hat{\psi}e^{ik(-y\sin\alpha + z\cos\alpha + ct)}, \tag{8.13}$$

where k, c, α and $\hat{\psi}$ are constants. These correspond with travelling waves of frequency $\omega = ck$ and total wave number k, travelling in the direction

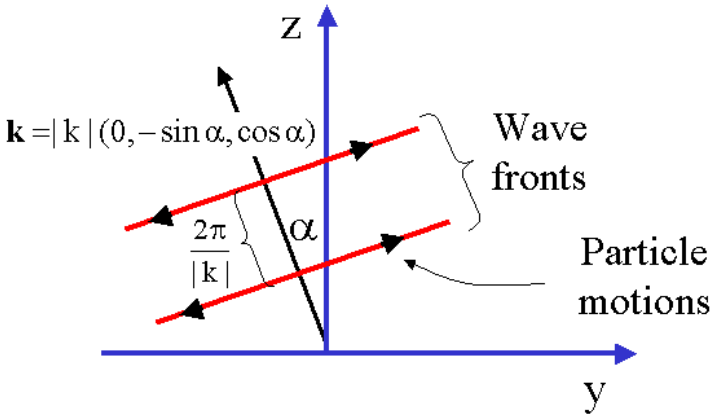

Figure 8.4:

$(0, -\sin\alpha, \cos\alpha)$ as shown. Note that, as for all transverse wave motions, the particle motions are normal to this direction.

Substitution of (8.13) into (8.12) gives

$$\omega^2 = N^2 \sin^2\alpha - 2S^2 \sin\alpha\cos\alpha + F^2\cos^2\alpha, \tag{8.14}$$

which is the dispersion relationship. Note that there is no wavelength dependence, there being no intrinsic length scale in the problem. Inertial oscillations in the horizontal ($\alpha = 0$, $\omega = F$) and buoyancy oscillations ($\alpha = \frac{\pi}{2}$, $\omega = N$) are special cases of (8.14). If the right-hand side of (8.14) is negative, ω is pure imaginary implying instability.

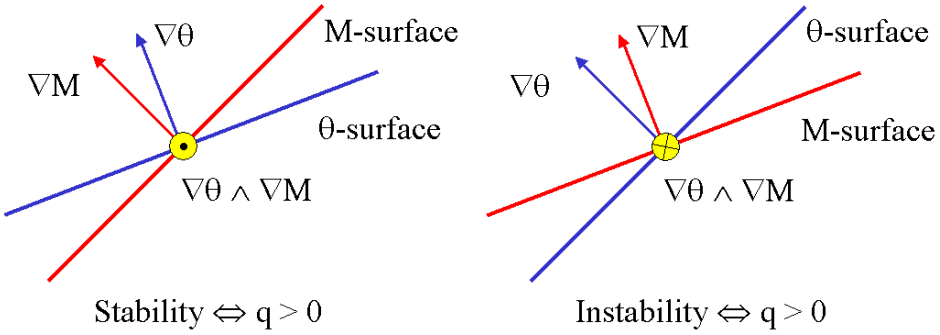

Figure 8.5:

Exercise

(8.4) Show that (8.14) can be written as

$$2\omega^2 = N^2 + F^2 - A\cos 2(\alpha - \alpha_1), \tag{8.15}$$

where α_1 is defined by

$$\sin 2\alpha_1 = 2S^2/A, \quad \cos 2\alpha_1 = (N^2 - F^2)/A \tag{8.16}$$

and

$$A = [(N^2 - F^2)^2 + 4S^4]^{1/2}.$$

According to (8.15), the minimum frequency, ω_{min}, corresponds with $\alpha = \alpha_1$, which is *slightly steeper* than the θ surfaces (since $N^2 >> F^2$, implying that $\tan 2\alpha_1 \approx 2S^2/N^2 \sim 10^{-1}$). Furthermore, the *maximum* frequency, ω_{max}, corresponds with $\alpha = \frac{\pi}{2} + \alpha_1$, a nearly vertical trajectory slope.

(8.5) Show that

$$\omega_{max}^2 \omega_{min}^2 = N^2F^2 - S^4. \tag{8.17}$$

The Ertel potential vorticity of the basic flow is

$$\begin{aligned} q &= \frac{g}{f\theta_0}\left[\frac{\partial U}{\partial z}\frac{\partial \theta}{\partial y} + \left(f - \frac{\partial U}{\partial y}\right)\frac{\partial \theta}{\partial z}\right] \\ &= \frac{g}{f\theta_0}\left[\frac{\partial M}{\partial z}\frac{\partial \theta}{\partial y} - \frac{\partial M}{\partial y}\frac{\partial \theta}{\partial z}\right] \\ &= \frac{1}{f^2}\left[-S^4 + F^2N^2\right], \end{aligned} \tag{8.18}$$

whereupon

$$\omega_{max}^2 \omega_{min}^2 = f^2 q. \tag{8.19}$$

We may now construct the graph of ω^2 versus ϕ. Since q is a conserved quantity, the rearrangement of the basic flow that makes it more stable to oscillations in the vertical (i.e. larger ω_{max}^2), makes it less stable to motions along the isentropes (i.e., smaller ω_{min}^2, which corresponds with $\alpha = \alpha_1$). The basic flow is *stable* if and only if $\omega_{min}^2 > 0$; i.e., $q > 0$, or equivalently,

$J(\theta, M) > 0$. Since[1] $J(\theta, M) = \mathbf{i} \cdot (\nabla\theta \wedge \nabla M)$, we have the two situations shown in Fig. 8.6. Thus the flow is *stable* if M-surfaces are more vertical than θ-surfaces, and *unstable* if the θ-surfaces are more vertical.

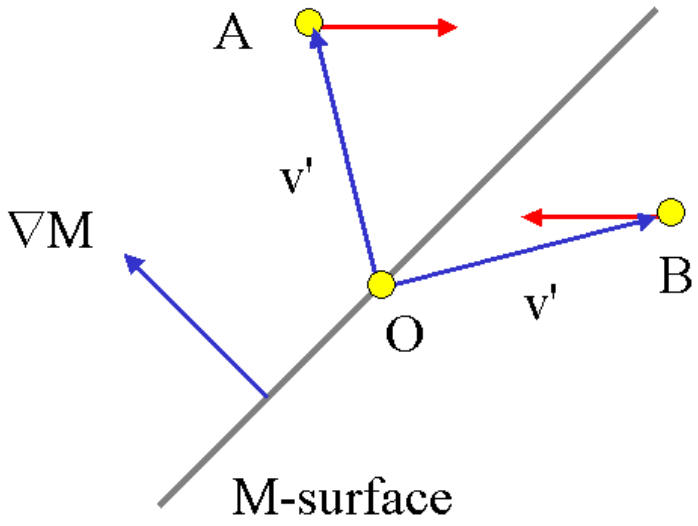

Figure 8.6:

Consider a perturbation in which a fluid parcel moves away from a point 0 on an M-surface to a point A or B as shown. Since $\partial u'/\partial t = -\mathbf{v}' \cdot \nabla M$, $(\partial u'/\partial t)_A < 0$, $(\partial u'/\partial t)_B > 0$, implying that $u'_A < 0$, $u'_B > 0$. Also, $\partial v'/\partial t = -fu' - \partial\phi/\partial y$, so that, in as much as the v' acceleration is due to the Coriolis torque, $-fu'$, then $(\partial v'/\partial t)_A > 0$ and $(\partial v'/\partial t)_B < 0$. Hence a perturbation away from an M-surface leads to a horizontal acceleration back to it.

In a similar way, we can show that a perturbation away from a θ-surface leads to a vertical acceleration back towards it (Fig. 8.7).

With these results, we can interpret the instability. In the case $q > 0$, a displacement leads to a positive restoring force; when $q < 0$, the restoring force is negative and leads to instability.

[1] $i \cdot (\nabla\theta \wedge \nabla M) = (1,0,0) \cdot (0, \theta_y, \theta_z) \wedge (0, M_y, M_z) = (1,0,0) \cdot (\theta_y M_z - \theta_z M_y, 0, 0)$.

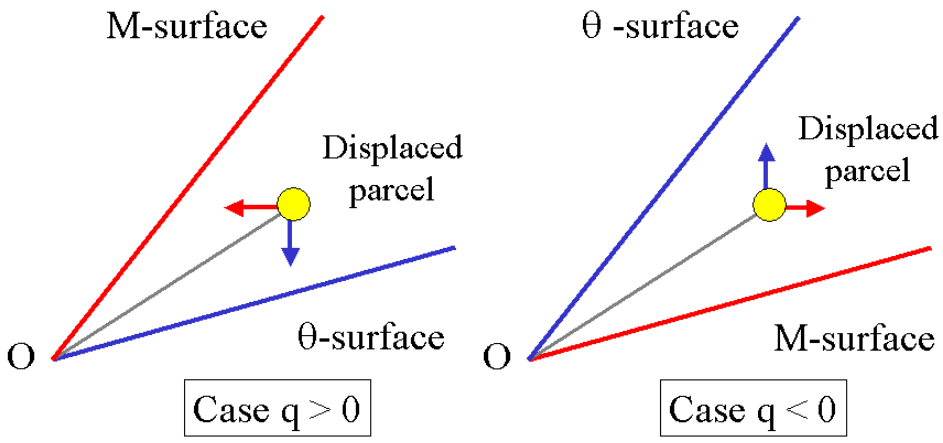

Figure 8.7:

8.1 Richardson number criterion

We may define a *Richardson number*, Ri, by

$$Ri = \frac{g}{\theta_0}\frac{\partial\theta}{\partial z}\Big/\left[\frac{\partial U}{\partial z}\right]^2 = \frac{f^2N^2}{S^4}.$$

Then $q = F^2N^2 - S^4 < 0$ is equivalent to $F^2N^2/S^4 < 1$ or $f^2N^2/S^4 < f^2/F^2$; i.e.,

$$Ri < \left[1 - \frac{1}{f}\frac{\partial U}{\partial y}\right]^{-1}. \tag{8.20}$$

For flows with no horizontal shear, the condition for symmetric instability becomes

$$Ri < 1. \tag{8.21}$$

Stone (1966) showed that for the simple Eady basic state of a constant shear in the vertical, Eady baroclinic waves dominate for $Ri > 0.95$ and Kelvin-Helmholtz waves for $Ri < 0.25$. In the range $0.25 < Ri < 0.95$, the symmetric baroclinic waves have the largest growth rates.

Exercises

(8.6) Show that with χ, Λ and α defined in exercise (8.1), Eq. (8.14) can be written as

$$\omega^2 = S^2 \left[\frac{\sin\ \alpha}{\sin\ \Lambda}\ \sin\ (\alpha - \Lambda) + \frac{\cos\ \alpha}{\cos\ \chi}\ \sin\ (\chi - \alpha) \right].$$

(8.7) Show that if the hydrostatic approximation is made, the dispersion relation becomes

$$\omega^2 = N^2 \tan^2 \alpha - 2S^2 \tan \alpha + F^2$$

and that the stability criterion is again $q > 0$ for stability.

It appears that the instability condition is rarely satisfied in the atmosphere, although there is evidence that symmetric instability modified by latent heat release may play a role in the generation of frontal rainbands (Bennetts and Hoskins, 1978; Emanuel, 1983).

Chapter 9

GEOSTROPHIC ADJUSTMENT

We have studied geostrophic, quasi-geostrophic, and semi-geostrophic motions of various types; now we illustrate how the adjustment to geostrophy takes place by considering one particularly simple flow[1]. We consider a homogenous layer of fluid of mean depth H with a free surface. At the initial time, $t = 0$, the surface has the form of a small step in height along the y-axis ($x = 0$): see Fig. 9.1. The initial fluid depth is represented by the formula:

$$h(x) = H + H\eta_o \mathrm{sgn}(x), \tag{9.1}$$

where

$$\mathrm{sgn}(x) = \begin{cases} 1 \text{ for } & x \geq 0, \\ -1 \text{ for } & x < 0. \end{cases}$$

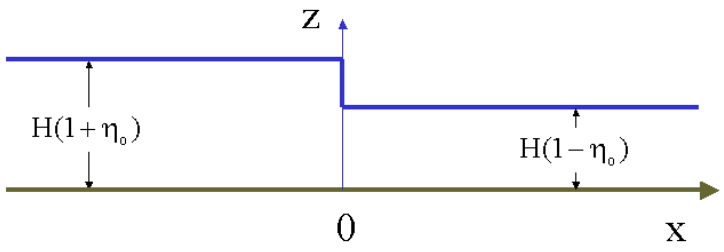

Figure 9.1: The initial surface displacement in Eq. (9.1).

The subsequent motion is assumed to be given by the linearized equations:

[1]This problem is discussed by Gill (1982; see sections 5.6, 7.2 and 7.3)

$$\frac{\partial u}{\partial t} - fv = -c^2 \frac{\partial \eta}{\partial x}, \tag{9.2}$$

$$\frac{\partial v}{\partial t} + fu = -c^2 \frac{\partial \eta}{\partial y}, \tag{9.3}$$

$$\frac{\partial \eta}{\partial t} + \frac{\partial u}{\partial x} + \frac{\partial v}{\partial y} = 0, \tag{9.4}$$

where $c = \sqrt{gH}$ (see DM, Chapter 11). Taking the divergence of (9.2) and (9.3) and using (9.4) to eliminate the horizontal divergence gives

$$\frac{\partial^2 \eta}{\partial t^2} - c^2 \left(\frac{\partial^2 \eta}{\partial x^2} + \frac{\partial^2 \eta}{\partial y^2} \right) + f\zeta = 0, \tag{9.5}$$

where $\zeta = \partial v/\partial x - \partial u/\partial y$ is the relative vorticity.

9.1 The nonrotating case $(f = 0)$

In this case the motion remains irrotational ($\zeta = 0$) and Eq. (9.5) reduces to the wave equation for two-dimensional motion ($\partial/\partial y \equiv 0$). The well-known solution to this equation is $\eta(x,t) = \frac{1}{2}\left[F(x-ct) + G(x+ct)\right]$, where F and G are arbitrary functions of their arguments. The solution represents the sum of a pair of disturbances with elevations $F(x)$ and $G(x)$ at $t = 0$ propagating in opposite directions with uniform speed c. In the case of the initial step profile with the fluid initially at rest, it is easily verified that

$$\eta(x,t) = -\tfrac{1}{2}\eta_o \left[\mathrm{sgn}(x-ct) + \mathrm{sgn}(x+ct)\right] \tag{9.6}$$

and

$$u(x,t) = \tfrac{1}{2}\eta_o \left[\mathrm{sgn}(x-ct) - \mathrm{sgn}(x+ct)\right].$$

Note that $u(x,t) = g\eta_o/c$ for $|x| < ct$ and is zero for $|x| > ct$. The evolution of this solution is illustrated in Fig. 9.2. It consists of a step of elevation propagating in the positive x-direction and a step of depression propagating in the negative x-direction. The flow is uniform and from right to left for $|x| < ct$ and zero elsewhere.

9.2 The rotating case $(f \neq 0)$

In this case the flow between the two moving steps will experience a Coriolis force acting to the right in the Northern Hemisphere; this will lead to a flow

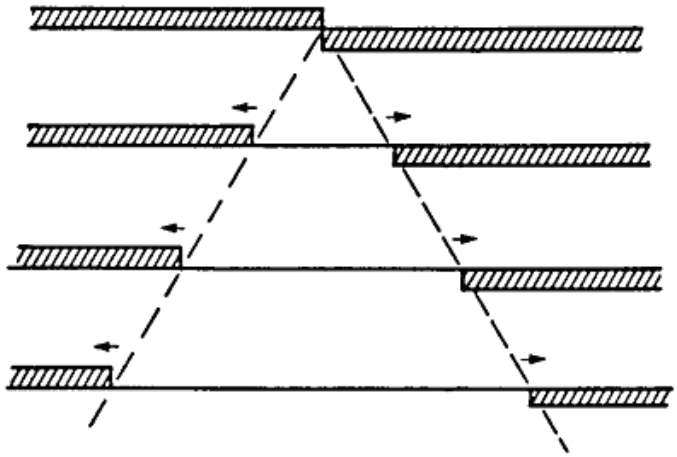

Figure 9.2: Solution of the shallow-water wave equation for the initial surface displacement in Eq. (9.1). Waves of elevation and depression move out from the initial discontinuity with speed c, leaving behind zero displacement, but a steady motion from right to left with speed $c\eta_o$ (From Gill, 1982).

in the negative y-direction. In turn this flow will be subject to a Coriolis force acting in the negative x-direction which will oppose the flow between the steps. The final adjusted state may be calculated without consideration of the transients. The (vertical) vorticity equation is obtained by taking the curl of (9.2) and (9.3) to give:

$$\frac{\partial \zeta}{\partial t} + f\left(\frac{\partial u}{\partial x} + \frac{\partial v}{\partial y}\right) = 0.$$

Eliminating the horizontal divergence using (9.4) leads to the equation:

$$\frac{\partial}{\partial t}\left(\frac{\zeta}{f} - \eta\right) = 0. \tag{9.7}$$

This is just the linearized form of the potential vorticity equation for a homogeneous rotating fluid (DM, Eq.6.5). The quantity Q', defined by

$$Q' = \zeta - f\eta,$$

is the perturbation potential vorticity and (9.7) expresses the fact that retains its initial value at each point for all time, i.e.

$$Q'(x, y, t) = Q'(x, y, 0).$$

One can exploit this infinite memory of an inviscid rotating fluid to find the final equilibrium solution for a particular initial state *without considering* details of the transient motions.

In the present case, at $t = 0$, $u = v = 0$ and $\eta = \eta_o \ \mathrm{sgn}(x)$, whereupon

$$\zeta/f - \eta = \eta_o \mathrm{sgn}(x).$$

Substitution into (9.5) gives:

$$\frac{\partial^2 \eta}{\partial t^2} - c^2 \frac{\partial^2 \eta}{\partial x^2} + f^2 \eta = -f^2 \eta_o \mathrm{sgn}(x). \tag{9.8}$$

In the steady state ($\partial/\partial t = 0$) this reduces to

$$c^2 \frac{d^2 \eta}{dx^2} - f^2 \eta = f^2 \eta_o \mathrm{sgn}(x). \tag{9.9}$$

The solution for $\eta(x)$ in Eq. (9.9) that is continuous and symmetric about $x = 0$ is:

$$\eta(x) = \eta_o \times \begin{cases} -1 + \exp(-x/L_R) & \text{for} \quad x \geq 0 \\ 1 - \exp(x/L_R) & \text{for} \quad x < 0 \end{cases} \tag{9.10}$$

where $L_R = c/|f| = \sqrt{gH}/|f|$ is the Rossby radius of deformation. The corresponding velocity field is:

$$v(x) = -\frac{gH\eta_o}{fL_R} \exp(-|x|/L_R). \tag{9.11}$$

Note that the ultimate flow is *not* in the direction of the pressure gradient, but at right angles to it. The solution is shown in Fig. 9.3.

9.3 The transient problem

To obtain a complete solution of the adjustment problem, i.e. of (9.8), we put $\eta_1 = \eta - \eta_{\text{steady}}$ with η_{steady} given by (9.10). Then η_1 satisfies the homogeneous equation[2]

$$\frac{\partial^2 \eta_1}{\partial t^2} - c^2 \frac{\partial^2 \eta_1}{\partial x^2} + f^2 H \eta_1 = 0. \tag{9.12}$$

subject to the initial condition

[2]Equation (9.12) is sometimes called the Klein-Gordon equation: see Gill (1982, p196).

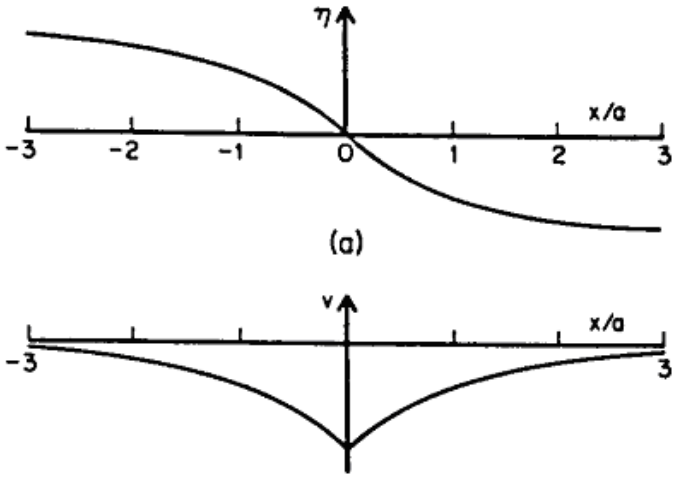

Figure 9.3: The geostrophic equilibrium solution corresponding to adjustment from an initial state that one of rest, but has uniform infinitesimal surface elevation $-\eta_o$ for $x > 0$ and η_o for $x < 0$. (a) The equilibrium surface level η, which tends towards the initial level as $x \to \pm\infty$. The distance unit is the Rossby radius of deformation (here denoted by a). (b) The corresponding equilibrium velocity distribution: there is a "jet" directed along the initial discontinuity in level with maximum speed equal to $c\eta_o$ (From Gill, 1982).

$$\begin{aligned} \eta_1 &= -\eta_o \mathrm{sgn}(x) - \eta_{steady} \\ &\qquad \text{at } t = 0. \\ &= -\eta_o \exp(-|x|/L_R)\mathrm{sgn}(x) \end{aligned} \tag{9.13}$$

The equation has wave-like solutions of the form

$$\eta_1 \propto \exp[i(kx - \omega t)] \tag{9.14}$$

where ω satisfies the dispersion relation

$$\omega^2 = f^2 + k^2 c^2. \tag{9.15}$$

The solution of the transient problem can be obtained by finding a suitable superposition of solutions. The appropriate combination of waves is the one that gives the initial distribution (9.13) and this can be found from tables of integral transforms [see e.g. Erdelyi *et al.* (1954, Vol. 1, p72)]; it is

$$\eta_1 = -\frac{2\eta_o}{\pi}\int_0^\infty \frac{k\sin kx}{k^2+\mu^2}dk \tag{9.16}$$

where $\mu = L_R^{-1}$. At later times, η_1 will consist of the same superposition of waves, with due allowance made for their propagation. Thus $2\sin kx$ in (9.16) must be replaced by the combination of waves that preserves antisymmetry, namely:

$$\sin(kx+\omega t) + \sin(kx-\omega t) = 2\sin kx\cos\omega t,$$

whereupon the solution at time t is

$$\eta_1 = -\frac{2\eta_o}{\pi}\int_0^\infty \frac{k\sin kx\cos\omega t}{k^2+\mu^2}dk, \tag{9.17}$$

The solutions for u and v can be obtained by reference to the standing-wave solutions that follow directly from (9.3) and (9.4) with $\partial/\partial y = 0$, i.e.

$$\begin{aligned} \eta_1 &= \sin kx\cos\omega t \\ u &= -\frac{\omega}{k}\cos kx\sin\omega t. \\ v &= -\frac{f}{k}\cos kx\cos\omega t \end{aligned}$$

For example,

$$u = \frac{2gH\eta_o}{\pi c}\int_0^\infty \frac{\cos kx\sin\omega t}{\sqrt{k^2+\mu^2}}dk, \tag{9.18}$$

where ω is given by Eq. (9.15). It happens that the transform on the right-hand-side can be evaluated exactly (Erdelyi *et al.* 1954, Vol. 1, p26); giving

$$u = \begin{cases} (gH\eta_o/c)J_0(f(t^2-x^2/c^2)^{1/2}) & \text{for } |x| < ct, \\ 0 & \text{for } |x| \geq ct, \end{cases} \tag{9.19}$$

where J_0 is the Bessel function of order zero. This is a special solution of the Klein-Gordon equation, corresponding to a point impulse at $x = 0$ at $t = 0$ (Morse and Feshbach, 1953, p139). The acceleration $\partial u/\partial t$ has the form of a delta function as a result of the infinite pressure gradient that exists at the initial instant.

Figures 9.4 - 9.6 show the solutions for η, u and v. Instead of the wave front having the form of a translating step as in the nonrotating solution, the step is now followed by a "wake" of waves that trail behind it because of dispersion. The shorter waves that contribute to the step still travel at speed c, but longer waves travel more slowly (they have smaller group velocity)

and lag behind. This is illustrated by the behaviour at a fixed point (Fig. 9.6) where the frequency (the time between wave crests) decreases after the passage of the wave front, eventually approaching the inertial frequency, f. Figure 9.6b shows how u varies with time at $x = L_R$.

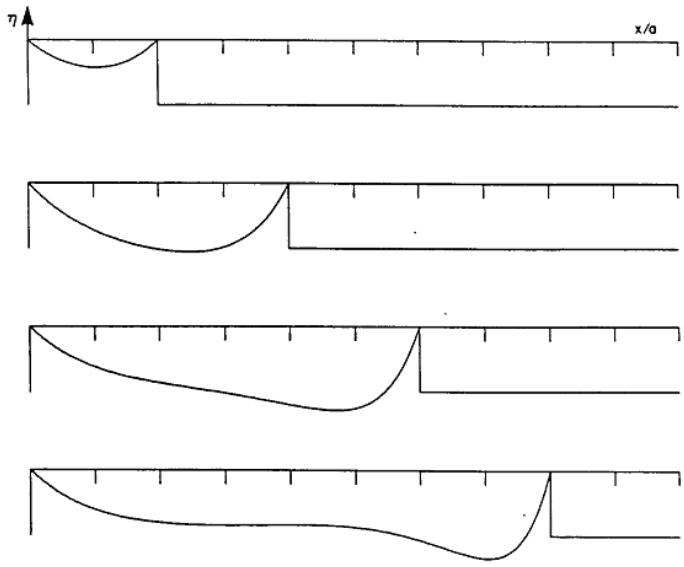

Figure 9.4: Transient profile of h for adjustment under gravity of a fluid with an initial infinitesimal discontinuity in level of $2\eta_o$ at $x = 0$. The solution is shown in the region $x > 0$, where the surface was initially depressed, at time intervals of $2/f$. The marks on the x-axis are at intervals of a Rossby radius of deformation. The solutions retain their initial values until the wave front arrives; this travels out from the position of the initial discontinuity with speed c. When the front arrives, the surface elevation rises abruptly to η_o and the u component of velocity jumps to $c\eta_o$ (see Fig. 9.5), just as in the nonrotating case illustrated in Fig. 9.2. This is because the first wave components to arrive are the very short waves, which are unaffected by rotation. Behind the front, however, is a "wake" of waves produced by dispersion. The width of the front narrows inversely with time. Well behind the front, the solution adjusts to the geostrophic equilibrium solution shown in Fig. 9.3 (From Gill, 1982).

Note how the length scale shortens just behind the wave front at $x = ct$ in Figs. 9.4 - 9.6. To see this put $x = ct + x'$ where $|x'| << |x|$. Then the expression in (9.18) is approximated by

$$t^2 - x^2/c^2 \equiv (2t + x'/c)(-x'/c) \approx 2tx'/c) = -x'/(c/2t)$$

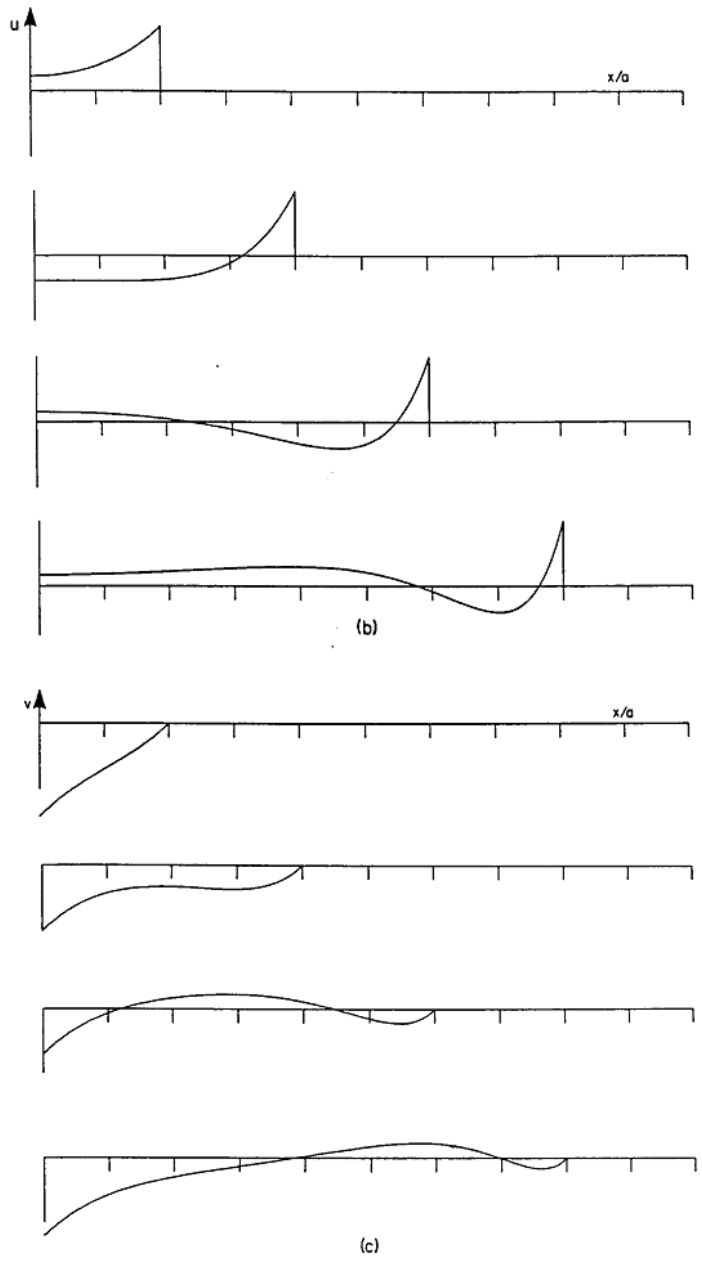

Figure 9.5: Transient profiles of (a) u and (b) v corresponding with the solution for h shown in Fig. 9.4 (From Gill, 1982).

and the length scale $c/(2t)$ diminishes inversely with time. Moreover the solution approaches the steady solution as time proceeds.

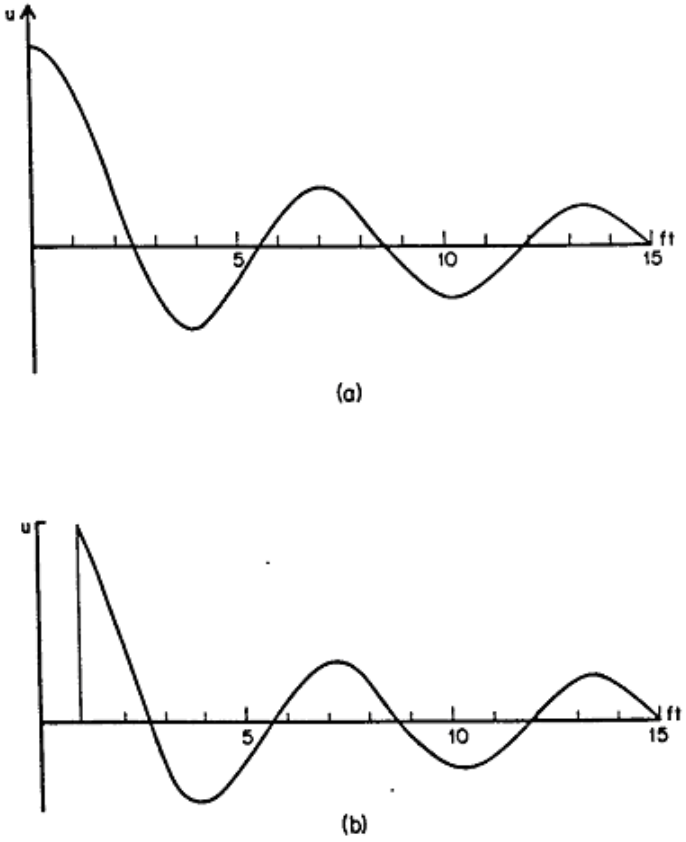

Figure 9.6: The u velocity as a function of time t (a) at the position of the initial discontinuity in level and (b) one Rossby radius away. The time is in units of $1/f$. The solutions show oscillations with frequency near f and decay with time like $1/\sqrt{t}$ at large times (From Gill, 1982).

9.4 Energy considerations

The perturbation energy equation for the shallow-water system is obtained by multiplying (9.1) by ρuH, (9.2) by ρvH and (9.3) by $\rho gH\eta$ and adding. It is easy to show that

$$\frac{\partial}{\partial t}\left[\tfrac{1}{2}\rho H(u^2+v^2)+\tfrac{1}{2}\rho gH^2\eta^2\right]+\frac{\partial}{\partial x}(\rho gHu\eta)+\frac{\partial}{\partial y}(\rho gHv\eta)=0. \qquad (9.20)$$

Note that the Coriolis terms cancel in this procedure and do not appear *explicitly* in the energy equations; this is because the Coriolis force is at right

angles to the velocity vector and therefore does no work. For the special case in which $\partial/\partial y = 0$, the integral of (9.20) over the region $|x| < X$ gives

$$\partial E/\partial t + F(X,t) - F(-X,t) = 0, \tag{9.21}$$

where

$$E = \int_{-X}^{X} \left[\tfrac{1}{2}\rho H(u^2+v^2) + \tfrac{1}{2}\rho g H^2 \eta^2\right] dx \tag{9.22}$$

is the total perturbation energy per unit length in the y-direction in the region $|x| < X$ and

$$F(x,t) = \rho g H u \eta \tag{9.23}$$

is the rate of energy transfer in the x-direction at the position x per unit length in the y-direction.

The total perturbation wave energy density is the sum of the kinetic energy $\frac{1}{2}\rho H(u^2+v^2)$ and the potential energy $\frac{1}{2}\rho g H^2\eta^2$. In the nonrotating situation shown in Fig. 9.2, the potential energy per unit area in the undisturbed region is $\frac{1}{2}\rho g H^2 \eta_o^2$ and the kinetic energy is zero. With the passage of the wave, the potential energy drops to zero while the kinetic energy jumps to the value $\frac{1}{2}\rho H u^2 = \frac{1}{2}\rho H (c\eta_o)^2$. Thus there is no change in total energy, but there is an instantaneous conversion from potential energy to kinetic energy as the wave passes. After a sufficient length of time, therefore, all the perturbation potential energy in a fixed region will be converted into the kinetic energy associated with the steady current that remains after the wave front has passed.

Although the Coriolis forces do not directly appear in the energy equations, the energy changes in the adjustment problem are profoundly affected by rotation. The change in potential energy per unit area at a particular value of x between the initial state and the steady equilibrium state is:

$$\begin{aligned} \Delta PE = \int_{-X}^{X} \left[\tfrac{1}{2}\rho g H^2(\eta_o^2 - \eta_{steady}^2)\right] dx &= \tfrac{1}{2}\rho g H^2 \eta_o^2 \int_0^\infty \left[1 - (1 - e^{-x/L_R})\right] dx \\ &= \tfrac{3}{2}\rho H c^2 \eta_o^2 L_R. \end{aligned} \tag{9.24}$$

In the nonrotating case, all the potential energy is converted to kinetic energy. However, in the present case, the amount of kinetic energy in the equilibrium state per unit length in the y-direction is

$$
\begin{aligned}
KE &= \int_{-X}^{X} \left[\tfrac{1}{2}\rho H v_{steady}^2\right] dx \\
&= 2 \times \tfrac{1}{2}\rho g H^2 \eta_o^2 \int_0^{\infty} \left[e^{-2x/L_R}\right) dx \qquad (9.25) \\
&= \tfrac{1}{2}\rho H c^2 \eta_o^2 L_R,
\end{aligned}
$$

which is only one third of the potential energy released. The remainder is radiated away as inertia-gravity waves in the transient part of the solution.

9.5 Discussion

The foregoing problem gives a great many insights into the response of a rotating fluid to gravitational forces:

- The energy analysis indicates that *energy is hard to extract* from the *available* potential energy in a rotating fluid. The reason is that the geostrophic equilibrium state established retains a certain amount of the initial *available* potential energy.
- The steady solution is *not* one of rest, but is a geostrophically-balanced flow.
- The steady solution is *degenerate* in the sense that any velocity field in geostrophic balance satisfies the continuity equation exactly. Therefore the steady solution cannot be found by looking for a solution of the steady-state equations - some other information is needed.
- The required information is supplied by the principle that potential vorticity is materially conserved (or locally conserved in the linear problem). With this knowledge, a steady solution can be found.
- The equation for the steady solution contains a length scale, $L_R = c/|f|$, where $c = \sqrt{(gH)}$ is the wave speed in the absence of rotation. If $f \to 0$, then $L_R \to \infty$, indicating that for length scales small compared with L_R, rotation effects are small, whereas for scales comparable with or large compared with L_R, rotation effects are important.

The geostrophic adjustment problem considered above explains why the atmosphere and oceans are nearly always close to geostrophic equilibrium on scales comparable with or larger than the Rossby radius of deformation. This is because if any force tries to upset such an equilibrium, the gravitational force acts as described above to restore a near-equilibrium.

9.6 More on the Rossby radius of deformation, L_R

The Rossby radius of deformation is a fundamental length scale in atmosphere-ocean dynamics. In essence, it is the *horizontal* scale at which the gross effects of *rotation* are of comparable importance with *gravitational* (or *buoyancy*) effects. To be specific, it is the scale for which the middle and last terms on the left-hand side of Eq. (9.8) are of the same order.

In the early stages of adjustment from the initial discontinuity in the transient problem discussed above, the change in level is confined to a small distance and the horizontal pressure gradient is comparatively large. Accordingly, gravity dominates the flow behaviour. Thus at scales small compared with the Rossby radius, the adjustment is approximately the same as in a nonrotating system. Later, as the change in surface elevation is spread over a distance comparable with the Rossby radius, the Coriolis acceleration becomes just as important as the pressure gradient term and thus rotation leads to a response that is radically different from that in the nonrotating case.

As shown in DM, Chapter 11, the same is true of inertia-gravity waves; the short waves with wavenumbers much less than L_R behave very much like pure gravity waves. For waves comparable in scale with the radius of deformation, the buoyancy term k^2c^2 in the dispersion relation (9.15) is comparable with the rotation term f^2. In contrast, long waves ($1/k >> L_R$) are dominated by rotation effects and have frequency close to the inertial frequency f. As we have seen, the Rossby radius of deformation is also an important scale for the geostrophic equilibrium solution as well. In the problem analysed above, the discontinuity did not spread out indefinitely, but only over a distance of the order of the Rossby radius.

For geostrophic, or quasi-geostrophic flow, the Rossby radius is the scale for which the two contributing terms to the perturbation potential vorticity Q' are of the same order. For a sinusoidal variation of surface elevation with wavenumber k, the ratio of the vorticity term to the gravitational term in Q' is $\zeta/(f\eta) = L_R^2k^2$. Therefore, for short waves ($1/k << L_R$) the vorticity term dominates while for long waves ($1/k >> L_R$) gravitational effects associated with the free surface perturbation dominate.

For quasi-geostrophic wave motions, the ratio $L_R^2k^2$ characterizes not only the partition of perturbation potential vorticity, but also the *partition of energy*. The perturbation potential energy integrated over one wavelength is

$$PE = \tfrac{1}{2}\rho g H^2 \int_{wavelength} \eta^2 dx, \tag{9.26}$$

whereas the kinetic energy is

$$KE = \tfrac{1}{2}\rho H \int_{wavelength} (u^2 + v^2) dx. \tag{9.27}$$

For quasi-geostrophic waves periodic in x, one can show that (see exercise 9.2) the ratio

$$\frac{KE}{PE} = L_R^2 k^2. \tag{9.28}$$

Thus short-wavelength geostrophic flow contains mainly kinetic energy, while long-wavelength geostrophic flow has most of its energy in the potential form. The situation is different, however, for inertia-gravity waves (see exercise 9.2).

Note that changes in η are associated with changes in the mass field, whereas changes in ζ are associated with changes in the velocity field. Thus for large scales, the potential vorticity perturbation is mainly associated with perturbations in the mass field and energy changes are mainly a result of potential energy changes. On the other hand, for small scales, the potential vorticity perturbation is mainly associated with perturbations in the velocity field and energy changes are mainly a result of kinetic energy changes. It follows that a distinction can be made between the adjustment processes at different scales. At large scales ($1/k >> L_R$), it is the mass field that is determined by the initial potential vorticity, and the velocity field is merely that which is in geostrophic equilibrium with the mass field. In other words, the large-scale velocity field adjusts to be in equilibrium with the large-scale mass field. In contrast, at small scales ($1/k << L_R$), it is the velocity field that is determined by the initial potential vorticity, and the mass field is merely that which is in geostrophic equilibrium with the velocity field. In other words, the mass field adjusts to be in equilibrium with the velocity field.

9.7 Balanced adjustment

In some cases, if the forcing evolves slowly on the time-scale of an inertial period, $2\pi/f$, the response of a rotating stratified fluid to a particular type of forcing may proceed through a series of quasi-balanced states, with negligible generation of inertia-gravity waves. We consider now some simple flow examples of this type. Again we consider flows involving a single layer of homogeneous fluid (Fig. 9.7).

Let $h(x,t)$ be the local fluid depth and let $S(x,t)$ be the mass *entering* the fluid layer per unit length in the x- and y-directions. For simplicity, it

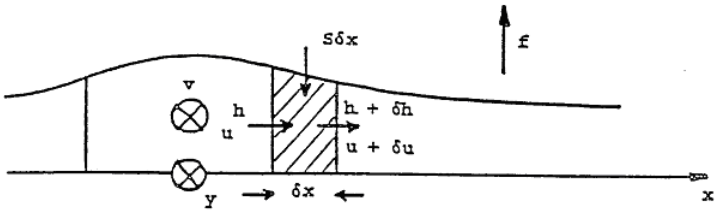

Figure 9.7: Simple flow configuration to illustrate geostrophic adjustment.

is assumed that the fluid entering does not possess horizontal momentum. The fluid may be driven in the y-direction by a body force distribution F per unit height and per unit length in the x-direction.

Conservation of mass in the shaded fluid element in Fig. 9.7 requires that

$$uh - (u + \delta u)(h + \delta h) + S\delta x = (\delta/\delta t)(h\delta x),$$

which in the limit as $\delta x \to 0$ gives

$$\frac{\partial h}{\partial t} + \frac{\partial}{\partial x}(uh) = S, \tag{9.29}$$

The momentum equations are

$$\frac{\partial u}{\partial t} + u\frac{\partial u}{\partial x} - fv = -g\frac{\partial h}{\partial x}, \tag{9.30}$$

and

$$\frac{\partial v}{\partial t} + u\left[\frac{\partial v}{\partial x} + f\right] = F. \tag{9.31}$$

For the moment, we assume that any motions are such that the first two terms in (9.30) are small enough for v to remain geostrophically-balanced, i.e.

$$fv = g\frac{\partial h}{\partial x}. \tag{9.32}$$

Then, differentiating (9.32) with respect to time and using (9.29) and (9.31) to eliminate time derivatives yield a diagnostic equation for u, namely

$$\frac{\partial^2}{\partial x^2}(hu) - \frac{f}{gh}\left(f + \frac{\partial v}{\partial x}\right)(hu) = -\frac{f}{g}F + \frac{\partial S}{\partial x}. \tag{9.33}$$

The solution procedure is then as follows: given F and/or S, Eq. (9.33) can be solved for u, following which h and v can be predicted at the next

time level using (9.29) and (9.31). The associated dynamical processes are brought out by considering special examples.

I. Assume S = 0; $F > 0$ for $-a < x < a$ and $F = 0$ for $|x| \geq a$; see Fig 9.8(a). Also $v(x, 0) = 0$ and $h(x, 0) = H$, a constant

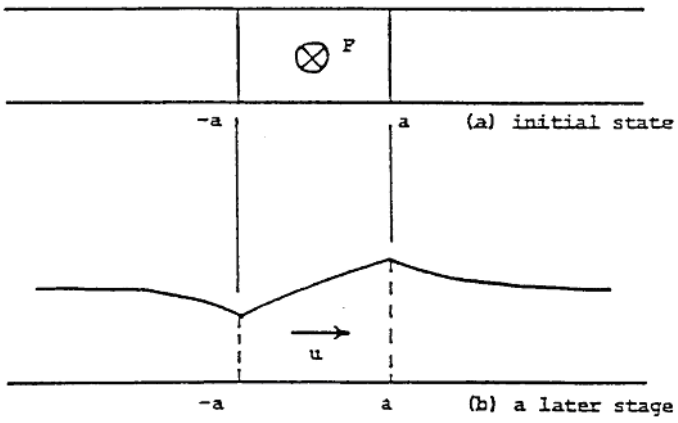

Figure 9.8: Illustration of (a) the initial state, and (b) the adjusted state. See text for details.

Physically, what happens is as follows. As time increases v increases accordingly to (9.31). The Coriolis torque acting to the right of v (for $f > 0$) generates flow to the right in the region $-a < x < a$ as shown in Fig. 9.8(b). According to our balance assumption, $\partial u/\partial t$ and $u\partial u/\partial x$ remain small so that this Coriolis torque is balanced by the negative pressure gradient force $(-g\partial h/\partial x)$. Our interest lies in the horizontal extent of the disturbance outside the forcing region $(-a, a)$.

Let us study the linear problem in which F is a constant in $(-a, a)$ and zero for $|x| > a$. If $h = H(1 + \eta)$, then (9.29), (9.31), (9.32) and (9.33) become

$$\frac{\partial \eta}{\partial t} + \frac{\partial u}{\partial x} = 0, \tag{9.34}$$

$$\frac{\partial v}{\partial t} + fu = F, \tag{9.35}$$

$$fv = gH\frac{\partial \eta}{\partial x}, \tag{9.36}$$

and

$$\frac{\partial^2 u}{\partial x^2} - \frac{u}{L_R^2} = \frac{F}{fL_R^2}, \tag{9.37}$$

where

$$L_R = \sqrt{gH}/f, \tag{9.38}$$

is the *Rossby radius of deformation*. The solution of (9.37) which is continuous and has a continuous x-derivative[3] at $x = -a$ and a, and which decays to zero as $|x| \to \infty$ is (see Ex. 9.1)

$$u(x) = \left(\frac{F}{f}\right) \times \begin{cases} \sinh(a/L_R)\ e^{x/L_R}, & x \le -a \\ \left[1 - e^{-a/L_R}\ \cos\ h\ (x/L_R)\right], & |x| \le a \\ \sinh(a/L_R)\ e^{-x/L_R}, & x \ge a \end{cases} \tag{9.39}$$

Note that this solution is independent of time. Moreover, the influence of forcing has an e-folding decay-scale equal to the Rossby radius L_R. From (9.34) it follows that

$$\frac{h(x,t)}{H} = \begin{cases} 1 - (Ft/L_R f)\ \sinh(a/L_R)\ e^{x/L_R} & x \le -a, \\ \left[1 + (Ft/L_R f)e^{-a/L_R}\ \sinh\ (x/L_R)\right] & |x| \le a, \\ 1 + (Ft/L_R f)\sinh(a/L_R)\ e^{-x/L_R} & x \ge a, \end{cases} \tag{9.40}$$

and from (9.36) that

$$v(x,t) = Ft \times \begin{cases} -\ \sinh(a/L_R)\ e^{x/L_R} & x \le -a, \\ e^{-a/L_R}\ \cosh\ (x/L_R) & |x| \le a, \\ -\sinh(a/L_R)\ e^{-x/L_R} & x \ge a, \end{cases} \tag{9.41}$$

The profiles of $u/(F/f)$, $[H^{-1}h(x,t) - 1]/(Ft/af)$, and $v/(Ft)$, are shown in Fig. 9.9 for the three values of L_R: $\frac{1}{2}a$, a and $2a$. Note also that the disturbance is dispersed further from the forcing region as L_R is increased. Note that u is positive for all values of x. Accordingly, the associated Coriolis torque implies a negative v velocity component, except in the forcing region where this torque is outweighed by the body force F. The discontinuity in $\partial h/\partial x$ at $x = \pm a$ and the corresponding discontinuity in v are consistent features within the inviscid model, but would be smeared out by viscosity in a real fluid.

[3]From (10.6) it is clear that continuity of u_x ensures continuity of h_t and hence of h, and finally of pressure.

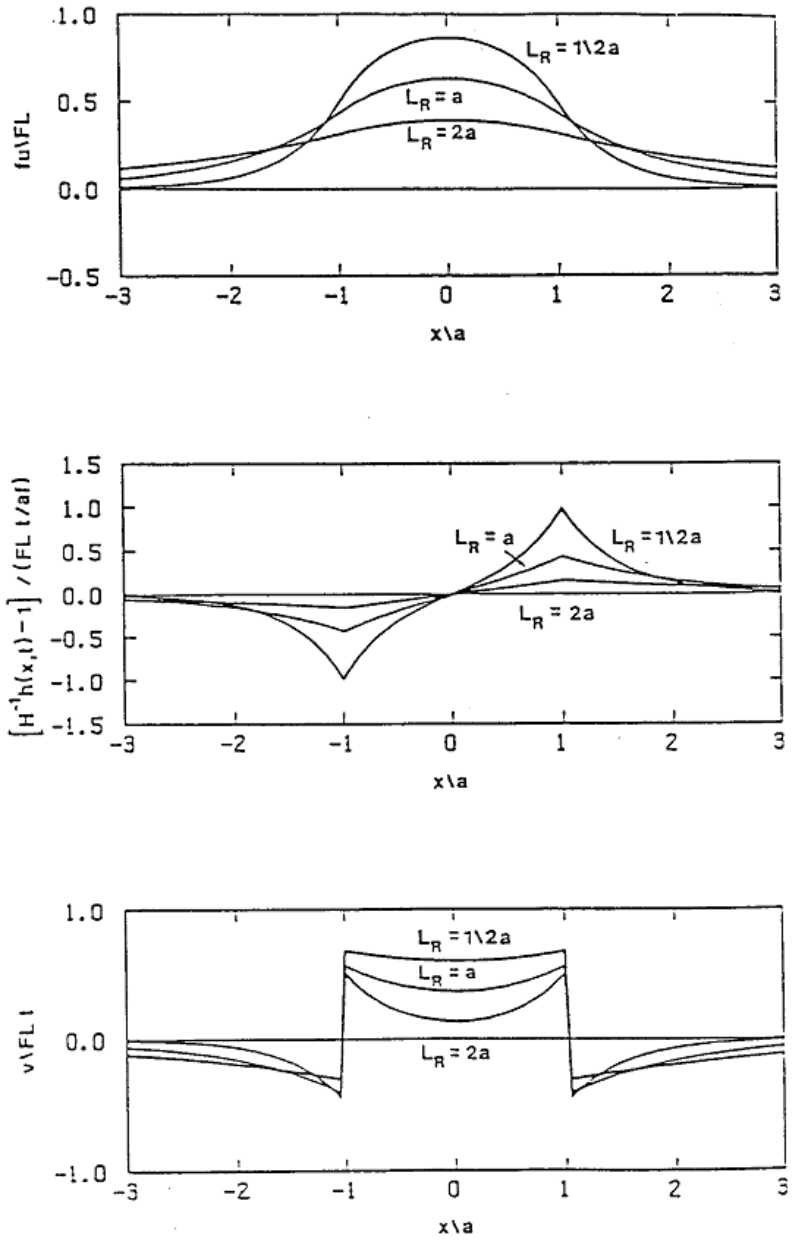

Figure 9.9: Nondimensional solutions for u, h and v from Eqs. (9.39) - (9.41) for different values of L_R as indicated.

II. Assume that $F \equiv 0$, but that $S \neq 0$ in the region $-a < x < a$. Assume again that $v(x,0) = 0$ and $h(x,0) = H$, a constant (see Fig. 9.10).

The physics of the example provides much insight into the adjustment

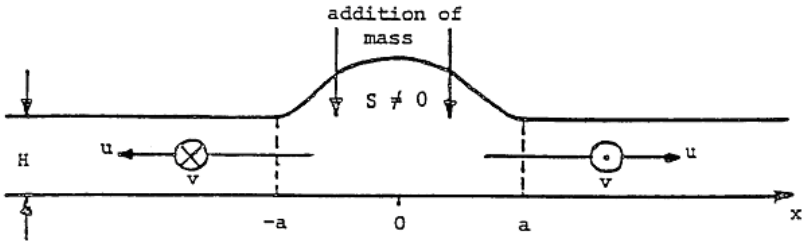

Figure 9.10: Geostrophic adjustment in response to the addition of mass.

process. Clearly, the addition of mass will lead to an outward pressure gradient which, if S is symmetric about $x = 0$, leads to a positive u for $x > 0$ and a negative u for $x < 0$. Hence the associated Coriolis torques imply sgn $(v) = -sgn(u)$ from (9.35). But the Coriolis torques associated with v oppose the x-component of pressure gradient and this feedback again limits the spread of the disturbance. To be specific, suppose that

$$S(x) = \begin{cases} S_0\,(x+a)/a & \text{if} \quad -a \le x \le 0, \\ S_0\,(a-x)/a & \text{if} \quad 0 \le x \le a, \\ 0 & \text{if} \quad |a| \le x. \end{cases} \tag{9.42}$$

If we assume the disturbance to be of small amplitude so that the governing equations may be linearized, the problem can be readily solved to give

$$u(x) = \begin{cases} \overline{S}\left[1 - e^{-x/L_R} - e^{-\mu}\,\sinh(x/L_R)\right] & \text{for} \quad 0 \le x \le a, \\ \overline{S}\,\left[\cosh\,\mu - 1\right]\;e^{-x/L_R} & \text{for} \quad a \le x, \end{cases} \tag{9.43}$$

$$h(x,t) = \begin{cases} \overline{S}\,t\mu\,\left[e^{-\mu}\,\cosh(x/L_R) - e^{-x/L_R} - \mu(x-1)\right] & \text{for} \quad 0 \le x \le a, \\ \overline{S}\,t\mu\,[\cosh\,\mu - 1]\;e^{-x/L_R} & \text{for} \quad a \le 0, \end{cases} \tag{9.44}$$

$$v(x,t) = \begin{cases} \overline{S}\,ft\,\left[e^{-x/L_R} + e^{-\mu}\sinh(x/L_R) - 1\right] & \text{for} \quad 0 \le x \le a, \\ \overline{S}\,ft\,[1 - \cosh\,\mu]\;e^{-x/L_R} & \text{for} \quad a \le x, \end{cases} \tag{9.45}$$

where $\overline{S} = aS_0/m^2H$, and $\mu = a/L_R$, and where $u(x)$ and $v(x,t)$ are odd functions of x and $h(x,t)$ is an even function. The curves representing $u(x)/\overline{S}$, $h(x,t)/\overline{S}t$ and $v(x,t)/\overline{S}ft$ as functions of x/a are shown in Fig. 9.11. Once more, the e-folding decay scale for the disturbance is the Rossby

radius of deformation and if this is small compared with a, the disturbance is effectively confined by the Coriolis forces to the neighbourhood of the forcing region.

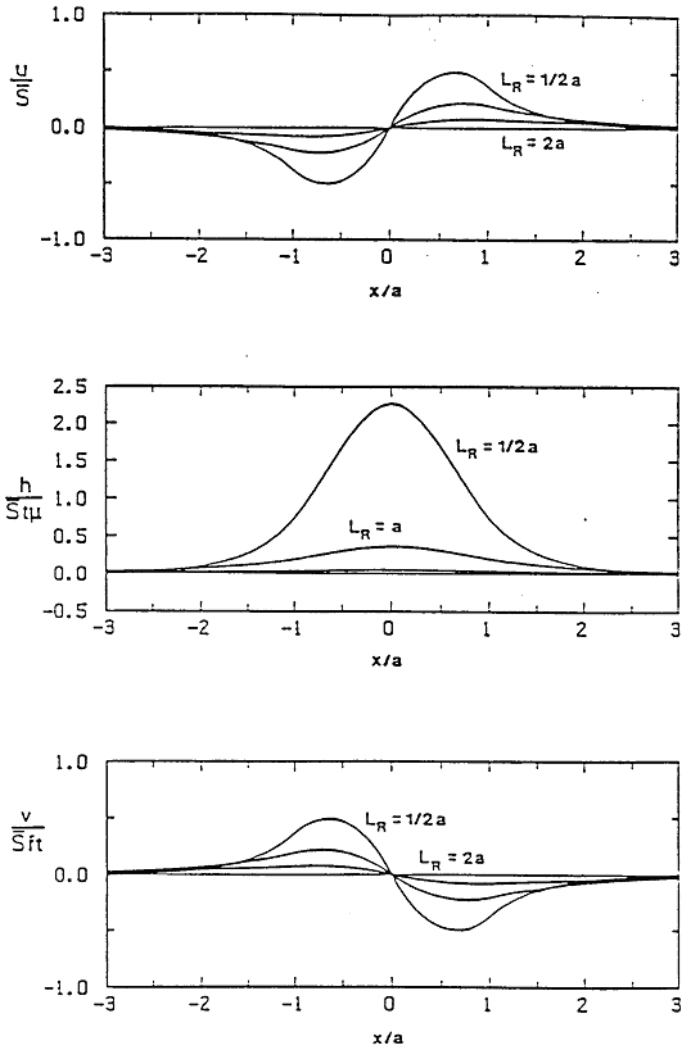

Figure 9.11: Nondimensional solutions for u, h and v from Eqs. (9.39) - (9.41) for different values of H_R as indicated.

Evidently, if the Coriolis effects are large ($L_R << a$), the mass field is unable to redistribute and the wind field adjusts to the mass field. Conversely, if Coriolis effects are small ($L_R >> a$), the mass disperses and thereby adjusts to the wind field, in this case zero. Even at this stage of our analysis, there is the suggestion that this may be a rather general result in the response

of rotating stratified fluid system to forcing, provided, of course, that the forcing does not act too quickly to invalidate the assumption of balance in Eq. (9.36).

Exercise

(9.1) Show that the solution of (9.37) that is continuous and has continuous x-derivatives at $x = -a$ and a, that decays to zero as $|x| \to \infty$ given by (9.39).

(9.2) Show that for quasi-geostrophic waves that are periodic in x,

$$\tfrac{1}{2}\rho g H^2 \int_{\text{wave}} \eta^2 dx = \tfrac{1}{2}\rho g H^2 \int_{\text{wave}} (u^2 + v^2) dx.$$

Using the fact that for such waves, $\zeta/f\eta = L_R^2 k^2$ (see page 86), verify the result (9.27). [Hint: consider $\int_{\text{wave}} \zeta\eta dx$ with z calculated geostrophically in terms of η].

Starting from the equations for small-amplitude inertia-gravity waves propagating in the x-direction, show that

$$\frac{KE}{PE} = 1 + \frac{2}{L_R^2 k^2},$$

and contrast the implications of this formula with those from Eq. (9.27).

Chapter 10

VERTICAL COORDINATE TRANSFORMATIONS

Let $\varepsilon = \varepsilon(x, y, z, t)$ be a new vertical coordinate in place of z. Then, any dependent quantity ψ can be expressed either as $\psi(x, y, z, t)$, or as $\psi(x, y, \varepsilon, t)$, where

$$\psi(x, y, \varepsilon(x, y, z, t), t) = \psi(x, y, z, t) \tag{10.1}$$

Differentiating with respect to x (or y, or t)

$$\left.\frac{\partial \psi}{\partial x}\right|_{\varepsilon} + \left.\frac{\partial \psi}{\partial \varepsilon}\right. \left.\frac{\partial \varepsilon}{\partial x}\right|_{z} = \left.\frac{\partial \psi}{\partial x}\right|_{z}, \tag{10.2}$$

and with respect to z,

$$\frac{\partial \psi}{\partial \varepsilon}\frac{\partial \varepsilon}{\partial z} = \frac{\partial \psi}{\partial z}. \tag{10.3}$$

The material derivative at constant z may be transformed thus:

$$\begin{aligned} \left.\frac{D}{Dt}\right|_{z} &= \left.\frac{\partial}{\partial t}\right|_{z} + u \left.\frac{\partial}{\partial x}\right|_{z} + v \left.\frac{\partial}{\partial y}\right|_{z} + w\frac{\partial}{\partial z} \\ &= \left.\frac{\partial}{\partial t}\right|_{\varepsilon} + u \left.\frac{\partial}{\partial x}\right|_{\varepsilon} + v \left.\frac{\partial}{\partial y}\right|_{\varepsilon} + \dot{\varepsilon}\frac{\partial}{\partial \varepsilon}, \end{aligned} \tag{10.4}$$

where

$$\dot{\varepsilon} = \frac{\partial \varepsilon}{\partial t} + u\frac{\partial \varepsilon}{\partial x} + v\frac{\partial \varepsilon}{\partial y} + w\frac{\partial \varepsilon}{\partial z} = \frac{D\varepsilon}{Dt}. \tag{10.5}$$

Note that u, v remain *horizontal* velocity components, but are calculated at the local value of ε instead of the corresponding value of z. The quantity $\dot{\varepsilon}$

plays a role in the transformed equations analogous to the vertical velocity component w in height coordinates.

Equation (10.1) can be written in the alternative form

$$\psi(x, y, z, t) = \psi(x, y, z(x, y, \varepsilon, t), t), \tag{10.6}$$

from which we can deduce that

$$\left.\frac{\partial \psi}{\partial x}\right|_{\varepsilon} = \left.\frac{\partial \psi}{\partial x}\right|_{z} + \left.\frac{\partial \psi}{\partial z}\,\frac{\partial z}{\partial x}\right|_{\varepsilon}, \tag{10.7}$$

and

$$\frac{\partial \psi}{\partial \varepsilon} = \frac{\partial \psi}{\partial z}\frac{\partial z}{\partial \varepsilon}. \tag{10.8}$$

Define

$$\nabla_z = \left(\frac{\partial}{\partial x},\ \frac{\partial}{\partial y},\ 0\right)_z. \tag{10.9}$$

Then using (10.7) we have

$$\nabla_z = \left(\frac{\partial}{\partial x},\ \frac{\partial}{\partial y},\ 0\right)_{\varepsilon} - \left(\frac{\partial z}{\partial x},\ \frac{\partial z}{\partial y},\ 0\right)_{\varepsilon} \frac{\partial}{\partial z} = \nabla_\varepsilon - (\nabla_\varepsilon z)\,\frac{\partial}{\partial z}\,. \tag{10.10}$$

10.1 Possible choices for ε

Coordinate transformations can be particularly useful when the motions are of a large enough scale for the hydrostatic approximation to be valid. Possible choices for ε are then the pressure p, or some function thereof; e.g.

- $\varepsilon = -Rlnp$: this is proportional to height in an isothermal atmosphere and can be a convenient coordinate to use in the stratosphere;
- $\varepsilon = (H_s/\kappa)[1 - (p/p_*)\kappa]$: this is proportional to height in an adiabatic atmosphere and was introduced by Hoskins and Bretherton (1972):
- $\varepsilon = p/p_s(x, y, t)$, where p_s is the surface pressure: this is the so-called sigma coordinate introduced by Phillips (1957), and is favoured in operational numerical weather prediction models;
- $\varepsilon = \theta$, the potential temperature: this leads to simplifications of the equations which prove useful in diagnostic interpretations of adiabatic, frictionless motion.

- We confine our attention here to the so-called isentropic coordinate system with $\varepsilon = \theta$.

10.2 Isentropic coordinates $\varepsilon = \theta$

In isentropic coordinates, the 'pseudo-vertical velocity' is identically zero for adiabatic motion, i.e.

$$\dot{\varepsilon} = \frac{D\theta}{Dt} = 0. \tag{10.11}$$

In other words, the vertical motion field is implicit in the coordinate transformation and need not be considered directly. However, this can lead to difficulties at boundaries (see Andrews, 1983).

10.3 The horizontal momentum equation

The horizontal pressure gradient transforms as follows. From Eq. (10.10),

$$\begin{aligned} -\alpha\nabla_z p &= -\alpha\nabla_\theta p + \alpha\frac{\partial p}{\partial z}\nabla_\theta z \\ &= -\frac{RT}{p}\nabla_\theta p - g\nabla_\theta z, \end{aligned} \tag{10.12}$$

using the hydrostatic equation ($\alpha\partial p/\partial z = -g$) and the gas equation ($p\alpha = RT$). Now $ln\ \theta = ln\ T + \kappa\ ln\ p_* - \kappa\ ln\ p$, whereupon, at constant θ, $R\ ln\ p = c_p\ ln\ T$ + constant. It follows that

$$\frac{R}{p}\nabla_\theta p = \frac{c_p}{T}\nabla_\theta T$$

and then from (10.12) that

$$-\alpha\nabla_z p = -\nabla_\theta(c_p T + gz). \tag{10.13}$$

The quantity $c_pT + gz$ is called the *Montgomery potential*, denoted by M. Using (10.4), (10.11) and (10.13), the horizontal momentum equation for adiabatic motion can be written as

$$\frac{\partial}{\partial t}\mathbf{u}_h + \mathbf{u}_h \cdot \nabla_\theta \mathbf{u}_h + f\mathbf{k} \wedge \mathbf{u}_h = -\nabla_\theta M. \tag{10.14}$$

If the motion is geostrophic, then we can solve for $\mathbf{u_h}$ in the normal way to obtain

$$\mathbf{u}_h = \frac{1}{f}\mathbf{k} \wedge \nabla_\theta M. \tag{10.15}$$

Thus the geostrophic wind blows parallel to the isopleths of constant M on an isentropic surface. The wind speed is proportional to the gradient of M and the blows with low values of M to the left (right) in the northern (southern) hemisphere.

10.4 The vertical momentum equation

When hydrostatic balance is satisfied, the vertical momentum equation is $0 = -\alpha\partial p/\partial z + g$. We wish to express this in terms of M. First note that $\theta = T(p_*/p)^\kappa$ implies that $c_p\ ln\ \theta = c_p\ ln\ T - R\ ln\ p$ + constant, since $\kappa = R/c_p$. Then, differentiating gives

$$\frac{c_p}{\theta} = \frac{c_p}{T}\frac{\partial T}{\partial \theta} - \frac{R}{p}\frac{\partial p}{\partial \theta},$$

or

$$c_p\frac{T}{\theta} = \frac{\partial}{\partial \theta}(c_p T) - \alpha\frac{\partial p}{\partial \theta}. \tag{10.16}$$

But in z-coordinates, the hydrostatic equation, $\alpha\partial p/\partial z = -g$, transforms to $\alpha(\partial p/\partial\theta)(\partial\theta/\partial z) = -g$, or

$$\alpha\frac{\partial p}{\partial \theta} = -g\frac{\partial z}{\partial \theta}. \tag{10.17}$$

Combining (10.16) and (10.17) gives

$$\frac{\partial M}{\partial \theta} = c_p\frac{T}{\theta}, \tag{10.18}$$

which is the isentropic-coordinate form of the hydrostatic equation.

10.5 The continuity equation

In height-coordinates the full continuity equation takes in the form

$$\left(\frac{\partial u}{\partial x} + \frac{\partial v}{\partial y}\right)_z + \frac{\partial w}{\partial z} = -\frac{1}{\rho}\frac{D\rho}{Dt}, \tag{10.19}$$

which, using (10.10), transforms to

$$\left(\frac{\partial u}{\partial x}+\frac{\partial v}{\partial y}\right)_\theta+\frac{\partial u}{\partial\theta}\frac{\partial\theta}{\partial x}+\frac{\partial v}{\partial\theta}\frac{\partial\theta}{\partial y}+\frac{\partial w}{\partial\theta}\frac{\partial\theta}{\partial z}=-\frac{1}{\rho}\frac{D\rho}{Dt}. \tag{10.20}$$

Now

$$\frac{\partial\dot\theta}{\partial\theta}=\frac{\partial}{\partial\theta}\frac{D\theta}{Dt}=\frac{D}{Dt}\left(\frac{\partial\theta}{\partial\theta}\right)+\frac{\partial u}{\partial\theta}\frac{\partial\theta}{\partial x}+\frac{\partial v}{\partial\theta}\frac{\partial\theta}{\partial y}+\frac{\partial w}{\partial\theta}\frac{\partial\theta}{\partial z}. \tag{10.21}$$

Also, from the hydrostatic equation, $\rho=-g^{-1}(\partial p/\partial\theta)(\partial\theta/\partial z)$, so that

$$ln\ \rho=ln(\partial\theta/\partial z)+ln(-\partial p/\partial\theta)-ln\ g.$$

Then

$$\frac{D}{Dt}\ln\rho=\frac{D}{Dt}\ln\left(\frac{\partial\theta}{\partial z}\right)+\frac{D}{Dt}\ln\left(\frac{\partial p}{\partial\theta}\right). \tag{10.22}$$

Also

$$\frac{D}{Dt}\left(\frac{\partial\theta}{\partial z}\right)=\frac{\partial}{\partial z}\left(\frac{D\theta}{Dt}\right)-\left(\frac{\partial u}{\partial\theta}\cdot\nabla\theta\right)\frac{\partial\theta}{\partial z}$$
$$=\left[\frac{\partial\dot\theta}{\partial\theta}-\frac{\partial u}{\partial\theta}\cdot\nabla\theta\right]\frac{\partial\theta}{\partial z}\equiv 0\,,\ \text{using (10.21)}\,,$$

whereupon, using (10.19) to (10.22) we obtain the unapproximated continuity equation in isentropic coordinates as

$$\left(\frac{\partial u}{\partial x}+\frac{\partial v}{\partial y}\right)_\theta+\frac{\partial\dot\theta}{\partial\theta}=-\left(\frac{\partial p}{\partial\theta}\right)^{-1}\frac{D}{Dt}\left(\frac{\partial p}{\partial\theta}\right).$$

This is often written in the form:

$$\frac{\partial\sigma}{\partial t}+\frac{\partial}{\partial x}(\sigma u)+\frac{\partial}{\partial y}(\sigma v)+\frac{\partial}{\partial\theta}(\sigma\dot\theta)=0, \tag{10.23}$$

where $\sigma=-(1/g)(\partial p/\partial\theta)=\rho(\partial z/\partial\theta)$ is called the *pseudo-density*. The integral of σ between two isentropic surfaces is just the mass of air between these surfaces per unit horizontal area.

For adiabatic motion, $\dot\theta\equiv 0$ and (10.23) simplifies further to acquire a quasi-two-dimensional form. An alternative derivation of the continuity equation is given by Pichler, (1984, pp. 239-240).

10.6 The vorticity equation

The horizontal momentum equation in its most general (nonadiabatic) form can be written as

$$\left.\frac{\partial \mathbf{u}_h}{\partial t}\right|_\theta + \tfrac{1}{2}\nabla_\theta \mathbf{u}_h^2 + (f\mathbf{k} + \nabla_\theta \wedge \mathbf{u}_h) \wedge \mathbf{u}_h + \dot{\theta}\frac{\partial \mathbf{u}_h}{\partial \theta} = -\nabla_\theta M.$$

Taking $\mathbf{k} \times \nabla_\theta \wedge$ of this equation gives

$$\left.\frac{\partial \eta_\theta}{\partial t}\right|_\theta + \nabla_\theta \cdot (\mathbf{u}_h \eta_\theta) = -\mathbf{k} \cdot \nabla_\theta \wedge \left(\dot{\theta}\frac{\partial \mathbf{u}_h}{\partial \theta}\right), \tag{10.24}$$

where

$$\eta_\theta = \zeta_\theta + f = \mathbf{k} \cdot \nabla_\theta \wedge \mathbf{u}_h + f, \tag{10.25}$$

is the *vertical component of absolute vorticity* in isentropic coordinates. Equation (10.24) is the vorticity equation in isentropic coordinates. The term on the right-hand side of (10.24) is analogous to the tilting term in height coordinates and here it vanishes for adiabatic motion when $\dot{\theta} \equiv 0$. In this case, the vorticity equation becomes

$$\frac{\partial \eta_\theta}{\partial t} + \mathbf{u}_h \cdot \nabla \eta_\theta = -\eta_\theta \nabla \cdot \mathbf{u}_h. \tag{10.26}$$

Combining this with the continuity equation, i.e., Eq.(10.23), we obtain

$$\frac{1}{\eta}\frac{D\eta}{Dt} = \left(\frac{\partial p}{\partial \theta}\right)^{-1} \frac{D}{Dt}\left(\frac{\partial p}{\partial \theta}\right)$$

or

$$\frac{D}{Dt}\left[(\zeta_\theta + f)\frac{\partial \theta}{\partial p}\right] = 0. \tag{10.27}$$

The quantity $-g(\zeta_\theta + f)(\partial\theta/\partial p)$ is called the *potential vorticity* (PV). It is equal to the *Ertel Potential Vorticity*, $\rho^{-1}(\boldsymbol{\omega} + \mathbf{f}) \cdot \nabla\theta$, defined in a height coordinate system. Equation (10.27) shows that the PV is conserved for frictionless, adiabatic motion.

Exercises

(10.1) Show that

$$\mathbf{u}_h \cdot \nabla \mathbf{u}_h = \tfrac{1}{2}\nabla_h \mathbf{u}_h^2 - \mathbf{u}_h \wedge (\nabla_h \wedge \mathbf{u}_h).$$

(10.2) Show that

$$\nabla_z \cdot \mathbf{u}_h = \nabla_\theta \cdot \mathbf{u}_h + \frac{\partial \theta}{\partial p}\left[\frac{\partial \mathbf{u}_h}{\partial \theta} \cdot \nabla_\theta \phi\right].$$

(10.3) Show that

$$\nabla_z \wedge \mathbf{u}_h = \nabla_\theta \wedge \mathbf{u}_h + \rho \frac{\partial \theta}{\partial p}\left[\nabla_\theta \phi \wedge \frac{\partial \mathbf{u}_h}{\partial \theta}\right].$$

(10.4) Show that the mass per unit horizontal area between two isobaric surfaces with pressures p_1 and $p_2\,(< p_1)$ is $(p_1 - p_2)/g$. Show that the same quantity between two isobaric surfaces with potential temperatures θ_1 and θ_2 can be written

$$\int_{\theta_1}^{\theta_2} \sigma d\theta, \quad \text{where} \quad \sigma = -\frac{1}{g}\frac{\partial p}{\partial \theta}.$$

(10.5) By cross differentiating the two components of Eq. (10.14) for the case in which a body force $F = (F, G, O)$ acts on the right-hand-side, show that

$$\frac{\partial}{\partial t}(\sigma Q) + \frac{\partial}{\partial x}\left(u\sigma Q + \dot{\theta}\frac{\partial v}{\partial \theta} - G\right) + \frac{\partial}{\partial y}\left(v\sigma Q - \dot{\theta}\frac{\partial u}{\partial \theta} + F\right) = 0, \tag{10.28}$$

where $Q = \partial v/\partial x - \partial u/\partial y + f$, is the vertical component of absolute vorticity in isentropic coordinates.

Show that the corresponding equation in pressure coordinates takes the form

$$\frac{\partial}{\partial t}\zeta_{ap} + \frac{\partial}{\partial x}\left[u\zeta_{ap} + \omega\frac{\partial v}{\partial p} - G\right] + \frac{\partial}{\partial y}\left[v\zeta_{ap} - \omega\frac{\partial v}{\partial x} + F\right] = 0, \tag{10.29}$$

where ζ_{ap} is equivalent to Q in (10.28).

Appendix A

Derivation of Eq. (4.41)

Equations (4.39), (4.38), (4.36) may be rearranged to give, respectively,

$$ik\hat{u}_2 = -im\hat{w}_2 - \hat{w}_{1Z} \tag{A.1}$$

$$i\omega^*\hat{\sigma}_2 = N^2\hat{w}_2 + \hat{\sigma}1T, \tag{A.2}$$

$$\begin{aligned} ik\hat{P}_2 &= i\omega^\star\hat{u}_2 - \hat{u}_{1T} - U_Z\hat{w}_1 \\ &= \frac{\omega^\star}{k}\left(-im\hat{w}_2 - \hat{w}_{1Z}\right) - \hat{u}_{1T} - U_Z\hat{w}_1, \end{aligned} \tag{A.3}$$

where (A.1) was used in deriving (A.3). Then substitution into (4.37) gives

$$\begin{aligned} -i\omega^\star\hat{w}_2 \;+\; & \frac{m}{k}\left[\frac{\omega^\star}{k}\left(-im\hat{w}_2 - \hat{w}_{1Z}\right) - \hat{u}_{1T} - U_Z\hat{w}_1\right] - \frac{1}{i\omega^\star}\left[N^2\hat{w}_2 + \hat{\sigma}_{1T}\right] \\ =\; & -\hat{w}_{1T} - \hat{P}_{1Z} \end{aligned}$$

or

$$\begin{aligned} \hat{w}_2\left[\omega^{*^2} + \omega^{*^2}\frac{m^2}{k^2} - N^2\right] - i\omega^{*^2}(m/k^2)\hat{w}_{1Z} \;-\; & \left(\hat{u}_{1T} + U_Z\hat{w}_1\right)\left(i\omega^* m/k\right) - \hat{\sigma}_{1T} \\ =\; & -i\omega^*\hat{w}_{1T} - i\omega^*\hat{P}_{1Z}. \end{aligned} \tag{A.4}$$

The coefficient of $\hat{w}_2$ is zero on account of (4.34). Now, using expressions connecting $\hat{u}_1$, $\hat{P}_1$ and $\hat{\sigma}_1$ with $\hat{w}_1$ from the formulae: $k\hat{u}_1 = -m\hat{w}_1$, $i\omega^*\hat{\sigma}_1 = N^2\hat{w}_1$, and $k\hat{P}_1 = \omega^*\hat{u}_1 = -(\omega^* m/k)\hat{w}_1$, obtained from the linear problem, (A.4) reduces to

$$2(m^2+k^2)\hat{w}_{1T} - 2m\omega^*_{1Z} - \omega^* m_Z \hat{w}_1 = 0. \tag{A.5}$$

Multiplication by the complex conjugate[1] of $\hat{w}_1$ and adding the resulting equation to its complex conjugate gives

$$\left[(m^2+k^2)|\hat{w}_1|^2/\omega^*\right]_T - \left[m|\hat{w}_1|^2\right]_Z = 0. \tag{A.6}$$

The mean wave-energy density E, is given by

$$E = \tfrac{1}{2}\rho^* \left|\hat{u}^2 + \hat{w}^2\right| = \tfrac{1}{2}\rho^* |\hat{w}|^2 \left[\frac{m^2}{k^2} + 1\right] \tag{A.7}$$

so that (A.6) becomes

$$\frac{\partial}{\partial T}\left[\frac{E}{\omega^*}\right] - \frac{\partial}{\partial Z}\left[\tfrac{1}{2}\rho^* \frac{m}{k^2}|\hat{w}|^2\right] = 0, \tag{A.8}$$

assuming that the mean density ρ^* is a constant (the Boussinesq approximation). Finally, differentiating (4.34) with respect to m gives

$$\omega^* \frac{\partial \omega^*}{\partial m} = \frac{-m\omega^{*2}}{k^2+m^2},$$

whereupon the second term in (A.8) becomes $-(E/^{\omega}*)w_g$, where $w_g = \partial\omega^*/\partial m = \partial\omega/\partial m$, and (A.8) is just (4.41) as required.

[1]Note that ω^* denotes the intrinsic frequency: it is a REAL quantity. Note also that $\bar{z}z_T + z\bar{z}_T = |z|^2_T$, where a bar denotes the complex conjugate.

Appendix B

Poisson Equation

Poisson's equation is the second-order, elliptic, partial differential equation

$$\frac{\partial^2 h}{\partial^2 x} + \frac{\partial^2 h}{\partial^2 y} = -F(x, y). \tag{B.1}$$

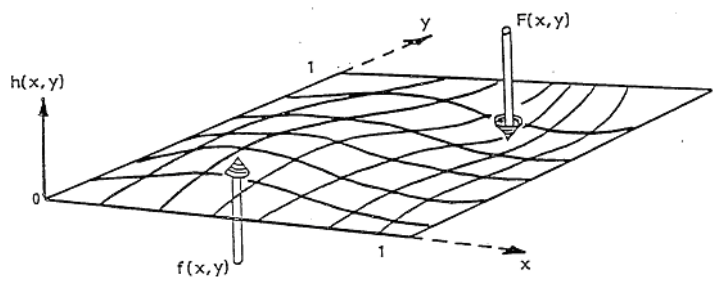

Figure B.1: Equilibrium displacement of a stretched membrane over a square under the force distribution $F(x, y)$.

Consider the solution in the square region $0 \leq x \leq 1$, $0 \leq y \leq 1$, subject to the (Dirichlet) boundary condition $h = 0$ on the boundary of the square. The equation with this boundary condition solves the problem of the equilibrium displacement of a stretched membrane over the square boundary when subjected to a force distribution per unit area proportional to $F(x, y)$ in a direction normal to the (x, y) plane. Of course, the boundary condition specifies zero displacement along the square boundary and the equation itself holds for small displacements of the membrane. The membrane analogy is useful as it allows us to use our intuition on how such a membrane would deform under a given force distribution (e.g., maximum displacement where

the force is a maximum) to anticipate the form of solution without having to solve the equation (Fig. B.1).

As a specific example, suppose there is a point force at the centre $(\frac{1}{2}, \frac{1}{2})$ of the unit square represented by delta-functions,

$$F(x, y) = \delta(x - \tfrac{1}{2})\delta(y - \tfrac{1}{2}). \tag{B.2}$$

We expect the solution to be symmetric about the diagonals of the square as shown in Fig. (B.2).

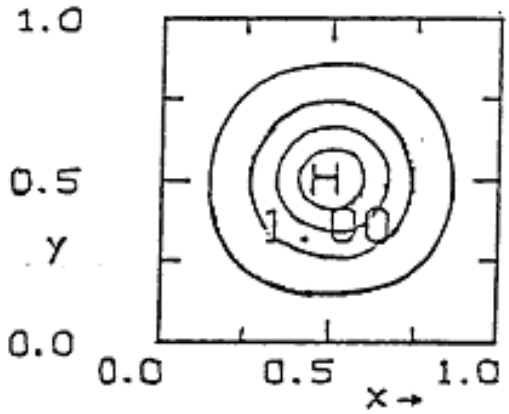

Figure B.2: Isopleths of membrane displacement subject to a point force at the centre point $(\frac{1}{2}, \frac{1}{2})$, giving rise to unit displacement at that point.

In fact, the isopleths of membrane displacement are determined analytically by the Green's function for the centre point, i.e.

$$h(x,y) = \begin{cases} 2\sum_{1}^{\infty} \dfrac{\sinh\ (n\pi x)\ \sinh\ (n\pi/2)\ \sin\ (n\pi y)\ \sin\ (n\pi/2)}{n\pi\ \sinh\ n\pi} & 0 \le x \le \frac{1}{2} \\ 2\sum_{1}^{\infty} \dfrac{\sinh\ (n\pi/2)\ \sinh\ (n\pi(1-x))\ \sin\ (n\pi y)\ \sin\ (n\pi/2)}{n\pi\ \sinh\ n\pi} & 0 \le x \le 1 \end{cases} \tag{B.3}$$

see Friedman, (1956; p. 262, Eq. 12.19), although Fig. B.2 was obtained by solving (B.1) numerically subject to an approximation to (B.2). Note especially that, although the force acts at a point, the response is distributed over the region. Now consider the response of the rectangular membrane $0 \le x \le 3$, $0 \le y \le 1$ due to a point force at the intersection of the diagonals

$(\frac{3}{2}, \frac{1}{2})$. The isopleths of membrane displacement, again normalized so that the maximum diaplacement is unity, are shown in Fig. B.3. Note that in

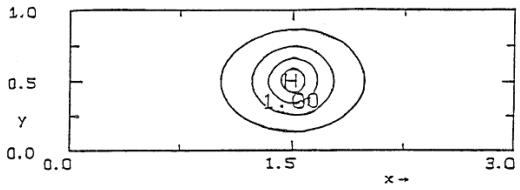

Figure B.3:

this case, the scales of response are set by the smallest rectangle length, in this case $\frac{1}{2}$.

Suppose, that we wish to infer the response of a membrane with nonuniform extension properties, as described for example by the equation

$$N^2 \frac{\partial^2 h}{\partial x^2} + f^2 \frac{\partial^2 h}{\partial z^2} = -F(x, z), \tag{B.4}$$

in the rectangular region $0 \leq x \leq L$, $0 \leq z \leq H$, again with $F(x, z)$ given by a point force proportional to $\delta(x - \frac{1}{2}L)\delta(z - \frac{1}{2}H)$. We consider the case $H << L$ and assume that N and f are constants. The equation may be transformed to one with unit coefficients by dividing both sides by N^2 and making the substitution $z = (f/N)Z$, whereupon

$$\frac{\partial^2 h}{\partial x^2} + \frac{\partial^2 h}{\partial Z^2} = -\frac{1}{N^2}\delta\left[x - \tfrac{1}{2}L\right]\ \delta\left[Z - \tfrac{1}{2}L_R\right], \tag{B.5}$$

where $L_R = HN/f$. The equation is valid for the region $0 \leq x \leq L$, $0 \leq Z \leq L_R$. In the case $L > L_R$, as exemplified in Fig. B.3, the response scale is the same, L_R, in both the x and Z directions. The latter corresponds with scale H for z. This last result is important in geophysical applications, for in a strably-stratified rotating fluid characterized by constant Brunt-Väisälä frequency N and constant Coriolis parameter f, we encounter equations of the type (B.4) for the streamfunction $\psi(x, z)$, usually in configurations where the aspect ratio of the flow domain, say H/L, is small. Typically, in the atmosphere, $f/N \sim 10^{-2}$. According to the foregoing results, provided $L > L_R$, then the horizontal length scale of the response is $L_R = HN/f$, which is just the *Rossby radius of deformation*. Since H is typically 10 km, the criterion $L > L_R$ requires that $L > 1000$ km. If $L < L_R$, the horizontal scale of response will be set by L and the vertical scale of response is then Lf/N, sometimes referred to as the *Rossby depth scale*. The former situation, which

is usually the case for geophysical flows, is illustrated in Fig. B.4 by numerical solutions of (B.4) in the region where $L = 2000$ km, $H = 10$ km, for four different values of L_R. Again a localized "force" $F(x, y)$ is applied at the point $(\frac{1}{2}L, \frac{1}{2}H)$ and the isopleths of "membrane displacement" are normalized so that the maximum displacement is unity. In all cases, $L > L_R$, but note how the horizontal scale of response decreases as L_R decreases. If other boundary conditions are imposed along all or part of the domain boundary, the foregoing ideas may have to be revised.

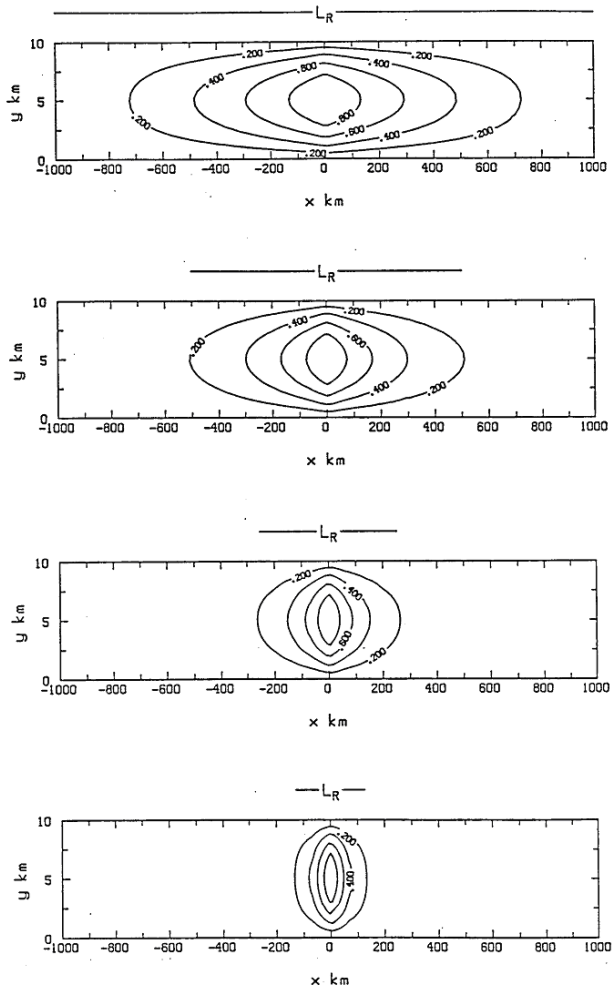

Figure B.4:

Bibliography

[1] Andrews, D. G., J. R. Holton and C. B. Leovy: 1987, Middle Atmosphere Dynamics, *Academic Press*, 489pp.

[2] Bluestein, H., 1992: Synoptic-Dynamic Meteorology in Middle Latitudes Vol. I: Principles of Kinematics and Dynamics. *Oxford Univ. Press*, 431pp. Vol. II: Observations and Theory of Weather Systems. *Oxford Univ. Press*, 1992, pp.

[3] Charney, J.G., 1973: Planetary Fluid Dynamics; Chapter in 'Dynamical Meteorology' (ed. Morel).

[4] Dutton, J. A., 1986: The Ceaseless Wind, *Dover*, 617pp.

[5] Etling, D., 1996: Theoretische Meteorologie: Eine Einführung. *Vierweg & Sohn*, Braunschweig/Wiesbaden, 318pp.

[6] Gill, A. E., 1982: Atmosphere - Ocean Dynamics. Academic Press, 662pp.

[7] Haltiner, G. J., 1980: Numerical Weather Prediction (2nd Edition). *Wiley*, 477pp.

[8] Holton, J. R., 1992: An Introduction to Dynamic Meteorology (3rd Edition) *Academic Press*, 507pp.

[9] Holton, J. R., 1975: The Dynamic Meteorology of the Stratosphere and Mesosphere. *Amer. Met. Soc. Monograph*, 216pp.

[10] James, I. N., 1994: Introduction to Circulating Atmospheres. *Cambridge University Press*, 422pp.

[11] Pedlosky, J., 1979: Geophysical Fluid Dynamics. *Springer*, 624pp.

[12] Pichler, H., 1986: Dynamik der Atmosphäre. *Bibliographisches Institut*, (2nd Edition) 456pp.

[13] Scorer, R.S., 1958: Natural Aerodynamics, *Pergamon Press*, 312pp.

[14] Smith, R. K., 1998: Lectures on Dynamical Meteorology. Referred to here as DM.

Bibliography

[1] Acheson, D. J., 1976. On over-reflection. *J. Fluid Mech.*, **77**, 433-472.

[2] Andrews, D. J., and M. E. McIntyre, 1978. An exact theory of nonlinear waves on a Lagrangian mean flow. *J. Fluid Mech.*, **89**, 609-646.

[3] Bannon, P. R., 1983. Quasi-geostrophic frontogenesis over topography. *J. Atmos. Sci.*, **40**, 2266-2277.

[4] Bannon, P. R., 1995. Potential vorticity conservation, hydrostatic adjustment, and the anelastic approximation. *J. Atmos. Sci.*, **52**, 2302-2312.

[5] Bennetts, D. A., and B. J. Hoskins, 1979. Conditional instability - a possible explanation for frontal rainbands, *Quart. J. Roy. Met. Soc.*, **105**, 945-962.

[6] Blumen, W., 1968. On the stability of quasi-geostrophic flow. *J. Atmos. Sci.*, **25**, 929-931.

[7] Blumen, W., 1972. Geostrophic Adjustment. *Rev. Geophys. Space Phys.*, **10**, 485-528.

[8] Booker, J. R., and F. P. Bretherton, 1967. The critical layer for internal gravity waves in a shear flow. *J. Fluid Mech.*, **27**, 513-539.

[9] Bretherton, F. P., 1966. Critical-layer instability in baroclinic flows. *Quart. J. Roy. Met. Soc.*, **92**, 325-334.

[10] Bretherton, F. P., 1971. GARP and Clear Air Turbulence. *Bull. Amer. Met. Soc.*, **52**, 17-21.

[11] Browning, K. A. and C. W. Pardoe, 1973. Structure of low-level jet streams ahead of mid-latitude cold fronts. *Quart. J. Roy. Met. Soc.*, **99**, 619-638.

[12] Charney, J. G. and M. Stern, 1962. On the stability of baroclinic jets in a rotating atmosphere. *J. Atmos. Sci.*, **19**, 159-172.

[13] Christie, D. R., 1992. The morning glory of the Gulf of Carpentaria: a paradigm for non-linear waves in the lower atmosphere. *Aust. Meteor. Mag.*, **41**, 21-60.

[14] Durran, D. R., 1989. Improving the anelastic approximation. *J. Atmos. Sci.*, **46**, 1453-1461.

[15] Durran, D. R., 1990. Reply. *J. Atmos. Sci.*, **47**, 1819-1820.

[16] Dutton, J. A., and G. H. Fichtl, 1969. Approximate equations of motion for gases and liquids. *J. Atmos. Sci.*, **26**, 241-254.

[17] Eliassen, A., 1949. The quasi-static equations of motion with pressure as independent variable. *Geofys. Publ.*, **17**, No. 3, 44pp.

[18] Eliassen, A., and E. Kleinschmidt, 1957. Dynamic meteorology. *Handbuch der Physik*, **58**, Berlin, Springer-Verlag, 1-154.

[19] Eliassen, A., and E. Palm, 1960. On the transfer of energy in stationary mountain waves. *Geofys. Publ.*, **22**, No 3, 1-23.

[20] Emanuel, K. A., 1983. The Lagrangian parcel dynamics of moist symmetric instability. *J. Atmos. Sci.*, **40**, 2368-2376.

[21] Erdélyi, A., W. Magnus, R. Oberhettinger, and F. G. Tricomi, 1954. Tables of Integral Transforms, Vol. I. McGraw-Hill, New York.

[22] Fiedler, B. H., 1990. Comments on "Improving the anelastic approximation". *J. Atmos. Sci.*, **47**, 1817-1818.

[23] Fjortoft, R.,1950.

[24] Fjortoft, R., 1962. Application of integral theorems in deriving criteria of stability for laminar flows and for the baroclinic circular vortex. *Geofys. Publ.*, **17**, No. 6, xxpp..

[25] Friedman, B., 1956. Principles and Techniques of Applied Mathematics, *Wiley*, New York.

[26] Garratt, J. R., W. L. Physick, R. K. Smith and A. J. Troup, 1985. The Australian summertime cool change. Part II: Mesoscale aspects. *Mon. Wea. Rev.*, **113**, 202-223.

[27] Hoskins, B. J., 1971. Atmospheric frontogenesis models: some solutions. *Quart. J. Roy. Met. Soc.*, **97**, 139-153.

[28] Hoskins, B. J., 1974. The role of potential vorticity in symmetric stability and instability. *Quart. J. Roy. Met. Soc.*, **100**, 480-482.

[29] Hoskins, B. J., 1975. The geostrophic momentum equation and the semi-geostrophic equations. *J. Atmos. Sci.*, **32**, 233-242.

[30] Hoskins, B. J., and F. B. Bretherton, 1972. Atmospheric frontogenesis models: mathematical formulation and solution. *J. Atmos. Sci.*, **29**, 11-37.

[31] Hoskins, B. J., and I. Draghici, 1977. The forcing of ageostrophic motion according to the semi-geostrophic equations and in an isentropic-coordinate model. *J. Atmos. Sci.*, **34**, 1859-1867.

[32] Hoskins, B. J., and N. V. West, 1979. Baroclinic waves and frontogenesis. Part II: Uniform potential vorticity jet flows - cold and warm fronts. *J. Atmos. Sci.*, **36**, 1663-1680.

[33] Hoskins, B. J., I. Draghici, and H. C. Davies, 1978. A new look at the w-equation. *Quart. J. Roy. Met. Soc.*, **104**, 31-38.

[34] Hoskins, B. J., and M. A. Pedder, 1980. The diagnosis of middle latitude synoptic development. *Quart. J. Roy. Met. Soc.*, **106**, 707-719.

[35] Jeffreys, H., and B. S. Jeffreys, 1956. Methods of Mathematical Physics, 3rd Edition, *Cambridge University Press*, pp.

[36] Klemp, J. B., and D. K. Lilly, 1975. The dynamics of wave-induced downslope winds. *J. Atmos. Sci.*, **32**, 320-339.

[37] Lamb, H., 1932. Hydrodynamics. Cambridge University Press, 6th Edition, pp.

[38] Leslie, L. M., and R. K. Smith, 1978. The effect of vertical stability on tornadogenesis. *J. Atmos. Sci.*, **35**, 1281-1288.

[39] Lilly, D. K., 1971. Wave Momentum flux - a GARP problem, BAMS, **33**, 17-23.

[40] Lipps, F. B., 1990. On the anelastic approximation for deep convection. *J. Atmos. Sci.*, **47**, 1794-1798.

[41] Lipps, F. B., and R. S. Hemler, 1982. A scale analysis of deep moist convection and some related numerical calculations. *J. Atmos. Sci.*, **39**, 2192-2210.

[42] Lipps, F. B., and Hemler, R. S., 1985. Another look at the scale analysis of deep moist convection. *J. Atmos. Sci.*, **42**, 1960-1964.

[43] McIntyre, M. E., 1970. On the nonseparable baroclinic parallel-flow instability problem. *J. Fluid Mech.*, **40**, 273-306.

[44] McIntyre, M. E., 1972. Baroclinic instability of an idealized model of the polar night jet. *Quart. J. Roy. Met. Soc.*, **98**, 165-174.

[45] Morse, P.M., and H. Feshbach, 1953. Methods of Theoretical Physics. Two parts. *McGraw-Hill, New York*.

[46] Nance, L. B., and D. R. Durran, 1994. A comparison of the accuracy of three anelastic systems and the pseudo-incompressible system. *J. Atmos. Sci.*, **51**, 3549-3565.

[47] Ogura, Y., and N. A. Phillips, 1962. Scale analysis of deep and shallow convection in the atmosphere. *J. Atmos. Sci.*, **19**, 173-179.

[48] Ooyama, K., 1966. On the stability of the baroclinic circular vortex: a sufficient criterion for stability. *J. Atmos. Sci.*, **23**, 43-53.

[49] Queney, P., 1948. The problem of airflow over mountain. A summary of theoretical studies. *Bull. Amer. Meteor. Soc.*, **29**, 16-26.

[50] Reed, R. J., 1955. A study of characteristic type of upper-level frontogenesis. *J. Meteor.*, **12**, 226-237.

[51] Reed, R. J., and E. F. Danielsen, 1959. Fronts in the vicinity of the tropopause. *Arch. Met. Geoph. Biokl. A*, **11**, 1-17.

[52] Sawyer, J. S., 1960. Numerical calculation of the displacements of a stratified airstream crossing a ridge of small height. *Quart. J. Roy. Met. Soc.*, **86**, 326-345.

[53] Scorer, R. S., 1972. Clouds of the World. *David & Charles (Publ.) Ltd, Newton Abbot, Devon*.

[54] Scorer, R. S., 1949. Theory of lee waves of mountains. *Quart. J. Roy. Met. Soc.*, **75**, 41-56.

[55] Simmons, A. J., 1974. Planetary-scale disturbances in the polar winter stratosphere. *Quart. J. R. Met. Soc.*, **100**, 76-108.

[56] Smith, R. B., 1979. The influence of mountains on the atmosphere. *Adv. in Geoph.*, **21**, 87-229.

[57] Smith, R. K., 1988. Waves and bores in the lower atmosphere: The 'morning glory' and related phenomena. *Earth Sci. Rev.*, **25**, 267-290.

[58] Stone, P. H., 1966. Frontogenesis by horizontal wind deformation fields. *J. Atmos. Sci.*, **23**, 455-465.

[59] Thorpe, S. A., 1971. Experiments on the instability of stratified shear flows: miscible fluids. *J. Fluid Mech.*, **46**, 299-319.

[60] Trenberth, K. E., 1978. On the interpretation of the diagnostic quasi-geostrophic omega equation. *Mon. Wea. Rev.*, **106**, 131-137.

[61] Williams, R. T., and J. Plotkin, 1968. Quasi-geostrophic frontogenesis. *J. Atmos. Sci.*, **25**, 201-206.

[62] Williams, R. T., 1972. Quasi-geostrophic versus non-geostrophic frontogenesis. *J. Atmos. Sci.*, **29**, 3-10.

[63] Williams, R. T., 1974. Numerical simulation of steady-state fronts. *J. Atmos. Sci.*, **31**, 1286-1296.